

University of Alberta

Metabolic Engineering of Central Carbon Metabolism for Production of
Isobutanol and other Higher Alcohol Biofuels in *Saccharomyces cerevisiae*

By

Ebele Ofuonye

A thesis submitted to the Faculty of Graduate Studies and Research
in partial fulfillment of the requirements for the degree of

Master of Science

Department of Biochemistry

©Ebele Ofuonye

Fall, 2012

Edmonton, Alberta

Permission is hereby granted to the University of Alberta Libraries to reproduce single copies of this thesis and to lend or sell such copies for private, scholarly or scientific research purposes only. Where the thesis is converted to, or otherwise made available in digital form, the University of Alberta will advise potential users of the terms of this thesis.

The author reserves all other publication and other rights in association with the copyright in the thesis and, except as herein before provided, neither the thesis nor any substantial portion thereof may be printed or otherwise reproduced in any material form whatsoever without the author's prior written permission.

Dedication

To my family

For their love and support

Abstract

The yeast *Saccharomyces cerevisiae* was engineered for production of high-value alcohols including isobutanol and isopentanol. This strategy uses the host's highly active valine amino acid biosynthetic pathway and diverts its 2-ketoacid intermediate for alcohol synthesis. A 2-ketoacid decarboxylase from *Lactococcus lactis* (*kdcA*) efficiently utilizes the branched chain precursor 2-ketoisovalerate to produce isobutyraldehyde, which can then be converted to isobutanol by alcohol dehydrogenase. In the presence of high concentration of valine, overexpression of *kdcA* and the *E. coli yqhD* alcohol dehydrogenase leads to increased isobutanol production of 15mg/g of valine. The valine biosynthetic pathway was also engineered for efficient production of alcohols from glucose by overexpressing the genes involved in valine biosynthesis (*ILV2*, *ILV6*, *ILV3* and *ILV5* genes) in addition to *kdcA* and *yqhD*. This strain produced ~150mg/liter of isobutanol; a yield of 1.88mg/g of glucose. Deletion of *LEU4*, *LEU9* and *BAT1* genes involved in competing reactions was not beneficial for isobutanol production.

Acknowledgement

My sincere appreciation goes to my supervisor, Dr. David Stuart for his guidance and encouragement throughout my studies. His willingness to provide hands-on support is truly appreciated. I am also indebted to my supervisory committee members: Dr Joel Weiner and Dr. Michael Ellison for constructive feedback on my research project.

My indebtedness goes to the members of the Stuart's lab both past and present for being a source of tremendous help in the course of this project. Many thanks to Kwesi Kutin for constructing the biobrick plasmids, Tete Li for performing the initial *kdcA* western blots and assays, Xiao Dong Liu, Isabella Wong and Diana Pham for providing an atmosphere conducive for learning.

I am most grateful to Dr. Ralf Kölling from Universität Hohenheim, Germany for generously providing the anti-Ilv2 polyclonal antibody, Jingui Lan from the Bressler lab in the department of Agriculture and Forestry, University of Alberta for helping with the Gas Chromatography assays and the members of the Biological conversions group of the Biorefining Conversions Network (BCN) at the University of Alberta for invaluable advice in the course of this project.

My gratitude extends to the faculty, staff and students of the Department of Biochemistry, University of Alberta for making my graduate school experience worthwhile. I want thank the graduate advisor; Kimberly Arndt, the members of the Schultz's lab, my classmates, and so many others too numerous to mention for their support and friendship.

Nothing reassures one more than the love of one's family. I would like to thank my husband; Chike Unaegbunam, my parents; Joseph and Louisa Ofuonye, my siblings; Ben, Chinedu, Ejike, Chinwe, Chinelo and Uche for the love and kindness shown to me over the years.

Finally, I am most grateful to God Almighty for countless graces.

Table of Contents

| | |
|--|----|
| Chapter One: Introduction | 1 |
| 1.1 Synthetic biology: An effective tool for biofuel production | 3 |
| 1.2 Current biofuel research | 5 |
| 1.2.1 Bioethanol production | 8 |
| 1.2.2 Isopropanol production | 10 |
| 1.2.3 Fermentative pathway for 1-butanol production | 12 |
| 1.2.4 Higher chain alcohol production via ketoacid pathways | 15 |
| 1.2.4.1 Isobutanol production | 15 |
| 1.2.4.2 2-Methyl-1-butanol(n-Pentanol) and 3-Methyl-1-butanol (Isopentanol) production | 19 |
| 1.2.4.3 Other non-natural alcohols | 23 |
| 1.2.5 Isoprenoid-derived biofuels | 23 |
| 1.2.6 Fatty acid-derived biofuels | 25 |
| 1.3 Alcohol cytotoxicity | 29 |
| 1.4 Research objectives | 30 |
| | |
| Chapter Two: Materials and methods | 31 |
| 2.1 General methods | 31 |
| 2.1.1 Reagents | 31 |
| 2.1.2 Growth and culture conditions | 31 |
| 2.1.3 Transformation of <i>S. cerevisiae</i> | 32 |
| 2.1.4 <i>E. coli</i> transformation | 33 |
| 2.1.5 DNA extraction and purification | 33 |
| 2.1.6 DNA modification | 34 |
| 2.1.7 Polymerase chain reaction | 34 |
| 2.1.8 DNA sequencing | 35 |
| 2.1.9 Agarose gel electrophoresis | 35 |

| | |
|---|----|
| 2.2 Strains and plasmid construction----- | 35 |
| 2.2.1 Oligonucleotide design----- | 35 |
| 2.2.2 Construction of biobrick vectors with yeast promoters----- | 37 |
| 2.2.3 Construction of <i>ILV</i> gene plasmids----- | 38 |
| 2.2.4 Construction of <i>MYC</i> -tagged alcohol dehydrogenase (ADH) plasmids-- | 40 |
| 2.2.5 Construction of HA-tagged 2-keto acid decarboxylase (<i>kdcA</i>) plasmid- | 41 |
| 2.2.6 Assembly of <i>ILV</i> gene array----- | 43 |
| 2.2.7 Construction of <i>leu4::kan^R leu9::loxP</i> , <i>bat1::loxP</i> and <i>leu4::kan^R</i> <i>leu9::loxP bat1::loxP</i> strains----- | 44 |
| | |
| 2.3 Experimental techniques----- | 46 |
| 2.3.1 Protein solubility assays----- | 46 |
| 2.3.2 SDS-PAGE electrophoresis and western blot----- | 47 |
| 2.3.3 Alcohol dehydrogenase assays----- | 48 |
| 2.3.4 Genetic complementation studies----- | 49 |
| 2.3.5 Gas chromatography assays----- | 49 |
| | |
| Chapter Three: Results----- | 51 |
| 3.1 Fusel Alcohol production by the classical Ehrlich pathway----- | 51 |
| 3.1.1 Isobutanol production in yeast overexpressing <i>Lactococcus lactis kdcA</i> ----- | 52 |
| 3.1.2 Determination of the optimal alcohol dehydrogenase activity for higher alcohol production----- | 54 |
| 3.2 Alcohol production in a media with branched-chain amino acids as sole nitrogen source----- | 58 |
| 3.3 Fermentative production of isobutanol in <i>S. cerevisiae</i> by overexpressing genes in the valine biosynthetic pathway----- | 59 |
| 3.3.1 Confirmation of <i>ILV</i> gene activity----- | 60 |
| 3.3.2 Isobutanol production by cells overexpressing the <i>ILV</i> pathway----- | 62 |
| 3.4 Comparing the effect of competing pathways on isobutanol production----- | 65 |
| 3.4.1 Isobutanol production in parental strain (WT) and <i>leu4::kan^R leu9::LoxP</i> strains----- | 69 |

| | |
|---|----|
| 3.4.2 Isobutanol production in <i>bat1::LoxP</i> and <i>leu4::kan^R leu9::LoxP bat1::LoxP</i> strains----- | 73 |
| 3.4.3 Comparing isobutanol production for WT, <i>leu4::kan^R leu9::LoxP</i> , <i>bat1::LoxP</i> and <i>leu4::kan^R leu9::LoxP bat1::LoxP</i> strains----- | 76 |
| 3.4.4 Isobutanol production in valine and isoleucine-deficient media----- | 79 |
| | |
| Chapter four: Conclusion----- | 80 |
| 4.1 Discussion----- | 80 |
| 4.2 Future directions----- | 84 |
| 4.3 Summary----- | 89 |
| References----- | 91 |

List of Tables

| | |
|--|----|
| Table 1: List of oligonucleotides used in this study----- | 36 |
| Table 2: List of plasmids used in this study----- | 42 |
| Table 3: List of strains used in this study----- | 46 |
| Table 4: In vitro alcohol dehydrogenase activity----- | 58 |
| Table 5: List and composition of strains used for isobutanol production----- | 69 |

List of Figures

| | |
|--|----|
| Figure 1.1: World energy consumption by fuel 1990-2035 in quadrillion Btu ----- | 2 |
| Figure 1.2: Global oil consumption, 1980-2002----- | 3 |
| Figure 1.3: The synthetic biology framework----- | 5 |
| Figure 1.4: Engineered pathways for microbial production of ethanol from carbohydrates----- | 9 |
| Figure 1.5: Metabolic pathway for isopropanol production in engineered <i>E. coli</i> ----- | 12 |
| Figure 1.6: Engineered pathway for 1-butanol production in <i>E. coli</i> ----- | 15 |
| Figure 1.7: Higher alcohol production via 2-ketoacid pathways----- | 16 |
| Figure 1.8: Pathway for isobutanol production from pyruvate----- | 17 |
| Figure 1.9: Pathway for 2-methyl-1-butanol production----- | 21 |
| Figure 1.10: Pathway for 3-methyl-1-butanol production in engineered <i>E. coli</i> ----- | 22 |
| Figure 1.11: Isoprenoid-derived biofuels----- | 25 |
| Figure 1.12: Schematic illustration of fatty acid pathway for biodiesel and long- chain alkanes/alkenes production----- | 28 |
| Figure 2.1: PCR fragments with 5' and 3' restriction sites----- | 39 |
| Figure 2.2: Assembly of <i>ILV</i> gene array----- | 43 |
| Figure 3.1: The Ehrlich pathway for valine degradation in <i>S. cerevisiae</i> ----- | 51 |
| Figure 3.2: Western blot of KdcA expressed in yeast using anti-HA----- | 53 |
| Figure 3.3: Alcohol production in yeast overexpressing KdcA versus empty vector (EV) control----- | 54 |

| | |
|---|----|
| Figure 3.4: In vivo alcohol production for yeast overexpressing <i>kdcA</i> and different ADHs----- | 56 |
| Figure 3.5: In vitro alcohol dehydrogenase activity----- | 57 |
| Figure 3.6: Fusel alcohol production under conditions of nitrogen limitation----- | 59 |
| Figure 3.7: Pathway for isobutanol production from pyruvate in <i>S. cerevisiae</i> --- | 60 |
| Figure 3.8: Confirmation of the activity of the cloned <i>ILV</i> genes----- | 61 |
| Figure 3.9: Isobutanol production in strain overexpressing the <i>ILV</i> gene array and <i>kdcA</i> ----- | 62 |
| Figure 3.10: <i>ILV2</i> is weakly expressed within the <i>ILV</i> array plasmid----- | 64 |
| Figure 3.11: Pathways for valine and leucine biosynthesis in yeast----- | 66 |
| Figure 3.12: Gene deletions by homologous recombination----- | 68 |
| Figure 3.13: Alcohol production for WT and <i>leu4::kan^R leu9::loxP</i> strains in 8% glucose----- | 72 |
| Figure 3.14: Alcohol production in <i>bat1::loxP</i> and <i>leu4::kan^R leu9::loxP bat1::loxP</i> strains in 2% glucose----- | 75 |
| Figure 3.15: Comparing the isobutanol production of WT, <i>leu4::kan^R leu9::loxP</i> , <i>bat1::loxP</i> , and <i>leu4::kan^R leu9::loxP bat1::loxP</i> strains in 4% glucose----- | 78 |
| Figure 3.16: Isobutanol production in a media deficient in valine and isoleucine----- | 79 |

List of Abbreviations

| | |
|-------------------|---|
| NEB | New England Biolabs |
| PEG | Poly Ethylene Glycol |
| PMSF | Phenylmethylsulfonyl fluoride |
| DMSO | Dimethyl sulfoxide |
| DNA | Deoxyribonucleic acid |
| RNA | Ribonucleic acid |
| PCR | Polymerase Chain Reaction |
| dNTPs | Deoxribonucleoside Triphosphates |
| LB | Luria Broth |
| IPTG | Isopropyl β -D-1-thiogalactopyranoside |
| YEPD | Yeast Extract-Peptone-Dextrose |
| Dex | Dextrose |
| Raff | Raffinose |
| Gal | Galactose |
| OD ₆₀₀ | Optical Density at 600nm |
| ACP | Acyl carrier protein |
| CoA | Coenzyme A |
| EDTA | Ethylene-Diamine-Tetra-Acetic acid |
| SDS-PAGE | Sodium dodecyl sulfate - polyacrylamide gel electrophoresis |
| DTT | Dithiothreitol |
| TCA | Trichloroacetic acid |
| GC | Gas Chromatography |
| FID | Flame ionization detector |
| 2MB | 2-Methyl-1- butanol |
| 3MB | 3-Methyl-1-butanol |
| 5-FOA | 5-Fluoroorotic acid |

| | |
|-------------------|--|
| KIV | 2-Ketoisovalerate |
| KIC | 2-Ketoisocaproate |
| KMV | 2-Keto-3-methylvalerate |
| IPP | Isoprenyl pyrophosphate |
| DMPP | Dimethylallyl pyrophosphate |
| GPP | Geranyl pyrophosphate |
| FPP | Farnesyl pyrophosphate |
| GGPP | Geranylgeranyl pyrophosphate |
| FAME | Fatty acid methyl esters |
| FAEE | Fatty acid ethyl esters |
| NADH | Nicotinamide adenine dinucleotide (reduced) |
| NAD ⁺ | Nicotinamide adenine dinucleotide (oxidized) |
| NADPH | Nicotinamide adenine dinucleotide phosphate (reduced) |
| NADP ⁺ | Nicotinamide adenine dinucleotide phosphate (oxidized) |
| rpm | Revolutions per minute |
| bp | Base pairs |
| G418 | Geneticin |
| Amp | Ampicillin |
| Kan | Kanamycin |
| ORF | Open reading frame |

Chapter One: Introduction

Increasing energy prices, concerns over the environment and depletion of total reserves of petroleum-derived fuels and chemicals are stimulating a worldwide effort towards synthesizing fuels from renewable sources. The advent of synthetic biology and metabolic engineering offers the possibility to engineer microbial vectors for efficient production of high value biofuels from readily available feedstocks.

The projection for world energy consumption by fuel source is depicted in figure 1.1. Given expectations that world oil prices will remain relatively high through most of the projection period, petroleum and other liquid fuels will be the world's slowest growing source of energy. It is projected that liquid fuel consumption will increase at an average annual rate of 1.0 percent from 2008 to 2035, whereas total energy demand will increase by 1.6 percent per year [110]. Renewable energy sources will be the fastest growing source of world energy, with consumption increasing by 2.8 percent per year. Although liquid fuels are expected to remain the largest source of energy, their share of world market energy consumption will decline from 34 percent in 2008 to 29 percent in 2035[110].

The industrialized countries are the largest consumers of oil. Regionally, the largest consuming area remains North America (dominated by the United States), followed by Asia (with Japan being the largest consumer (Figure 1.2)).

The United States and Canada use more oil for transportation than for heat and power, but the opposite pattern holds true for the rest of the world: most regions use more oil for heat and power than for transportation [111]. The increasing

dependence on petroleum for transportation fuels has led to an increased focus to find sustainable replacements or supplements to petroleum derived diesel fuel, jet fuel and motor gasoline [28].

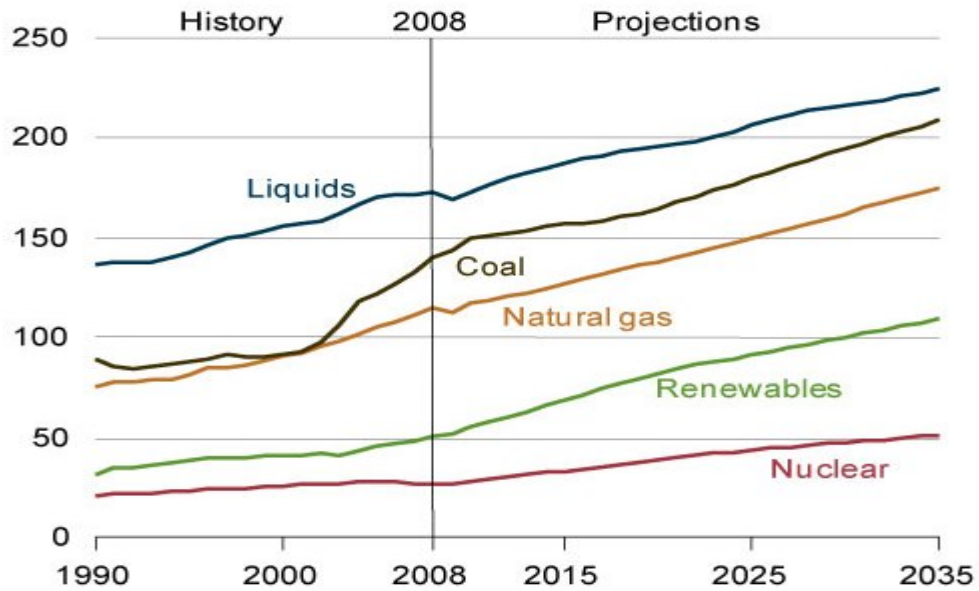


Figure 1.1: World energy consumption by fuel 1990-2035 in quadrillion Btu
Source: US energy information administration [110]

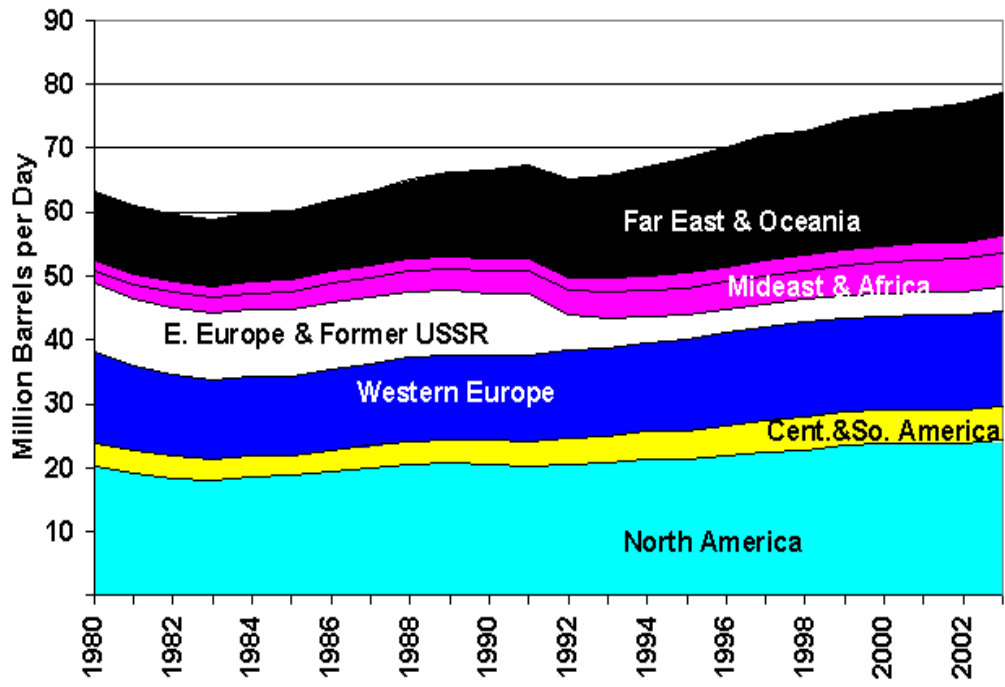


Figure 1.2: Global oil consumption by region, 1980-2002
 Source: US Energy information administration [111]

1.1 Synthetic biology: An effective tool for biofuel production

Humanity has long relied on microbial biocatalysts for production of fermented food and beverages [57]. Numerous microorganisms have been found to naturally produce a wide variety of compounds with uses as fuels, chemicals, and pharmaceutical products [24]. The concept of biofuels has been in existence since the nineteenth century; the invention of ignition engines was done with ethanol [1]. However, the discovery of fossil fuels was a major setback for biofuels. The large-scale oil crisis of 1970s and recent advances in synthetic biology, metabolic engineering and systems biology have generated a renewed interest in the production of biofuels [33].

Synthetic biology aims to design, synthesize and characterize new biological elements, or redesign natural systems [28, 70]. In synthetic biology, biological components are classified in a hierarchy as parts, devices, systems and chassis as shown in figure 1.3. The lowest level is the part and is defined as a single basic biology function e.g. a ribosome binding site, DNA, protein etc. Various tools and techniques inform the design of potential parts. Through clever design, these parts are then combined to form a device. These devices are then integrated into systems that can achieve more complex functionality through a variety of interactions. Finally, these systems are assembled into an optimized chassis to accomplish an astounding array of functions such as hunting for tumor cells, acting as biosensors or operating as a microbial cell factory [70].

Much of the work accomplished in biofuel research until now has relied on the identification of target pathways and the design of synthetic expression systems for enzymes responsible for fuel production [28]. As these technologies progress and mature, the design, implementation and optimization of new functions, as well as the upgrading and rewiring of existing components will be essential for the successful discovery and production of new biofuels [28].

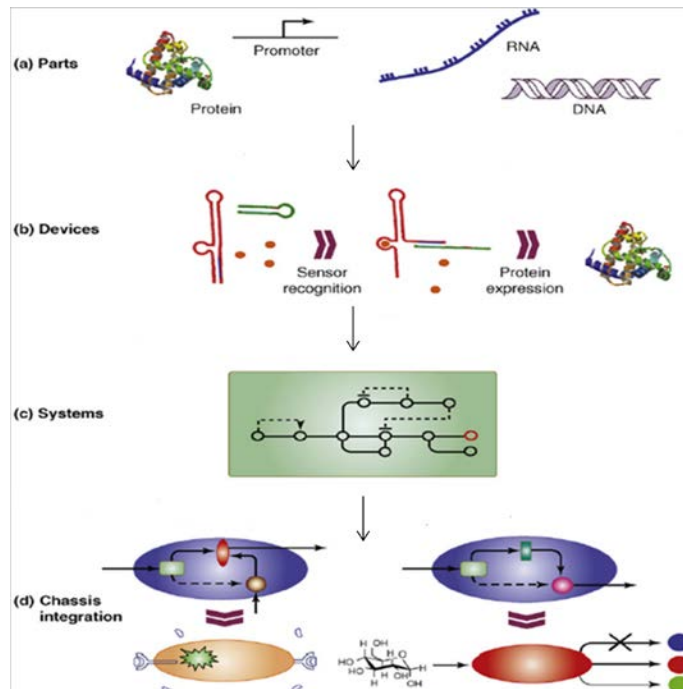


Figure 1.3: The synthetic biology framework

a) The lowest level is the part. Examples include DNA, RNA, proteins etc. b) These parts are combined to form a device. The example shown here is the simple expression of a protein that performs a desired function in response to a signal. c) The devices are then integrated into systems that can achieve more complex functionality through a variety of interactions. In this example, the protein device forms part of a branched reaction pathway. d) Finally, these systems are assembled into an optimized chassis to accomplish an astounding array of functions, such as hunting for human tumor cells, acting as biosensors, or operating as a microbial cell factory. Culled from Leonard, E. et al. [70]. Used with permission.

1.2 Current biofuel research

To address the challenges associated with use of fossil fuels, several compounds are being investigated as either replacements or supplements to fossil-derived fuels. Some examples include: bioethanol, biobutanol, isoprenoid-derived biofuels and biodiesel.

Ethanol produced from starch remains the most abundantly produced biofuel with production levels reaching 52.6 billion liters (13.9 billion gallons) in the United States alone in 2011 [83, 123]. Brazil trails the United States in terms of volumetric ethanol production since 2006 [12, 114]. The United States produces ethanol from corn while Brazil uses sugar cane. Ethanol is the first widely used

commercially available transportation fuel derived from renewable sources. The use of ethanol is a first step away from the dependence on fossil fuels and towards a new era of sustainable energy. Ethanol as a fuel however, is not perfect. Pure ethanol cannot be combusted in standard contemporary automotive engines due to its chemical properties [41, 84]. Ethanol has a higher vapor pressure than gasoline, which at operating temperatures, could produce vapor bubbles within the fuel lines. The “vapor lock” can cause the car to hesitate and stall due to inadequate fuel delivery [84]. Another main concern with ethanol is that it has a higher latent heat of vaporization, which requires more heat to vaporize the ethanol fuel than gasoline, which can reduce the ability of the car’s engine to ignite the fuel at lower temperatures [84]. Most internal combustion engines can operate with 10% ethanol and 90% gasoline mixtures without modifications, but only new engines especially modified for E85 gasoline blend can utilize 85% ethanol, 15 % gasoline mixture. The chemical properties of ethanol also make ethanol incompatible with current fuel transportation infrastructure and distribution. Ethanol’s lower solubility in gasoline, high solubility in water, and hygroscopic nature present an immense problem in fuel transportation. Currently, gasoline is primarily transported through pipelines. Moisture that seeps into transportation pipelines is normally not a problem due to water’s low solubility in gasoline. Since ethanol is hygroscopic, a gasoline/ethanol mixture permits water contamination in fuel, which may cause corrosion and damage to engine parts. The polar nature of ethanol molecules creates strong hydrogen bonds with water. Since water easily separates from gasoline, water contamination causes a

temperature dependent phase separation of gasoline and ethanol/water mixture. Low temperature is a major concern since it increases phase separation of water contaminated gasoline/ethanol mixture which may lead to frozen fuel lines during the winter. The added corrosiveness of ethanol and water also makes it less suitable for pipeline transportation. To mitigate this problem, ethanol requires its own separate transportation system and needs to be mixed with gasoline at the pumping station to avoid water contamination and fuel separation [84].

Another problem with ethanol is that current production requires use of sugar or starch as feedstock, which in turn drives up the cost of both food and fuel [84]. A shift to lignocellulosic ethanol would remedy this problem. Continual usage of ethanol as a fuel will require a drastic overhaul of the fuel infrastructure. A shift to higher alcohol biofuel may be required to move beyond the problems associated with ethanol use. The new fuel must be cost-effective, high in energy, and/or does not require much change in current delivery systems [84].

Biobutanol and other four carbon alcohols are currently being investigated as possible replacements for gasoline because they have superior fuel properties over ethanol. Biodiesel is expected to substitute petroleum-based diesel fuel. Fatty acid-derived and isoprenoid-based biofuels are being investigated as possible replacements for jet fuel [84].

1.2.1 Bioethanol production

Bioethanol C_2H_5OH is a two carbon alcohol derived from biomass feedstock by fermentation. The industrial production of ethanol from refined sugars of starch or sugar cane is done almost exclusively using baker's yeast. The yeast *Saccharomyces cerevisiae* produces ethanol in batch fermentation with CO_2 and small amounts of methanol, glycerol and other byproducts [1, 91]. Typical fermentations will yield up to 20% v/v ethanol by using glucose derived from starch, owing to inhibitor resistance, ethanol tolerance and ethanol-specific productivity of modern industrial yeast strains [1, 33, 91].

Most of the raw materials currently used for bioethanol production are from corn and sugar cane, however, future limitation in the supply of these materials is inevitable because they are also used as food crops [91]. Therefore, lignocellulosic biomasses are considered attractive raw materials for bioethanol production. Lignocellulosic biomass is composed of 40-50% cellulose, 25-35% hemicellulose and 15-20% lignin [91]. Many industrial yeast strains produce ethanol solely from six carbon sugars ($C_6H_{12}O_6$) but are unable to ferment five carbon sugars ($C_5H_{10}O_5$) such as xylose and arabinose, which are the most abundant lignocellulosic sugars next to glucose [33]. To combat this problem, recent efforts have been focused on the fermentation of pentose sugars. Two approaches have been taken to accomplish this. The first is to transfer pentose degrading pathways from other organisms into ethanologenic organisms such as the conventional yeast *S. cerevisiae* or ethanologenic bacterium *Zymomonas mobilis* and the other is to engineer natural pentose utilizing organisms such as *E.*

coli, *Klebsiella oxytoca* and the yeast *Pichia stipitis* to increase ethanol yields [29, 33]. Figure 1.4 summarizes the recent efforts towards producing ethanol from pentose sugars.

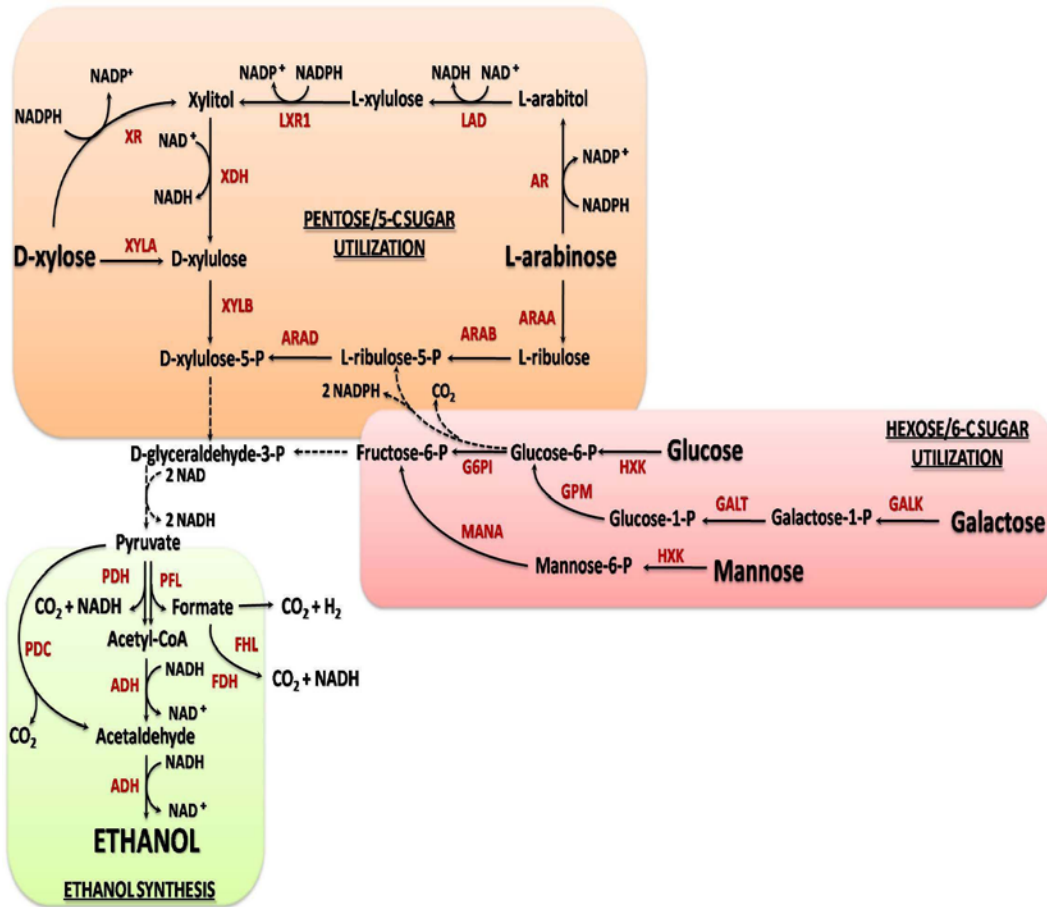


Figure 1.4: Engineered pathways for microbial production of ethanol from carbohydrates. Orange, red and green boxes indicate pathways for pentose and hexose sugar utilization, and ethanol synthesis respectively. The dashed lines indicate multiple steps. The conversion of D-xylose to D-xylulose is performed by xylose isomerase. Yeast can grow on and ferment xylulose, a heterologous xylose isomerase *xylA* gene from the anaerobic fungus *piromyces* sp E2a was expressed in *S. cerevisiae* for xylose catabolism. Xylose and arabinose metabolism was introduced into *Z. mobilis* by overexpressing *E. coli* genes involved in the conversion of these two pentoses to xylulose-5-P. This intermediate is channeled into the pentose phosphate pathway to yield glyceraldehyde-3-P, which is an intermediate in Embden-Meyerhof-Parnas (EMP) pathway. Abbreviations: ADH: alcohol dehydrogenase; AR: Aldose reductase; ARAA: L-arabinose isomerase; ARAB: L-ribulokinase; ARAD: L-ribosephosphate-4-epimerase; FDH: formate dehydrogenase; FHL: formate hydrogen lyase; LAD: L-arabitol-4-dehydrogenase; LXR1: L-xylulose reductase; PDC: pyruvate decarboxylase; PDH: pyruvate dehydrogenase, PFL: pyruvate formate lyase; XDH: xylitol dehydrogenase; XR: xylose reductase; XYLA: Xylose isomerase; XYLB: xylulokinase. Taken from Dellomonac et al. [33].

1.2.2 Isopropanol production

Isopropanol is a three carbon $(\text{CH}_3)_2\text{CHOH}$ alcohol, has an energy density of 23.9MJ/L, a high octane number and low solubility in water when compared with ethanol [83]. Isopropanol is both a desirable fuel and an important feedstock in the petrochemical industry. Its dehydrated product, propylene serves as the monomer for making polypropylene [4, 91, 119]. Isopropanol is currently used as an additive to petroleum-based fuels [83]. Isopropanol can be used in the esterification process of fats and oil in place of methanol to generate crystallization-resistant biodiesels [83, 119].

Isopropanol is one of the secondary alcohols produced naturally by Clostridial species from the acetone biosynthetic pathway [4]. However, as a native metabolite, it can only be produced in a limited amount for the host's own benefit as a detoxification response to low pH conditions [119]. The maximum titer reported in the native producer *Clostridium beijerinckii* was 1.8g/L [119]. The limited genetic tools available in Clostridium hinder the engineering of alcohol production to increase yields [83].

To overcome this problem, Hanai et al. [49] reconstructed the Clostridium biosynthetic pathway in *E. coli*. Acetone production from acetyl-CoA has previously been achieved in *E. coli* by introducing three *Clostridium acetobutylicum* genes: acetyl-CoA acyltransferase (*thl*), acetoacetyl-CoA transferase (*ctfAb*) and acetoacetate decarboxylase (*adc*) [4, 49, 83, 119]. To synthesize isopropanol, a secondary alcohol dehydrogenase (SADH) from *Clostridium beijerinckii* was overexpressed in combination with the acetone-

production pathway in *E. coli* in an NADPH-dependent reaction [49] (figure 1.5). In addition, the native *E. coli* acetyl-CoA acyltransferase (encoded by *atoB*) and acetoacetyl transferase (encoded by *atoAD*) were tested as pathway components. Furthermore, the activity of the secondary alcohol dehydrogenase from *C. beijerinckii* was compared to that of *Thermoanaerobacter brockii*. With these efforts, the strain with a combination of *C. acetobutylicum thl*, *E. coli atoAD*, *C. acetobutylicum adc* and *C. beijerinckii adh* achieved the highest isopropanol titer of 4.9g/L [49, 119].

Jojima et al. [58] has achieved isopropanol production levels of 13.6g/L in *E. coli* by reconstructing the Clostridal isopropanol pathway. This group expressed each of *thl*, *ctfAB* and *adc* genes from dedicated promoters rather than polycistronic expression of the *thl-ctfAD-adc* operon in a single vector. This could possibly explain the increased isopropanol yield [58, 83].

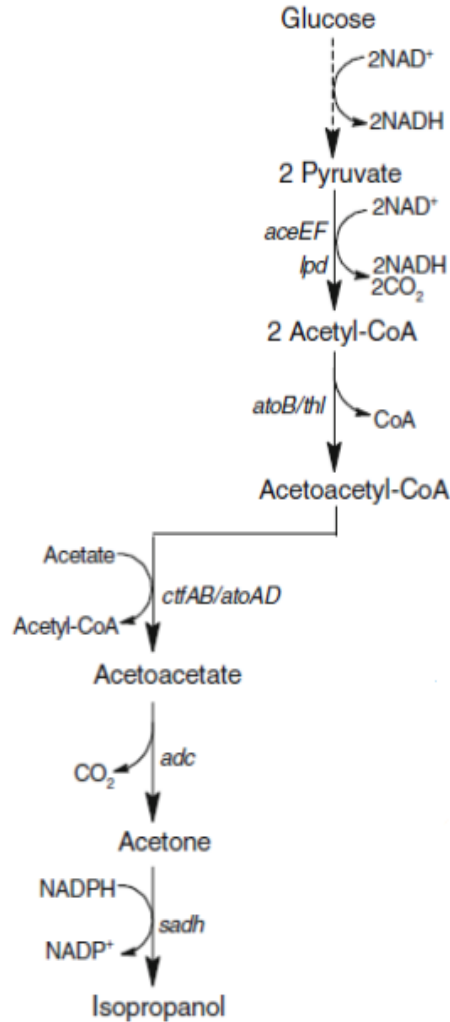


Figure 1.5: Metabolic pathway for isopropanol production in engineered *E. coli*.

The dashed line indicates omitted steps. Isopropanol pathway consists of four enzymatic steps from acetyl-CoA. *aceEF* and *lpd* encode pyruvate dehydrogenase; *atoB/thl* encodes acetyl-CoA acetyltransferase; *ctfAB/atoAD* encodes acetoacetyl-CoA transferase; *adc* encodes acetoacetate decarboxylase; *sadh* encodes secondary alcohol dehydrogenase. Adapted from Yan, Y. and Liao, J.C. [119].

1.2.3 Fermentative pathway for 1- butanol production

Butanol is a four-carbon (C_4H_9OH) alcohol, has an energy density of 29.2MJ/L, which is comparable to that of gasoline (32MJ/L). The chemical properties of butanol are similar to gasoline; butanol is hydrophobic, less hygroscopic and less corrosive than ethanol. These properties make it compatible with existing

infrastructure designed for petroleum products. Butanol can be used in pure form or blended to any concentration with gasoline [2]. All these qualities make butanol an ideal supplement or substitute to gasoline as a transportation fuel.

The microbial production of 1-butanol has a history of over 100 years [119]. Traditionally, 1-butanol was produced by *Clostridium* species through a process, which produces acetone/ butanol/ ethanol at a ratio of 3:6:1 [91]. This process is called the ABE (Acetone-Butanol-Ethanol) fermentation. However, microbial production of 1-butanol was made unprofitable by advancements in the petrochemical industry. 1-butanol concentrations ranging from 11.9-14.3g/L by *Clostridium berjerinckii* BA101 has been reported [24]. With renewed interest in alternative fuels; the production of 1-butanol has been investigated in *E. coli* and *S. cerevisiae*. These organisms unlike the native Clostridia producers are more amenable to genetic manipulations.

The engineered fermentative pathway for 1-butanol production in *E. coli* follows a similar strategy to that of isopropanol. The native pathway for 1-butanol production in *C. acetobutylicum* was transferred into *E. coli* to enable the conversion of acetyl-CoA to butanol (Figure 1.6). Unlike the successes achieved with isopropanol production in *E. coli*, the production of 1-butanol, however, has proven to be more difficult [28]. Initial efforts were able to produce 0.5 g/L using *E. coli* as a host. Construction of a new strain harboring a single construct resulted in an increase in production to 1.2 g/l [28]. In addition to *E. coli*, 1-butanol production has been investigated in *Pseudomonas putida*, *Bacillus subtilis*, and *S. cerevisiae* [28], although production in *E. coli* has thus far shown the most

promise. Each of these processes, however, is far from industrial feasibility, as yields (0.05 g/g) and productivities (0.01 g/L/h) must increase significantly to match the same figures for corn ethanol (0.5 g/g and 2 g/L/h). The advancement of these processes is thought to be limited by the low activity of pathway enzymes due to poor expression, solubility, or oxygen sensitivity, as well as metabolic imbalance introduced by these heterologous pathways [28].

Recently, Bond-Watt et al. [15] engineered 1-butanol production pathway in *E. coli* by replacing the *AtoB/Thl* and *Bcb/Etf* genes from the pathway in figure 1.6 with *PhaA* gene from *Ralstonia eutrophus* and a *ter* gene from the prokaryote *Treponema denticola*, respectively. To provide the additional NADH reducing equivalents to balance the production of 1-butanol from glucose, the pyruvate dehydrogenase complex *aceEF.lpd* was overexpressed. The combination of these modifications led to an *E. coli* strain that produced 4.65g/L of 1-butanol. These experiments point to upstream cellular pathways and decisions in carbon fate as the current limitation to *n*-butanol production rather than the synthetic pathway itself [15].

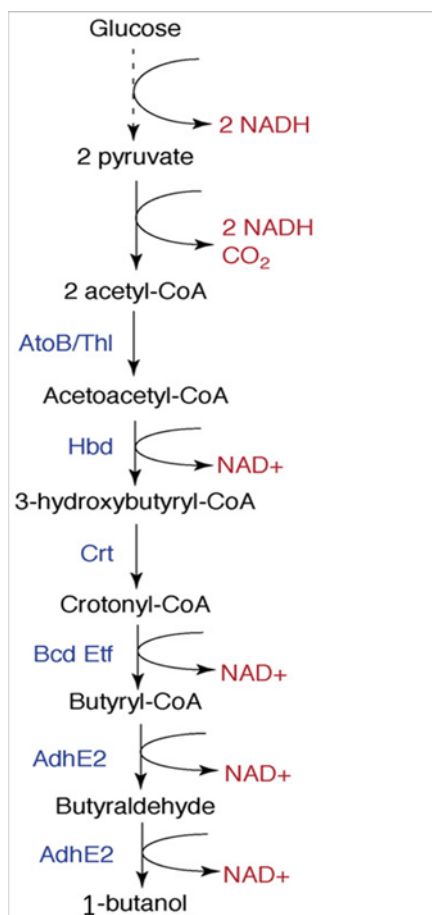


Figure 1.6: Engineered pathway for 1-butanol production in *E. coli*.

The engineered 1-butanol production pathway consists of six enzymatic steps from acetyl-CoA. *AtoB*, acetyl-CoA acetyltransferase; *Thl*, acetoacetyl-CoA thiolase; *Hbd*, 3-hydroxybutyryl-CoA dehydrogenase; *Crt*, crotonase; *Bcd*, butyryl-CoA dehydrogenase; *Etf*, electron transfer flavoprotein; *AdhE2*, aldehyde/alcohol dehydrogenase. Taken from Atsumi S. and Liao J.C [4] Used with permission.

1.2.4 Higher chain alcohol production via keto-acid pathways

Amino acid biosynthetic pathways generate a number of keto-acid intermediates.

The yeast *S. cerevisiae* can convert the keto-acids in the leucine, valine, isoleucine, phenylalanine, tryptophan and methionine pathways into various alcohols as byproducts of fermentation through the Ehrlich pathway [51]. The Ehrlich pathway consists of a two-step reaction in which a 2-ketoacid is first decarboxylated into an aldehyde through the action of 2-ketoacid decarboxylase

(KDC) and subsequently, the aldehyde is reduced to an alcohol by an alcohol dehydrogenase (ADH) [3, 51, 83]. By insertion of the Ehrlich pathway in *E. coli*, Atsumi et al. [3] were able to produce various higher alcohols as shown in figure 1.7.

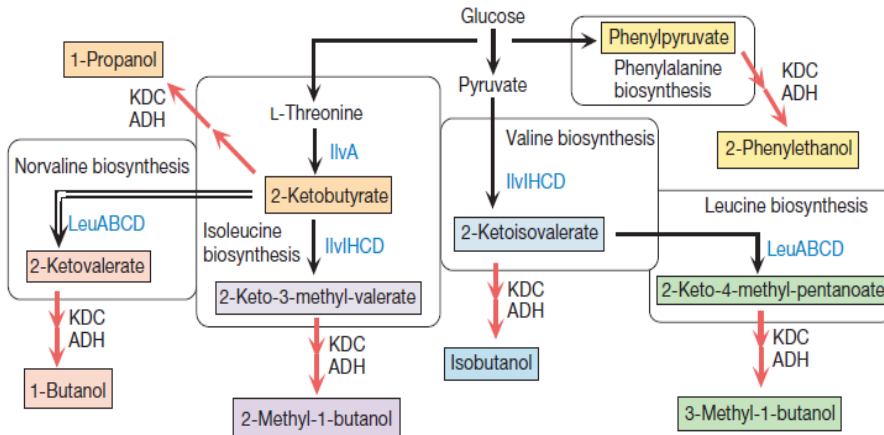


Figure 1.7: Higher alcohol production via 2-ketoacid pathways.

Red arrows represent the 2-keto acid decarboxylation and reduction pathway. Blue enzyme names represent amino acid biosynthesis pathways. The double lines represent a side pathway leading to norvaline and 1-butanol biosynthesis. Taken from Atsumi et al. [3]. Used with permission.

1.2.4.1 Isobutanol production

Isobutanol is an isomer of butanol. It has similar physico-chemical properties to 1-butanol [119]. Isobutanol like other higher alcohols is a potential biofuel because it has the capacity to replace gasoline. Isobutanol is produced biologically as a byproduct of yeast fermentation [69]. Isobutanol production has been engineered in *E. coli*, *Bacillus subtilis*, *Corynebacterium glutamicum*, *S. cerevisiae* and the cyanobacterium; *Synechococcus elongatus* using a common strategy as shown in figure 1.8. Isobutanol production in these organisms was accomplished by overexpressing 2-ketoacid decarboxylase (KDC) and alcohol dehydrogenase (ADH). In addition, the overexpression of three key enzymes:

(acetohydroxyacid synthase (AHAS), acetohydroxyacid isomeroreductase (AHAIR) and Dihydroxyacid dehydratase (DHAD)) involved in the conversion of pyruvate to 2-ketoisovalerate – an intermediate in valine biosynthesis leads to increased isobutanol production due to an increased drain off of pyruvate and increased 2-ketoisovalerate availability [14].

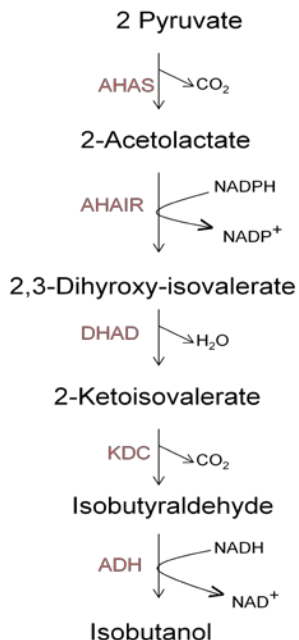


Figure 1.8: Pathway for isobutanol production from pyruvate.

AHAS, Acetohydroxyacid synthase; AHAIR, Acetohydroxyisomeroreductase; DHAD, Dihydroxyacid dehydratase; KDC; 2-Ketoacid decarboxylase; ADH, Alcohol dehydrogenase.

The AHAS enzyme from *E. coli*, *B. subtilis* and *C. glutamicum* have lower affinities towards pyruvate compared with other competing enzymes such as pyruvate formate lyase, pyruvate dehydrogenase complex, or lactate dehydrogenase. Increasing the intracellular pyruvate availability by knockout of the respective genes proved to be beneficial for isobutanol production [14].

In *E. coli*, the stepwise deletion of genes *adhE*, *ldhA*, *frdAB*, *fnr*, *pta* and *pflB* (encoding alcohol dehydrogenase, D-lactate dehydrogenase, fumarate reductase,

transcriptional regulator FNR, phosphateacetyltransferase and formate lyase respectively) and the overexpression of acetohydroxyacid synthase *alsS* from *Bacillus subtilis*, which has high affinity for pyruvate led to a drastic increase in isobutanol production when compared to the strain overexpressing only the pathway depicted in figure 1.8 [14, 119]. With the combination of these genetic modifications and overexpressions, the engineered *E. coli* strain was able to produce isobutanol at a titer of 20g/L and 86% of the theoretical yield [119].

Smith K.M and Liao J.C. [101], developed a rapid evolutionary strategy for isolating strains of *E. coli* that effectively produce isobutanol from glucose using random mutagenesis and growth selection scheme. By selecting for mutants capable of growing in the presence of the valine analog; norvaline, isobutanol titer of 21.2g/L was reported. In another study, Baez et al. [10] employed a batch fermentation technique that was integrated with gas stripping. This technique allowed in situ product removal and reduces isobutanol toxicity during the growth phase. Isobutanol production titer of 50g/L was achieved with engineered *E. coli* after 72 hours.

In *C. glutamicum* and *B. subtilis*, isobutanol titer of 4.9g/L and 2.62g/L respectively [65, 71, 100], has been achieved by employing similar strategies used in *E. coli*.

Isobutyraldehyde and isobutanol production by photosynthetic CO₂ recycling has also been accomplished in the cyanobacteria; *Synechococcus elongatus*. To achieve this, Atsumi et al. [7] integrated the *kdcA* gene from *Lactococcus lactis*,

the *alsS* from *Bacillus subtilis* and the *ilvC* and *ilvD* genes from *E. coli* into the genome of the cyanobacterium. In addition, the overexpression of ribulose 1, 5-bisphosphate carboxylase/oxygenase (Rubisco) enzyme that catalyze CO₂ fixation reaction in the Calvin-Benson-Bassham (CBB) lead to the production of an isobutyraldehyde titer of 1.1g/L after 8 days.

In yeast, isobutanol is produced naturally via the Ehrlich pathway. *S. cerevisiae* has been engineered for increased isobutanol production by overexpression of the genes involved in valine biosynthesis; *ILV2*, *ILV3* and *ILV5*. This led to production of 4.12mg/g glucose of isobutanol [21]. In another study, an isobutanol production of 6.6g/g glucose was achieved by overexpressing *kdcA*, *ADH6* and *ILV2* in a *pdclΔ* strain of *S. cerevisiae* [64]. Engineering *S. cerevisiae* for efficient production of isobutanol from pyruvate is one of the thrusts of this thesis.

1.2.4.2 2-methyl-1-butanol (n-Pentanol) and 3-methyl-1-butanol (Isopentanol) production

2-methyl-1-butanol (2MB) and 3-methyl-1-butanol (3MB) were first isolated as by-products of yeast fermentation. They are normally used as apple or banana flavoring agents for wines. They are also used as chemical intermediates and solvents in pharmaceutical products [115]. These compounds are currently derived from the chlorination of pentane followed by hydrolysis or by the oxo process [115]. Due to depleting fossil resources, organisms that are capable of producing 2MB and 3MB by fermentation are being developed [20, 26].

Production of 2MB in *E. coli* begins with the synthesis of 2-keto-3-methylvalerate (KMV) from a combination of the threonine and isoleucine biosynthetic pathways (figure 1.9). KMV synthesis begins with the carboligation of pyruvate and 2-ketobutyrate catalyzed by acetohydroxyacid synthase (AHAS). To shift the carbon flux towards 2MB production, overexpression of the threonine operon (*thrABC*), the deletion of *metA* and *tdh* competing pathways upstream of threonine production and the disruption of leucine biosynthesis (*leuABCD* operon) proved beneficial for 2MB production [20, 24, 119].

Cann et al. [20] found that AHASII from *Salmonella typhimurium* (*ilvGM*) and a threonine deaminase encoded by *C. glutamicum* (*ilvA*) were more suitable for 2MB production than the enzymes from *E. coli*. The combinations of these approaches gave an *E. coli* strain that produced 1.25g/L 2MB in 24 hrs [20, 119].

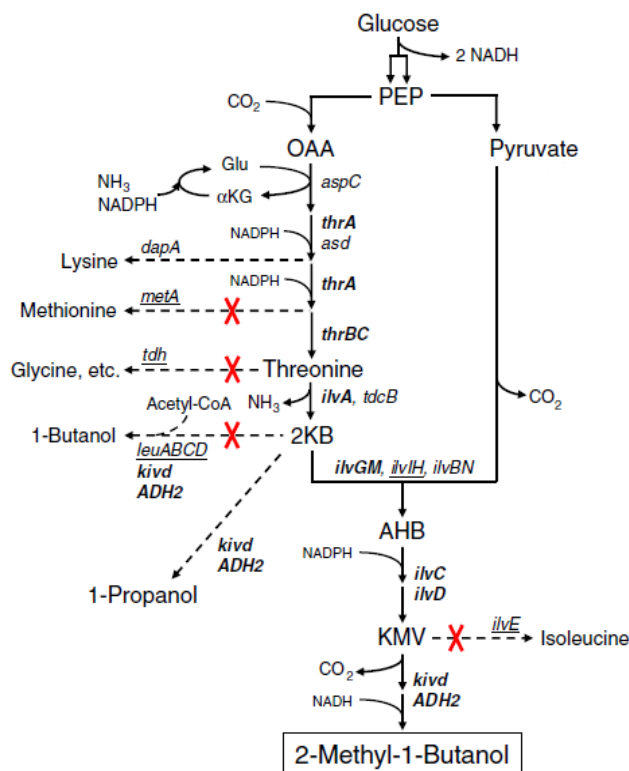


Figure 1.9: Pathway for 2-Methyl-1-butanol production.

Genes in bold were overexpressed while underlined genes are knocked out. PEP; phosphoenolpyruvate, OAA; oxaloacetic acid, α KG; α -keto-glutarate, 2KB; 2-ketobutyrate, AHB; 2-aceto-2-hydroxybutyrate, KMV; 2-keto-3-methylvalerate. Adapted from Cann et al. [20].

The 3-methyl-1-butanol (3MB) pathway makes use of the valine pathway for isobutanol production which generates the precursor 2-ketoisovalerate (KIV) and the leucine biosynthetic pathway (*leuABCD*), which converts KIV into 2-ketoisocaproate (KIC) with the addition of acetyl CoA [26]. 3MB and isobutanol compete for the same substrate KIV (figure 1.10). Initial production of 3MB was low due to feedback inhibition of isopropylmalate synthase by leucine. A leucine resistant mutant and additional deletion of *tyrB* and *ilvE* created a strain that produced 1.28g/L 3MB in 28 hrs [24, 26, 119]. To further increase 3MB yield, a mutagenesis approach that leverages selective pressure towards L-leucine

biosynthesis was employed [27]. Random mutagenesis of the previously engineered *E. coli* strain and selection with 4-aza-D, L-Leucine, a structural analogue of L-leucine resulted in a new strain able to produce 4.4g/L of 3MB. The production of 3MB in 4-aza-D, L-Leucine is limited by the toxicity of the alcohol. A two-phase fermentation system that involves continuously removing the 3MB from the aqueous cellular environment lead to a total 3MB titer of 9.5g/L after 60hrs [27].

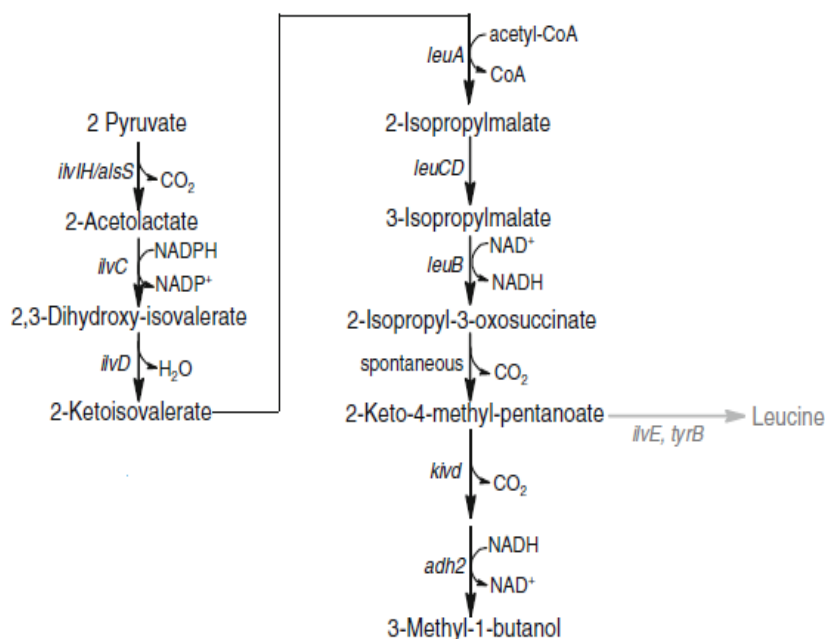


Figure 1.10: Pathway for 3-Methyl-1-butanol production in engineered *E. coli*

ilvH/alsS encodes acetolactate synthase; *ilvC* encodes acetohydroxy acid isomeroeductase; *ilvD* encodes dihydroxy acid dehydratase; *ilvE* encodes leucine transaminase; *tyrB* encodes leucine aminotransferase; *leuA* encodes 2-isopropylmalate synthase; *leuCD* encodes 2-isopropylmalate isomerase; *leuB* encodes 3-isopropylmalate dehydrogenase; *kivd* encodes ketoisovalerate decarboxylase; *adh2* encodes alcohol dehydrogenase. Adapted from Yan Y. and Liao J.C [119]

1.2.4.3 Other non-natural alcohols

The leucine biosynthetic pathway has been expanded to produce non-natural 5 to 8 carbon alcohols by engineering the chain elongation activity of 2-Isopropylmalate synthase (*leuA*) (figure 1.10) and the substrate chain length of 2-ketoacid decarboxylase [24, 120]. These modifications led to the production of 1-pentanol, 1-hexanol, 4-methyl-1-hexanol and 5-methyl-1-heptanol.

1.2.5 Isoprenoid-derived biofuels

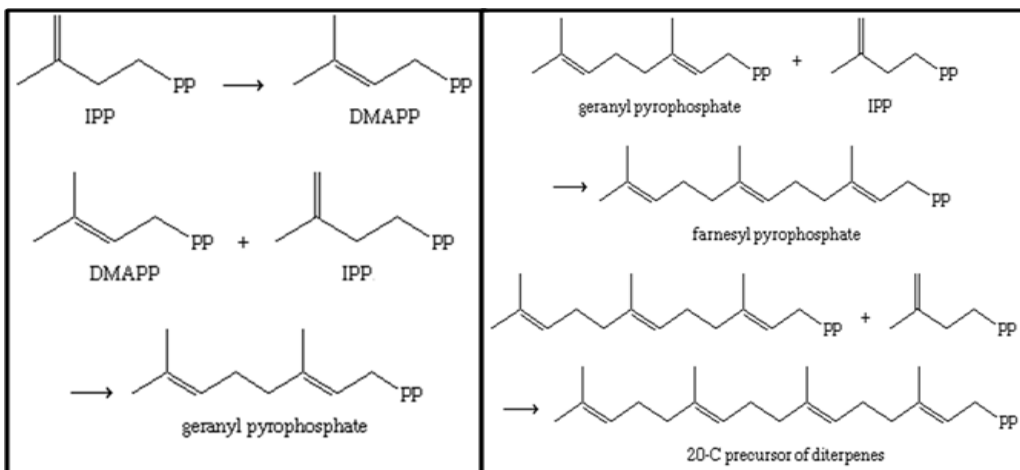
Isoprenoids are the oldest known biomolecules, encompassing over 30,000 compounds and serve numerous biochemical functions [67]. They are intermediates in sterol biosynthesis and have been produced naturally in plants, animals and bacteria for many years for their pharmaceutical and nutritional value [24]. Isoprenoids are synthesized from the 5-carbon isoprenoid units; isoprenyl pyrophosphate (IPP) and its isomer dimethylallyl pyrophosphate (DMAPP) [4, 24, 67]. These molecules are synthesized from glyceraldehyde-3-phosphate and pyruvate via the Methylerythritol pathway or from acetyl CoA via the mevalonate pathway [4, 90]. IPP and DMAPP can be conjugated together to form monoterpene (C10), sesquiterpene (C15), and diterpene precursors; geranyl pyrophosphates (GPP), farnesyl pyrophosphate (FPP) and geranylgeranyl pyrophosphate (GGPP) as shown in figure 1.11a [24, 90]. Isoprenoid alcohols and olefins can be synthesized from IPP, GPP, FPP or GGPP in a single step through the actions of phosphatases, pyrophosphatases and terpene synthases as shown in figure 1.11b [24, 90]. Because isoprenoids possess vast structural diversity,

including saturated, unsaturated, branched or cyclic alkenes or alkanes, their potential as fuel candidates, such as isopentenol (C5) for motor gasoline, isoprene as jet fuel and farnesene for diesel fuel is promising [28].

An *E. coli* strain engineered to overproduce isopentenol, a 5-carbon unsaturated alcohol has been reported [19]. Isopentenol can be produced by the dephosphorylation of the isoprenoid building blocks IPP and DMAPP (figure 1.11b). To produce isopentenol in *E. coli*, the isoprenyl biosynthetic pathway was combined with the overexpression of *nudF*, a pyrophosphatase-like enzyme from *Bacillus subtilis*. Isopentenol concentration of 110mg/L was achieved [4, 19, 28].

Farnesol and farnesene, which are derived from FPP, have been produced in *E. coli* and *S. cerevisiae* using a truncated yeast alkaline phosphatase *Pho8* lacking 62 amino acids from the N-terminus [90, 103] and a Norway spruce terpene synthase respectively [76, 90]. These sesquiterpenes are being developed as precursors to diesel fuels.

a)



b)

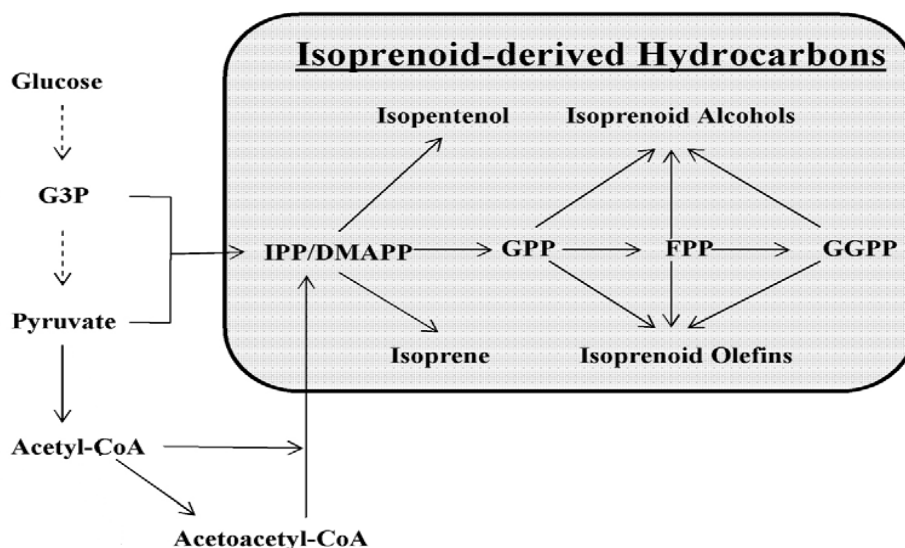


Figure 1.11: Isoprenoid-derived biofuels

a) Structures of different isoprenoids. b) Pathway for isoprenoid-derived hydrocarbons
G3P; glyceraldehyde-3-phosphate, CoA; coenzyme A, IPP; isopentenyl pyrophosphate, DMAPP; dimethylallyl pyrophosphate, FPP; farnesyl pyrophosphate, GPP; geranyl pyrophosphate, GGPP; geranylgeranyl pyrophosphate. Adapted from Rude et al. [90]. Used with permission.

1.2.6 Fatty-acid derived biofuels

The fatty acid biosynthetic pathways are of great importance to the production of biofuels. Fatty acid biosynthesis involves the condensation of two carbon units into a growing fatty acyl chain. It begins with the carboxylation of acetyl CoA to malonyl CoA. After the transacylation of the acetyl CoA and malonyl CoA to acyl carrier protein, acetyl-ACP and malonyl-ACP are condensed into acetoacetyl-ACP (figure 1.12). This molecule is then reduced, dehydrated and reduced a second time to form 2, 3, 4-saturated fatty acyl-ACP. In each subsequent elongation cycle, malonyl-ACP is condensed with the saturated fatty acyl-ACP to add 2 carbons. The branch from saturated to unsaturated pathway occurs when the chain length is ten carbon chain backbone. Due to variability in chain length and

degree of saturation, fatty acids can be converted into different potential biofuels (figure 1.12).

The esterification of fatty acyl-CoA with short-chain alcohols generates biodiesel. The fatty acyl-CoA can also be reduced to their corresponding aldehydes, which can in turn be decarbonylated to long-chain alkanes/alkenes or further reduced to fatty alcohols that can also be esterified to biodiesel with acetyl-CoA [119].

Biodiesel is a monalkyl ester of fatty acids. Biodiesel is currently made from plant oils through transesterification of triacylglycerols with short chain alcohols such as methanol and ethanol to form fatty acid methyl esters (FAMES) and fatty acid ethyl esters (FAEE) respectively [28, 91]. However, this process is not sustainable because transesterification requires high energy and cheap sources of vegetable oil are scarce [91]. There are three major investigations in biodiesel production: the use of lipase with whole cell biocatalysts technology, biodiesel production from microalgae and the use of metabolically engineered microorganisms [91].

The Microbial production of biodiesel has been approached from two angles: First, by producing short chain alcohols and performing the transesterification in vivo with exogenously added fatty acids and second, by producing free fatty acid that can be harvested for transesterification in vitro [28]. The in vivo production of biodiesel using endogenously produced ethanol has been reported [28]. The expression of the ethanol production pathway from *Zymomonas mobilis* along with a broad substrate range acyltransferase (*atfA*) from *Acinetobacter baylyi* in *E.*

E. coli lead to the production of FAEEs at a titer of 1.28g/L using glucose and oleic acid as substrates in fed batch fermentation [28, 119]. Recently, Steen et al. [104] engineered an *E. coli* strain that produced FAEEs from glucose. To do this, the ethanol production pathway from *Z. mobilis* (*pdh*, *adhB*) was overexpressed to produce ethanol for FAEE production. By combining this pathway with a cytosolic version of an endogenous thioesterase (*tesA*) and an ester synthase from *A. baylyi* (*atfA*), a fatty acid oxidation deficient strain of *E. coli* (Δ *fadE*) was able to produce 37mg/L of FAEE directly from glucose [28, 104]. To increase the production of FAEE, two CoA ligases, *fadD* from *E. coli* and *FAA2* from *S. cerevisiae*, were overexpressed along with another copy of *atfA* to bring production of FAEE up to 674 mg/L.

Overexpressing a fatty acyl-CoA reductase encoded by *acr1* from *Acinetobacter calcoaceticus* BD413 resulted in the production of medium chain fatty alcohols up to ~60mg/L [104].

Schirmer et al [93] engineered the alkane biosynthesis pathway from cyanobacteria in *E. coli* by overexpressing a fatty aldehyde-generating acyl-ACP reductase from *Synechooccus elongatus* PCC7942_orf1594 and a cocktail of fatty aldehyde decarbonylases from *Nostoc punctiforme* PCC73102, *Thermosynechococcus elongatus* BP-1, *Synechococcus* sp. Ja-3-3Ab, *Prochlorococcus marinus* MIT9313, *Prochlorococcus marinus* NATL2A, and *Synechococcus* sp. RS9117 [93]. The *E. coli* strain produced a variety of hydrocarbons ranging from tridecane to heptadecene depending on cyanobacteria species from which the decarbonylase was sourced.

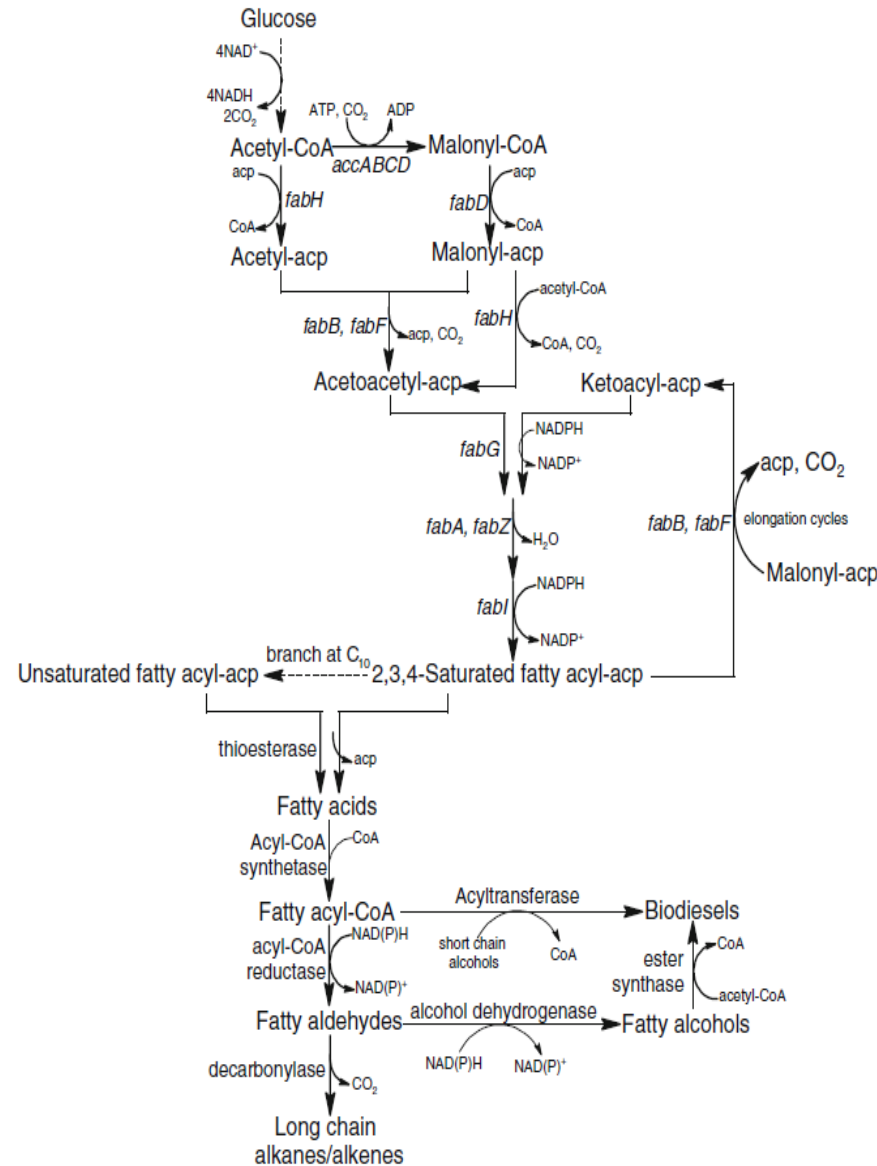


Figure 1.12: Schematic illustration of fatty acid pathway for biodiesel and long-chain alkanes/alkenes production.

The dashed line indicates omitted steps. *acp* means acyl carrier protein; *accABCD* encodes acetyl-CoA carboxylase; *fabD* encodes malonyl-CoA-ACP transacylase; *fabH* encodes ketoacyl-ACP synthase III; *fabB* encodes ketoacyl-ACP synthase I; *fabF* encodes ketoacyl-ACP synthase II; *fabG* encodes ketoacyl-ACP reductase; *fabA* encodes hydroxydecanoyl-ACP dehydratase; *fabZ* encodes hydroxyacyl-ACP dehydratase; *fabI* encodes enoyl-ACP reductase. The acyl-CoA synthetase is an acyl-coA ligase *fadA* from *E. coli* and *FAA* gene from *S. cerevisiae*. The ester synthase could be the *AtfA* gene from *Acinetobacter baylyi*. Acyl-CoA reductase is *acrI* gene from *Acinetobacter calcoaceticus* or the fatty aldehyde-generating acyl-ACP reductase from *Synechooccus elongatus* PCC7942_orf1594. The decarbonylase can be sourced from different species of cyanobacteria. Adapted from Yan, Y. and Liao J.C. [119], Steen et al.[104] and Schirmer et al. [93].

1.3 Alcohol cytotoxicity

One of the greatest challenges to large-scale microbial production of alcohols is cytotoxicity. The effects of ethanol on *E. coli* and 1-butanol on *Clostridium acetobutylicum* are well documented [17]. In general, the cytotoxicity of these alcohols has been attributed to membrane disruption, which is thought to occur by direct insertion of lipophilic side chain into the cellular membrane [17]. In *C. acetobutylicum*, butanol is believed to interact with the cell thereby altering the fluidity of the membrane, decreasing the intracellular pH and ATP concentration and inhibiting the uptake of glucose [8]. In *E. coli*, isobutanol causes similar effects, with growth retardation at 8g/L although production continued up to 20g/L [8].

The effect of stress caused by ethanol, 1-butanol and isobutanol on *E. coli* was recently studied by Brynildsen M. P and Liao J.C [17] using genomic analysis. This study reveals that the isobutanol stress response is qualitatively similar to that of 1-butanol with respect to the transcriptional levels except for increased repression of amino acid biosynthesis by 1-butanol [8, 17]. The response to ethanol however differs significantly from that to 1-butanol and isobutanol. This difference was attributed to the regulation of genes responsible for membrane potential management. These results indicated that the cytotoxicity of longer chain alcohols is unlike ethanol cytotoxicity despite the fact that all three alcohols commonly disrupt the cell membrane.

Atsumi et al. [8] used a sequential transfer method in which the isobutanol concentration in the growth media was increased after every 15 transfers to evolve

a strain of *E. coli* that was tolerant to increased levels of isobutanol. In another study to mitigate the effect of cytotoxicity of isobutanol during fermentation using engineered *E. coli*, Baez et al [10], continuously removed the isobutanol formed using gas stripping. Gas stripping is a simple and efficient way to recover solvent from fermentation broths. With this technique, the isobutanol titer reached 50g/L after 72 hours, an indication that in situ product removal can effectively overcome isobutanol toxicity in *E. coli*.

1.4 Research objectives

The aim of this research project was to manipulate carbon and amino acid metabolism in yeast and assemble novel metabolic pathways that would allow the synthesis of higher alcohol biofuels particularly isobutanol from carbohydrate precursors.

This research comprises of the following key parts:

- Manipulate the Ehrlich pathway for amino acid degradation for production of higher alcohols
- Determine the optimal alcohol dehydrogenase activity for conversion of 2-keto aldehydes to alcohols
- Engineer the valine biosynthetic pathway for efficient production of alcohols from pyruvate by overexpression of valine biosynthesis and the Ehrlich pathway genes
- Evaluate how the competing reaction in the isobutanol pathway impact on alcohol production

Chapter Two: Materials and Methods

2.1 General methods

2.1.1 Reagents

Restriction enzymes used in this study were either from New England Biolabs (Ipswich, MA, USA) or Invitrogen (Carlsbad, CA USA). Taq and Vent DNA polymerases were from New England Biolabs. PGEM-T vector system for PCR cloning was from Promega (Madison, WI USA). Oligonucleotides were synthesized by Integrated DNA Technologies (Coralville IA, USA).

2.1.2 Growth and culture conditions

Luria Broth (LB) media for bacterial growth consisted of 1% tryptone, 0.5% Yeast Extract, 1% NaCl and 1.5% Agar for plates. Components for growth media were purchased from Fisher Scientific (Fair Lawn New Jersey). Ampicillin, Xgal and Isopropyl β -D-1-thiogalactopyranoside (IPTG) were added to a final concentration of 100 μ g/mL, 20mg/mL and 0.1mM respectively. Yeast strains were routinely propagated in rich YEP (1% Yeast Extract, 2% Peptone, 30mg/L adenine sulphate and 30mg/mL tryptophan, supplemented with 2% Sugar (usually one of dextrose, galactose or raffinose). Selective media lacking uracil and/or one or more amino acids consisted of 1.6g/L Difco Yeast Nitrogen Base (Becton, Dickson and Co.), 5g/L ammonium sulphate, 2% sugar (unless otherwise stated), 15g/L agar (for plates) and 2g/L amino acid drop-out mixtures. Drop-out mixtures typically contained 0.5g adenine sulphate, 2g uracil, 4g leucine and 2g of every

other amino acid as required. Sporulation media consisted of 1% Potassium acetate and 1.5% agar. 5-Fluoro-orotic acid (5-FOA) plates consists of 15g/L agar, 1.7g/L Yeast Nitrogen Base, 5g/L ammonium sulphate, 20mg/L of each of adenine sulphate, tryptophan, leucine, histidine, arginine and any other amino acids, 2% glucose, 35mg/L uracil, and 1g/L 5-FOA. The amino acid-enriched media typically consisted of 10g/L of the enriched amino acids, 10g/L raffinose, 1.8g/L Yeast Nitrogen Base and 10mg/L of each of adenine, histidine and tryptophan.

2.1.3 Transformation of *S. cerevisiae*

50mL cultures of cells were grown at 30°C overnight in rich or selective medium. The cells were diluted into fresh medium and allowed to grow to $OD_{600} = 0.5$. Cells were recovered using Beckman CPR centrifuge at 3000 rpm for 1 minute. The supernatant was discarded and the cell pellet were then washed in 50mL of sterile water and recovered by centrifugation. The pellet were resuspended in 1mL LiAc solution (10mM Tris-HCl pH 8.0 and 0.1M LiAc) and incubated with gentle agitation for 10-15minutes at 30°C or room temperature. 5µL of 10mg/mL of Salmon Sperm DNA and 1-5µg of plasmid DNA was added to 100µL of the cell suspension and incubated at room temperature for 5 minutes. 280µL Polyethylene Glycol (PEG) solution (50% PEG 4000 in 0.1M LiAc pH 8.0) was added to the cell and DNA mixture and mixed by inverting the tube several times. This was incubated at 30°C for 1-4 hours. 43µl of DMSO was added to the mixture and mixed by inverting several times and heat-shocked at 42°C for 5 minutes. After heat-shock, cells were recovered by centrifugation using an Eppendorf centrifuge

5415C at full speed for 1 minute. The PEG solution was aspirated and the cell pellet was washed with 1mL of sterile water. The water was aspirated and the cells resuspended in 60µL of sterile water and spread onto selective plates. The plates were incubated at 30°C until colonies began to appear.

2.1.4 *E. coli* transformation

Competent cells were made as previously described by Inoue et al. [56] and frozen. 0.5-1µg of plasmid DNA was added to 50µl of thawed cells. The cell and DNA mixture was incubated on ice for 15 minutes and heat-shocked for 45seconds at 42°C. After heat-shock, the cell/DNA mixture was immediately transferred to ice for additional 10 minutes. 1mL of LB was added to the reaction mixture and this was incubated at 37°C for 1 hour. After incubation the mixture was centrifuged using an Eppendorf centrifuge 5415C at full speed for 1 minute. Some of the LB was discarded and the pellet was resuspended in the remainder of the media and spread to the appropriate selective media.

2.1.5 DNA extraction and purification

Yeast genomic DNA was extracted from 10-30mL of log phase yeast culture. Cells were harvested using Beckman CPR Centrifuge at 3000rpm for 1 minute. The pellet was then resuspended in 400µL of “Crush” buffer (50mM Tris-HCl, 50mM EDTA and 1% SDS). 0.5mm glass beads (Biospec products Inc.) were added to meniscus of the sample. The mixture was vortexed for 15 minutes at 4°C or 5X for 2 minutes each at room temperature with 1 minute on ice between bursts. The lysate was transferred to a new microtube and extracted with equal

volume of buffered phenol and chloroform. 40 μ l of 3M Sodium Acetate (NaOAc) and 2 volumes of isopropanol were added to the extract and allowed to precipitate on ice for 30 minutes. This was followed by centrifugation using an Eppendorf centrifuge 5415C for 20 minutes at full speed. The DNA pellet was washed with 70% ethanol and centrifuged again at full speed for 10 minutes. The pellet was allowed to air dry and then resuspended in 50 μ L of TE buffer or water with 5 μ l of 10mg/mL RNase A per 50 μ L of buffer and incubated at 37°C for 15 minutes.

Plasmid DNA was extracted with Qiagen QIAprep Spin miniprep kits as directed by the manufacturer. DNA extracted from agarose after electrophoresis was purified by Qiagen QIAquick gel extraction kits as directed by the manufacturer. PCR-DNA purification was done with Qiagen QIAquick PCR purification kits as directed by the manufacturer.

2.1.6 DNA modification

All restriction enzyme digestions were carried out as specified by the manufacturers. Typically, a 20 μ L reaction consisted of 5 μ L of miniprep plasmid DNA, 1X recommended buffer and 1 unit of restriction enzyme. DNA ligations were performed using 1 μ L T4 DNA ligase (New England Biolabs (NEB)) at room temperature for at least 1 hour or overnight at 16°C.

2.1.7 Polymerase chain reaction

Polymerase Chain Reaction was performed using either Taq or Vent DNA polymerase (NEB). A 100 μ L reaction typically contained 1X NEB thermopol reaction buffer, 1 unit of polymerase enzyme, 2mM dNTPs, 1 μ mol of primers and

1µl genomic DNA template or 1µL of miniprep plasmids. Typical reaction conditions were 30cycles; 1 minute at 95°C for denaturation, 1 minute at a variant annealing temperature (usually around 55°C) and variant time at 72°C for extension.

2.1.8 DNA sequencing

DNA sequencing was done at the Applied Genomics Centre at the University of Alberta. Primer concentration of 3.2pmol/µl and plasmid template concentration of 15-22.5ng/µl were used.

2.1.9 Agarose Gel Electrophoresis

DNA samples were electrophoresed through 0.7% agarose prepared by melting electrophoresis grade agarose in the microwave in 1X TAE buffer (4.84g/L Tris base, 1.14g/L glacial acetic acid and 1mM EDTA pH 8.0) 0.5mg/ml Ethidium bromide was added to the melted agarose. Gels were electrophoresed in 1X TAE buffer at 100V.

2.2 Strain and plasmid construction

2.2.1 Oligonucleotide design

Oligonucleotides were designed with the help of DNA strider 1.2.1 software program and synthesized by Integrated DNA Technologies (Coralville IA USA). All oligonucleotides used in this study are listed in Table 1.

Table 1: List of oligonucleotides used in this study

| Primer name | Sequence (5' → 3') |
|-------------|--|
| Bba 1 | AATTCCGTGCGGCCGCATCGTCTAGAAGCTCGATTAT |
| Bba 2 | TCGACATAATCGAGCTTCTAGACGATGCGGCCGCACG |
| Bba 3 | TCGAGTCGATTATTTGCATGACTAGTGAGCGCGGCCGCAATCTGCAGAG |
| Bba 4 | AGCTCTCTGCAGATTGGCGGCCGCGCTCACTAGTCATGCAAATAATCGAC |
| PGK750X | CACGTTCTAGAACGCACAGATATTATAACATCTG |
| PGK750S | CAGGTAAGTGTGTTTTATATTTGTTGTAAAAAGTAG |
| HXT400X | CACGTTCTAGACCACTACTTCTCGTAGGAAC |
| HXT400S | CAGGTAAGTGTGTTTTGATTAATAAATAAAAAACTTTTT |
| PDC800X | CACGTTCTAGACATGCGACTGGGTGAGCAT |
| PDC800S | CAGGTAAGTGTGTTTTGATTGATTTGACTGTGTTATT |
| PYK1000X | CACGTTCTAGAAATGCTACTATTTTGGAGATTAAT |
| PYK1000S | CAGGTAAGTGTGATGATGTTTTATTGTTTTG |
| TEF450X | CACGTTCTAGAATCACACCCAATCCCCAC |
| TEF450S | CAGGTAAGTGTGTAATTAATACTTAGATTAGATT |
| FBA830X | CACGTTCTAGAAGTTGATGGATCCAAGTGGC |
| FBA830S | CAGGTAAGTGTGTAATATGTATTACTTGGTTATG |
| ILV2-5' | CCGACGCCTAGGATGATCAGACAATCTACGCTA |
| ILV2-3' | CCAGCGCTGCAGGCGGCCGCGCTAGCACTTGAATTGAACTTATTATTCAT |
| ILV2in-5' | TTACCAAAGGATGTTACAGCAGC |
| ILV2in-3' | CAGTAGCACAAACCGTGCATAC |
| ILV2scrA | CCACCAGTTAAACCGACGAAAG |
| FBA1scr | AACAAGTGCACGTAACCAATG |
| ILV3-5' | CCGACGCCTAGGATGGGCTTGTTAACGAAAGTT |
| ILV3-3' | CCAGCGCTGCAGGCGGCCGCGCTAGCTAATTTCTAGATTATAATTAAGG |
| ILV5-5' | CCGACGTCTAGAATGTTGAGAACTCAAGCCGCC |
| ILV5-3' | CCAGCGCTGCAGGCGGCCGCACTAGTCATTGAATCATAATAAATATGTAA |
| ILV6-5' | CCGACGTCTAGAATGCTGAGATCGTTATTGCAAAGC |
| ILV6-3' | CCAGCGCTGCAGGCGGCCGCACTAGTGTGTCTTTAACCTTTTTATCT |
| ADH7-5' | CCGACGTCTAGAATGCTTTACCCAGAAAAATTTTCAGGGC |
| ADH7-3' | CCAGCGCTGCAGGCGGCCGCTAGGATCAAAATTTCCCTTAAGTTAAG |
| ADH7-myc | CTGCAGCTACTAACTAGTCTAAAGGT |
| ADHA-5' | GAGCTCTCTAGAATGAAAGCTGCCGTCGTTAGA |
| ADHA-myc | GGTACCCTGCAGTTAAAGGTCCTCCTCAGAGATTAATTTCTGTTACCTTTTGTGAAGTCTAT |
| YQHD-5' | CCGACGTCTAGAATGACCACCTTTAA |
| YQHD-3' | GTCGGCTGCAGGGGGCCGCACTAG T |
| KDCA-5' | CCGACGTCTAGAATGTATACCGTTGGTACTATTTG |
| KDCA-3' | CCAGCGCTGCAGGCGGCCGCGCTAGCTTAGGCATAGTCTGGGACGTC |
| M13F | GTTTTCCCAGTCACGAC |
| M13R | AACAGCTATGACCATG |
| AMSS-5' | CTAGTATGCTTTCACTACGTCAATCTATAAGATTTTTCAAGCCAGCCACAA GAACTTTGTCTAGATATCTGCTTGGCTAGCCTGCA |
| AMSS-3' | GGCTAGCAAGCAGATATCTAGAGCTACACAAAGTTCTTGTGGCTGGCTTG |

| | |
|-----------|---|
| | AAAAATCTTATAGATTGACGTAGTGAAAGCATA |
| MSS-5' | GATCCATGCTTTCACTACGTCAATCTATAAGATTTTTCAAGCCAGCCACAA GAACTTTGTGTAGCTCTAGATATCTGCTTGGTAC |
| MSS-3' | CAA GCA GAT ATC TAG AGC TAC ACA AAG TTC TTG TGG CTG GCT TGA AAA ATC TTA TAG ATT GAC GTA GTG GTG AAA GCA TG |
| PDCseq | ATT TCT TGT CAT ATT CCT TTC |
| GALF | GGG TAA TTA ATC AGC GAA GCG |
| LEU4D-5' | GGATTCTCACACTAGAAGTTTACTGT |
| LEU4D-3' | GTAAATAAATAAGTATAGAAATAAATA |
| LEU9KO-5' | TTATAAGGGTCTTCTCCTTAGGATAATACTATCGGCACATTATCATTAGC CGCGTAGCCACG ATT TAG GTG ACA CTA TAG |
| LEU9KO-3' | CATTTATAAATAAAAATACATATATATAAACATGAGTAATCATAAGCTAC TCCTTTCTAATTCATTAATGC AGGTTAACC |
| BAT1KO-5' | TTCGTTAGAATAAATCACCCATAAAC |
| BAT1KO-3' | AGTTCAAGTCGGCAACAGTTTTTGCAG |
| BAT1i 5' | TTTGAAAGCCTACAGAACTCC |
| BAT1i 3' | TTACCATAATTGACTCTCCG |
| BAT1e 5' | GAATGATCTTACTGATAGAGG |
| BAT1 e 3' | AAGTCCAGCGAGATACCTTGG |
| LEU4Dscr | GACCAGTAAAAAGAACTTACG |
| KANFscr | CCTCGACATCATCTGCCC |
| LEU9scr | CCTTACTTTACTCCACGAAAT C |
| LoxPscr | TAAGGGTTGTGACCTGCAG |
| ADHt-5' | GGATCTAGAGCGAATTTCTTATGATTT |
| ADHt-3' | GGACTGCAGGCGGCCGCACTAGTAG |
| HXTt-5' | GGATCTAGAACTAAACAAGCTCAATA |
| HXTt-3' | GGACTGCAGGCGGCCGCACTAGTAA |
| CYct-5' | GGATCTAGAACAGGCCCTTTTCCTT |
| CYct-3' | GGACTGCAGGCGGCCGCACTAGTAT |
| MYCBBB | GGCGGCCGCACTAGTTTAATTCAAGT |
| MYCBBT | CTAGAGAGCAAAAGCTCATTCTGAA |
| MYCscr | ACTAGTTTAATTCAAGTCCTC |
| XAx | CTAGTTTCCTAGGCTGG |
| XAE | AATTCCAGCCTAGGAAA |

2.2.2 Construction of biobrick vectors with yeast promoters

The biobrick vectors with different yeast promoters were constructed by Kwesi Kutin; a former technician in the lab. To construct these plasmids, YEplac195 plasmid originally from Gietz, R. D. and Sugino, A. [47] was digested with

EcoR1 and Sal1. The Bba1 and Bba2 oligonucleotides (see table 1) were hybridized. The duplex oligonucleotide sequence was then ligated into the digested vector. This created EcoR1-Not1-XbaI-Sal1 sites in the plasmid. Similarly, the new plasmid created was cut with Sal1 and HindIII, Bba3 and Bba4 oligonucleotides hybridized to form a duplex oligonucleotide sequence with Xho-Spe1-Not1-PstI-Hind III sites was ligated into digested plasmid. The resulting vector has EcoR1-Not1-Xba1----Spe1-Not1-Pst1 sites which is compatible for biobrick-style assembly.

To create biobrick vectors with yeast promoters, the following oligonucleotide pairs; PGK700X/PGK700S, PYK1000X/PYK1000S, TEF450X/TEF450S, HXT400X/HXT400S, FBA830X/FBA830S and PDC800X/PDC800S, were used to amplify the *PGK1*, *PYK1*, *TEF1*, *HXT7*, *FBA1* and *PDC1* promoters from *S. cerevisiae* strain W303 respectively. The PCR products were digested with Xba1 and Spe1 and ligated into the biobrick vectors digested with Xba1 and Pst1.

2.2.3 Construction of *ILV* plasmids

ILV2, *ILV3*, *ILV5* and *ILV6* genes were amplified using *ILV2* *ILV3*, *ILV5* and *ILV6* 5' and 3' oligonucleotides respectively (see table 1). This created PCR fragments with the restriction sites shown in figure 2.1. *ILV2* and *ILV3* have internal Xba1 sites and cannot be excised as Xba1 and Pst1 fragment from the YEplac 195 biobrick plasmids during sequential assembly of all the genes into a single plasmid. To get around this, a short nucleotide sequence designated as XAxb and XAE (see table 1) were hybridized and ligated into the XbaI cut vector

to destroy the Xba1 site thereby creating an AvrII site in the YEplac195 biobrick plasmids containing the *FBA1* and *HXT7* promoters. The YEplac195 biobrick plasmids containing the yeast promoters were digested with Spe1 and Pst1 and the *ILV* genes were ligated into them to place each *ILV* gene under the regulation of a different yeast promoter. For the purpose of this thesis, the YEplac195 plasmids harboring the *ILV* genes each under the regulation of different yeast promoters are called: *FBA1-ILV2*, *HXT1-ILV3*, *PGK1-ILV5* and *PDC1-ILV6* (see table 2).

The YIp-FBA1-ILV2 integrating plasmid was constructed by cutting *FBA1-ILV2* plasmid with AvrII and Pst1, the fragment was ligated into a YIplac204 vector (Gietz, R. D. and Sugino, A. [47]) digested with Xba1 and Pst1. The resulting vector was then cut within the *TRP1* gene with EcoRV to direct integration of the plasmid into the endogenous *TRP1* gene.

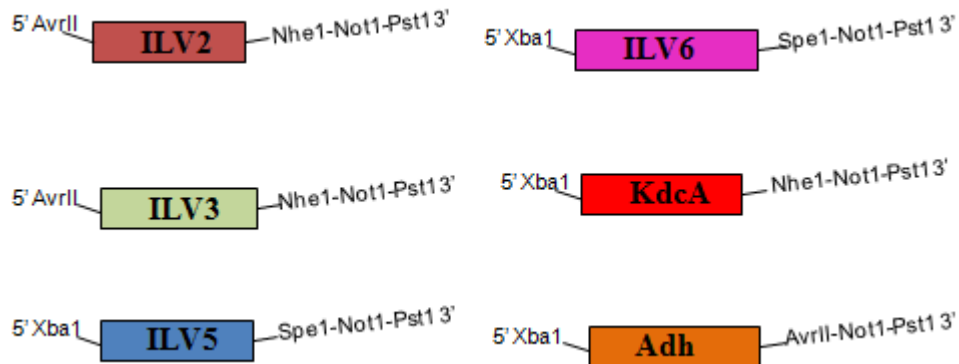


Figure 2.1: PCR fragments with 5' and 3' restriction sites.

2.2.4 Construction MYC-tagged alcohol dehydrogenase (ADH) plasmids

ADH7 was amplified from the yeast genomic DNA using the ADH7 5' and ADH7myc oligonucleotides (see table 1) and cloned into the biobrick vector with the *TEF1* promoter. This plasmid is called TEF1-ADH7myc

A plasmid (pMA-T-ADHA) containing a synthetic *Lactococcus lactis adhA* codon-optimized for expression in *S. cerevisiae* was synthesized by Mr Gene Inc. The *adhA* gene was amplified from the pMA-T-ADHA plasmid using ADHA5' and ADHAMyc oligonucleotides. The PCR product was digested with Xba1 and Pst1 and ligated into the TEF1 biobrick vector. Finally the TEF1-AdhA plasmid was digested with Spe1 and Pst1 and the *CYC1* yeast termination sequence (this was amplified from the yeast genomic DNA using CYCt 5' and 3' oligonucleotides see table 1) was ligated into it. This plasmid is designated as TEF1-ADHAMyc.

The *E. coli yqhD* was amplified from *E. coli* DH5 α strain using YQHD 5' and 3' oligonucleotides (see table 1) and ligated into the TEF1 biobrick plasmid. The MYC-tag oligonucleotides (MYC BBT and MYC BBB) were hybridized and ligated into a TEF1-YqhD plasmid digested with Spe1 and Pst1. This created TEF1-YqhDmyc. Lastly, TEF1-YqhDmyc was digested with Spe1 and Pst1 and a *CYC1* yeast termination sequence was added to it as described above.

An additional plasmid designed as TEF1-MSS-YqhD was also constructed. The yeast *COX4* signal sequence (hybridized AMSS5' and AMSS 3' oligonucleotides) was ligated as an Spe1 and Pst1 fragment in the TEF1 plasmid. The resulting

plasmid was cut open with NheI and PstI and a *yqhD* PCR fragment was ligated into it to give TEF1-MSS-YqhD plasmid.

2.2.5 Construction of HA-tagged 2-keto acid decarboxylase (*kdcA*) plasmid

A synthetic *kdcA* gene from *L. lactis* codon-optimized for expression in *S. cerevisiae* and harboring a HA-epitope tag (pMK-RQ-KdcA see table 2) was synthesized by Mr. GENE Inc. The gene was excised as KpnI and BamHI fragment and ligated into YCplac111-GAL plasmid.

KdcA was also ligated into a YEplac195 and pRS303 plasmids (see table 2). Firstly, *kdcA* was amplified with KDCA 5' and 3' oligonucleotides using the synthetic pMK-RQ-KdcA plasmid as template. This was then ligated into a YEplac195 biobrick vector containing *PYK1* yeast promoter. To clone *kdcA* to the pRS303 plasmid, YEplac-PYK1-KdcA plasmid was digested with EcoRI and NheI and was then ligated into a pRS303 plasmid digested with EcoRI and SpeI.

Table 2: List of plasmids used in this study

| Plasmid Name | Relevant Characteristics | Reference |
|---------------------|--|------------------|
| pGEM-T | Amp ^R | Promega |
| FBA1-ILV2 | <i>P_{FBA1}-ILV2</i> , <i>URA3</i> marker, Amp ^R | [47], this study |
| HXT7-ILV3 | <i>P_{HXT7}-ILV3</i> , <i>URA3</i> marker, Amp ^R | [47], this study |
| PGK1-ILV5 | <i>P_{PGK1}-ILV5</i> , <i>URA3</i> marker, Amp ^R | [47], this study |
| PDC1-ILV6 | <i>P_{PDC1}-ILV6</i> , <i>URA3</i> marker, Amp ^R | [47], this study |
| TEF1-ADH7myc | <i>P_{TEF1}-ADH7</i> , <i>URA3</i> marker, <i>MYC</i> tag, Amp ^R | [47], this study |
| TEF1-AdhAmyc | <i>P_{TEF1}-adhA</i> , <i>URA3</i> marker, <i>MYC</i> tag, Amp ^R | [47], this study |
| TEF1-YqhDmyc | <i>P_{TEF1}-yqhD</i> , <i>URA3</i> marker, <i>MYC</i> tag, Amp ^R | [47], this study |
| pMA-T-AdhA | Amp ^R | Mr. GENE |
| TEF1-MSS-YqhD | <i>P_{TEF1}-yqhD</i> , <i>COX4</i> signal sequence, <i>URA3</i> marker, Amp ^R | [47], this study |
| YIp-FBA1-ILV2 | <i>P_{FBA1}-ILV2</i> , <i>TRP1</i> marker, Amp ^R | [47], this study |
| YIplac204 | <i>TRP1</i> marker, Amp ^R | [47] |
| YCplac111-GAL | <i>P_{GAL}</i> , <i>LEU2</i> Marker, Amp ^R | [47], this study |
| YCplac-GAL-KdcA | <i>P_{GAL}-kdcA</i> , <i>LEU2</i> Marker, Amp ^R | [47], this study |
| YCplac-GAL-MSS-KdcA | <i>P_{GAL}-kdcA</i> , <i>LEU2</i> Marker, <i>COX4</i> Signal sequence, Amp ^R | [47], this study |
| YEplac-GAL-MSS-KdcA | <i>P_{GAL}-kdcA</i> , <i>TRP1</i> Marker, <i>COX4</i> Signal sequence, Amp ^R | [47], this study |
| PRS-PYK1-KdcA | <i>P_{PYK1}-kdcA</i> , <i>HIS3</i> marker, Amp ^R | [98], this study |
| YEplac-PYK1-KdcA | <i>P_{PYK1}-kdcA</i> , <i>URA3</i> marker, Amp ^R | [47], this study |
| pMK-RQ-KdcA | kan ^R | Mr. GENE |
| pRS303 | <i>HIS3</i> marker, Amp ^R | [98] |
| ILV array-Adh7 | <i>P_{FBA1}-ILV2</i> , <i>P_{HXT7}-ILV3</i> , <i>P_{PGK1}-ILV5</i> , <i>P_{PDC1}-ILV6</i> , <i>P_{TEF1}-ADH7</i> , <i>URA3</i> marker, Amp ^R | This study |
| ILV array-MSS-YqhD | <i>P_{FBA1}-ILV2</i> , <i>P_{HXT7}-ILV3</i> , <i>P_{PGK1}-ILV5</i> , <i>P_{PDC1}-ILV6</i> , <i>P_{TEF1}-yqhD</i> , <i>URA3</i> marker, <i>COX4</i> signal sequence, Amp ^R | This study |

2.2.6 Assembly of *ILV* gene array

Figure 2.2 shows the sequential assembly of the *ILV* genes and ADHs into a single multiple copy plasmid.

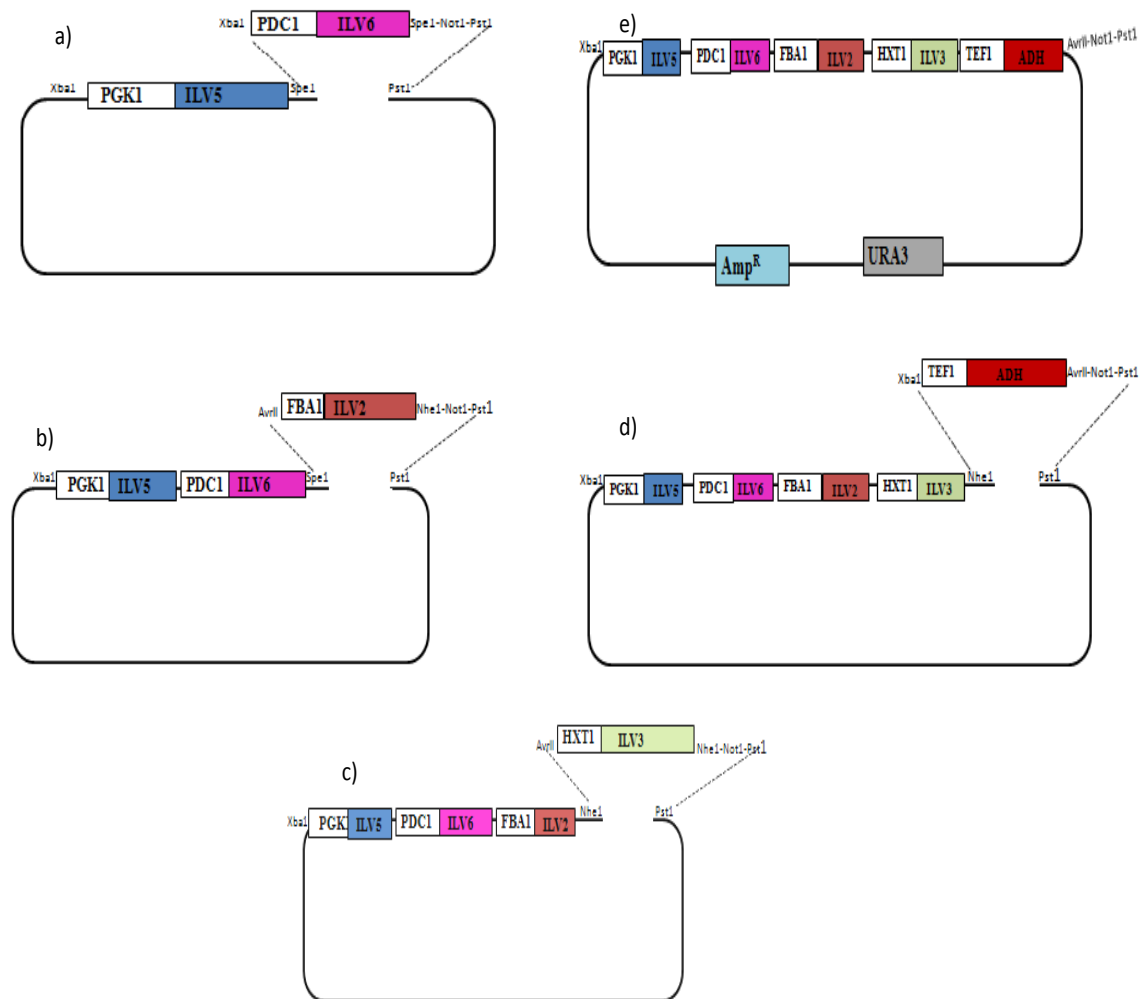


Figure 2.2: Assembly of *ILV* gene array

a) P_{PDC1} -*ILV6* was excise as *Xba*I and *Pst*I fragment and ligated into an *Spe*I and *Pst*I cut *PGK1-ILV5* plasmid b) P_{FBA1} -*ILV2* was excised from *FBA1-ILV2* plasmid as *Avr*II and *Pst*I fragment and ligated in an *Spe*I and *Pst*I cut plasmid from step a. c) P_{HXT1} -*ILV3* was excised as *Avr*II and *Pst*I fragment from P_{HXT1} -*ILV3* plasmid and ligated into the plasmid from step b. d) P_{TEF1} -*ADH* was excised from the biobrick vector as *Xba*I and *Pst*I fragment and cloned into an *Nhe*I and *Pst*I digested plasmid from step c. e) Assembled array of genes for isobutanol production in a multicopy plasmid under the regulation different yeast promoters.

2.2.7 Construction of *leu4::kan^R*, *leu4::kan^R leu9::loxP*, *bat1::loxP*, and *leu4::kan^R leu9::loxP bat1::loxP* strains

The LEU4D 5' and 3' oligonucleotides were used to amplify a Kanamycin resistance cassette from KanMX6 template [113]. The PCR product was then used to transform *S. cerevisiae* strain W303 and transformants were selected on YEPD plates containing 200µg/mL G418. Correct deletions were confirmed by PCR using LEU4Dscr and KANFscr oligonucleotides. These oligonucleotides bind 5' upstream of the *LEU4* gene and within the promoter of the *kan^R* gene respectively. Similarly, LEU9KO 5' and 3' oligonucleotides were used to amplify *Schizosaccharomyces pombe HIS5* gene that complements the *Saccharomyces cerevisiae his3* mutation from the pUG27 plasmid template [48]. Due to the flanking *loxP* sites the deletion marker can be removed by expressing *cre* recombinase. The product was used to transform the *leu4::kan^R* strain. The *HIS5⁺* transformants were selected on –His + Dex plates. Correct deletions were confirmed by PCR using LEU9scr and LoxPscr oligonucleotides. LEU9scr primes 5'upstream of the *LEU9* gene and LoxPscr hybridizes the LoxP site and allows synthesis upstream away from *HIS5* gene and to the 5' end of the gene being replaced.

To recycle the *HIS5* gene so that it could be used for further deletions, the *leu4::kan^R leu9::HIS5* strain was transformed with *GAL-Cre1* recombinase plasmid and plated on –URA + Dex plates. The recombinase loops out the *HIS5* gene from the chromosome leaving behind a LoxP site. *URA3⁺ leu4::kan^R leu9::HIS5* mutants harboring the *GAL-Cre1* plasmid were grown in –URA +

raffinose media overnight at 30°C. The cells were diluted to an OD₆₀₀ of 0.5 and the *GAL*-promoter was induced by the addition of galactose to a final concentration of 2% to allow the expression of the recombinase. The culture was incubated at 30°C for 2 hours. After 2 hours, 100µL of culture was transferred to 3ml of YEPD. A series of 10-fold dilutions 1:10, 1:100, 1:1000, 1:10000 were made and 100µL of each of the dilutions were spread on YEPD plates. Once colonies appeared, they were replica plated to –His + Dex plates. The YEPD and –His plates were marked carefully for identification and orientation. Once colonies begin to appear, colonies that grew on YEPD but not on –His plates were picked. These colonies were then streaked to –HIS plate to confirm that they did not grow on this medium. The *His*[–] cells were streaked to a 5-FOA plate. This medium kills *URA3*⁺ cells and so cells that had lost the *GAL-Cre1* plasmid were able to grow. Finally, several colonies from the 5-FOA plate were streaked to YEPD and to –URA + Dex plates. The colonies that showed no growth on medium lacking uracil were selected. These colonies had *leu4::kan^R leu9::loxP* deletions.

The *BAT1* gene was deleted using a similar strategy described above. Firstly, the *HIS5* gene was amplified from a pUG27 template using Bat1KO 5' and 3' oligonucleotides. The PCR product was used to transform the *leu4::kan^R leu9::loxP* strains and also a parental strain. Diagnostic PCR using Bat1e 5' and LoxPscr oligonucleotides were used to confirm the correct deletions. The Bat1e 5' binds 5' upstream of the *BAT1* gene and LoxPscr hybridizes the loxP site and

allows synthesis upstream away from *HIS5* and to the 5' end of the gene being replaced. The *HIS5* gene was looped out of the chromosome as described above.

Table 3: List of strains used in this study

| Strain | Relevant Characteristics | Reference |
|--|--|------------|
| <i>leu4::kan^R</i> | Leucine negative, G418 ^R | This study |
| <i>leu4::kan^R leu9::loxP</i> | Leucine negative, G418 ^R | This study |
| <i>leu4::kan^R leu9::loxP bat1::loxP</i> | Leucine negative, valine negative, G418 ^R | This study |
| <i>bat1::loxP</i> | Valine negative, | This study |
| <i>ilv2::kan^R</i> | Valine negative, G418 ^R | This study |
| <i>ilv3::kan^R</i> | Valine negative, G418 ^R | This study |
| <i>ilv5::kan^R</i> | Valine negative, G418 ^R | This study |

2.3 Experimental techniques

2.3.1 Protein solubility assays

The strains harboring each of GAL-KDCA, TEF1-Adh7myc, TEF1-AdhAmyc and TEF1-YqhDmyc plasmids were grown in 50mL of selective medium. Total protein extraction was performed with Trichloroacetic acid (TCA) as described by Foiani, M., et al. [43]. For soluble and insoluble protein extraction, cells were usually grown and harvested using Beckman CPR centrifuge at 3000rpm for 1 minute. The pellet was washed once with water and resuspended in 500µl of chilled extraction buffer (50mM Tris-HCl pH 7.4, 250mM NaCl, 0.1% NP-40, 1mM PMSF, 1µg/mL aprotinin, 0.5µg/mL leupeptin, 0.5µg/mL pepstatin, 1X phosphate inhibitors (IX phosphate inhibitor contained 10mM Sodium pyrophosphate, 5mM EDTA, 5mM EGTA and 0.1mM sodium orthovanadate))

and kept on ice. 0.5mm glass beads (Biospec Products Inc.) were added to meniscus of the sample and the mixture was vortexed 4X for 1 minute each with 1 minute on ice between. The tubes were punctured and the punctured tube containing the sample was fitted into a fresh microfuge tube. The two tubes were placed in a 15ml falcon tube. The lysate was filtered into the fresh tube by centrifuging the falcon tube using Beckman CPR centrifuge at 3000 rpm for 1minute. The lysate was further centrifuged in an Eppendorf 5415C centrifuge at full speed for 10 minutes at 4°C. The clarified supernatant was transferred to a fresh tube as the soluble fraction. The pellet containing the insoluble fraction was resuspended in 500µL 50mM Tris HCl pH 7.4. Soluble and insoluble fractions were visually assessed by western blotting.

2.3.2 SDS-PAGE electrophoresis /western blotting

2X laemmli buffer (100mM Tris-HCl pH 6.8, 4% SDS, 20% glycerol, 0.2% bromophenol blue, and 200mM Dithiothreitol (DTT)) was added to 20µL of each of the protein fractions. The samples were heated for 10 minutes at 65°C and centrifuged using an Eppendorf 5415C centrifuge for 5 minutes at full speed. The proteins were separated on 10% Polyacrylamide gels in 1X SDS running buffer pH 8.3 (25mM Tris-HCl, 0.25M Glycine, 0.1% SDS) at 100V.

Separated proteins were transferred to an Immobilon membrane (Millipore) using the semi-dry transfer method (Semi-dry transfer buffer contained 2.9g/L glycine, 5.8g/L Tris base, 0.37g/L SDS and 200mL methanol). After transfer, the membrane was blocked in 10% skim milk in 1X TBS-T(8g NaCl, 0.2g KCl, 3g

Tris Base, 2.7mL Tween-20/litre pH to 8.0 with HCl) in sealed bag and incubated for 4 hours at room temperature or overnight at 4°C. The membrane was then incubated in primary antibody (1 in 10,000 dilution in 5% skim milk prepared with 1X TBS -T) for 2 hours at room temperature or overnight at 4°C and then washed twice for 15 minutes with TBS-T. For the Ilv2 western blot, the Ilv2 antibody described in Dasari, S and Kölling R. [31] was used. This was followed by incubation in secondary HRP-conjugated antibody (1 in 5,000 dilution in 5% skim milk prepared with 1X TBS-T) for 2 – 4 hours at room temperature and again washed twice for 15 minutes with TBS-T.

The proteins were visualized by the Enhanced Chemiluminescence (ECL) technique. Membrane was immersed in ECL reagents (250mM Luminol, 90mM Cumaric acid, Tris-HCl pH 8.0 and 0.02% H₂O₂) for 1.5 minutes and exposed to Fuji SuperRX Xray film and processed using a Kodak X-OMAT 2000 M35 processor.

2.3.3 Alcohol dehydrogenase assay

Reductive alcohol dehydrogenase activity was detected by measuring NADPH oxidation at 340nm. Activities of the crude extract of cells overexpressing *yqhD*, *ADH7* and empty vector (EV) control were assessed in a 1mL reaction containing 545µL 50mM NaH₂PO₄ pH 7.0, 200µL 0.25mM NADPH, 250µL 25mM isobutyraldehyde and 5µL crude enzyme extract. The mixture containing the buffer, enzyme extract and NADPH was incubated at room temperature for 1 minute and the reaction was started with the addition of the isobutyraldehyde

substrate. The decrease in absorbance at 340nm was monitored every 1 minute using Biochrom ultrospec 3000 UV visible spectrophotometer. Total protein concentration was quantified by Bradford's method using Biorad protein assay kit (microassay procedure). The initial rate was taken as the change in absorbance between 1 and 5 minutes. The specific activity was determined by dividing the initial rate with the total protein concentration.

2.3.4 Genetic complementation studies

Heterozygous diploid strains harboring *ilv2::kan^R*, *ilv3::kan^R* and *ilv5::kan^R* deletions were sporulated on SPM (sporulation medium). Tetrads were dissected to haploids using an optic fiber needle. The haploids strains bearing the deletions were selected on G418 plates. The *ilv2::kan^R*, *ilv3::kan^R* and *ilv5::kan^R* were then grown in selective media and transformed with FBA1-ILV2, HXT1-ILV3 and PGK-ILV5 plasmids respectively. Empty vector controls were also performed for each of the strains. The functionality of the cloned genes was confirmed by genetic complementation of valine auxotrophy.

2.3.5 Gas chromatography assays

For the Ehrlich pathway experiments, cells overexpressing relevant plasmids were grown in 5mL of amino acid-enriched media with no other source of nitrogen for 96hours at 30°C in a rotator incubator. For fermentative isobutanol production, the cultures were grown in 20mL of synthetic complete media lacking histidine, uracil and tryptophan, and supplemented with 2% glucose (unless otherwise

stated) in 125mL shake flasks at 30°C with shaking at 220 rpm. Cultures were inoculated at OD₆₀₀ of 0.1 and assayed for isobutanol titers at 24 and 48 hours post-inoculation. Gas Chromatography (GC) analysis was performed as previously described by Gibreel, A. et al. [45] with some slight modifications. Isobutyraldehyde, isobutanol, isopentanol and pentanol were analyzed using n-hexanol as internal standard by gas chromatography (GC, Agilent Technologies 7890A GC System and 7693 Autosampler) using a Restek Stabilwax-DA column (30m by 0.53 mm inner diameter, 0.5- μ m film thickness), a 1 μ L injection in split mode (20:1 split ratio), an injector temperature of 170°C, an FID temperature of 190°C, and helium carrier gas in constant pressure mode (7.5 lb/in²). The oven program started at 35°C, held for 3 minutes, followed by 20°C /min to 190°C with a final hold of 1 minute. An aliquot of 800 μ L of the supernatant sample and 200 μ L of a 0.5% n-Hexanol internal standard solution were added to 1.5 mL GC vials and thoroughly mixed. For standards, 200 μ L of 0.5% pure isobutyraldehyde, isobutanol, isopentanol, n-pentanol and n-hexanol (internal standard) were used. Water was used as blank. The GC response factor for isobutyraldehyde, isobutanol, isopentanol and pentanol were determined and used with an internal standard correction to measure the concentration of the alcohols in the samples. The experiments were performed in triplicates for 3 independent colonies derived from each strain.

Chapter Three: Results

3.1 Fusel alcohol production by the classical Ehrlich pathway

The Ehrlich pathway is the pathway for branched-chain amino acid degradation in yeast [51]. It begins with the enzyme catalyzed deamination of a branched-chain amino acid to the corresponding 2-ketoacids (2-ketoisocaproic acid from leucine, 2-ketoisovaleric acid from valine and 2-keto-3-methylvaleric acid from isoleucine) [37]. The deamination reaction is catalyzed by a branched-chain amino acid transaminase (BAT). There are 2 isoforms of this enzyme; Bat1 and Bat2 which are found in the mitochondria and cytosol respectively [21]. The 2-ketoacids produced are then decarboxylated to their corresponding aldehyde by a decarboxylase enzyme and subsequently reduced to an alcohol by an alcohol dehydrogenase (ADH) (figure 3.1). The conversion of branch chain amino acids into their respective aldehyde and alcohols via the Ehrlich pathway resembles the fermentative metabolism of pyruvate, which yields ethanol and CO₂. In both cases, the decarboxylation of a 2-keto acid is followed by the reduction of the resulting aldehyde [108].

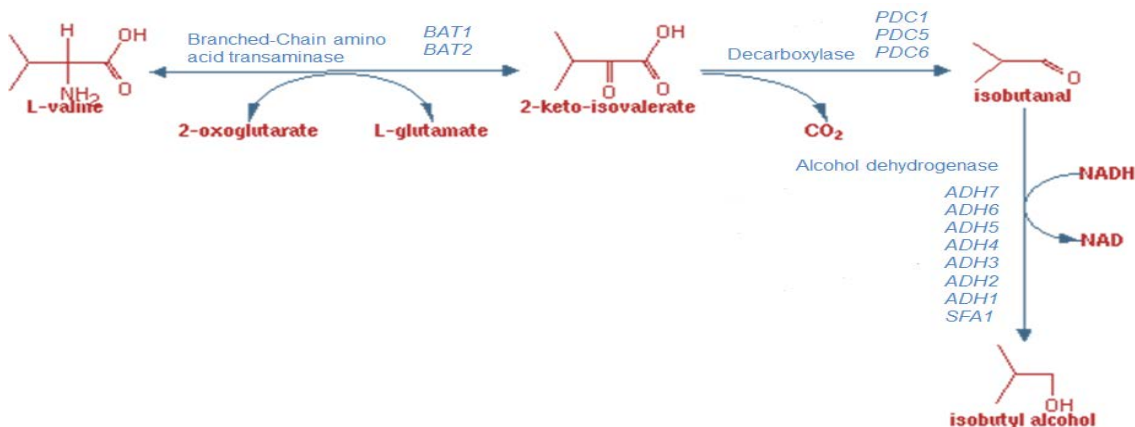


Figure 3.1: The Ehrlich pathway for valine degradation in *S. cerevisiae*.

3.1.1 Isobutanol production in yeast overexpressing *Lactococcus lactis* branched-chain 2-keto acid decarboxylase (*kdcA*)

2-ketoacid decarboxylases are involved in the catabolism of 2-ketoacids derived from aromatic and branched-chain amino acids. They are rare in bacteria but occur more frequently in plants, fungi and yeast [32]. At least six different 2-keto decarboxylases have been identified in *S. cerevisiae* namely: Phenylpyruvate decarboxylase, which is responsible for the decarboxylation of phenyl pyruvic acid to phenylacetaldehyde. Others are pyruvate decarboxylases *PDC1*, *PDC5* and *PDC6*, 2-ketoisocaproate decarboxylase *KID1* and the pyruvate decarboxylase-like enzyme YDR38w [32, 54]. *S. cerevisiae* harbors three structural genes *PDC1*, *PDC5* and *PDC6* that can each encode an active pyruvate decarboxylase. Although *PDC1*, *PDC5* and *PDC6* are able to catalyze the decarboxylation of branch-chain amino acids, they are not essential for fusel alcohol production by *S. cerevisiae* [108].

We have found that a 2-ketoacid decarboxylase known as *kdcA* from *Lactococcus lactis* efficiently converts the 2-ketoacid intermediates in the valine biosynthetic pathway to isobutyraldehyde. *L. lactis kdcA* is a 1647bp open reading frame that encodes a putative peptide of 61kDa. It is a member of the thiamine pyrophosphate (TPP)-dependent 2-ketoacid decarboxylase family and has been shown to have high affinity for 2-ketoisovalerate - an intermediate compound in valine and leucine biosynthesis [32, 54, 99].

A codon-optimized synthetic 2-ketoacid decarboxylase sourced from *Lactococcus lactis* was overexpressed in *S. cerevisiae* under the regulation of

the yeast *GALI* promoter and *ADHI* terminator. As shown in fig 3.2, the *L. lactis* *kdcA* is well expressed in yeast and a significant amount of the enzyme appeared to be in soluble fraction.

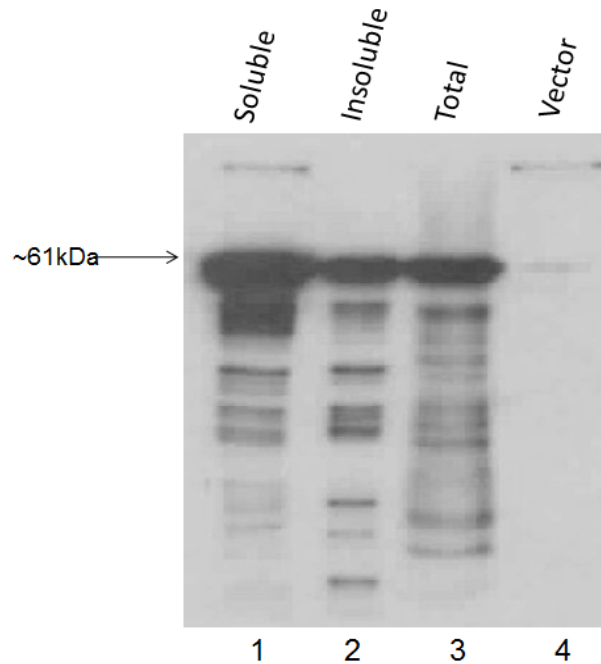


Figure 3.2: Western blot of KdcA expressed in yeast using anti-HA. Lanes 1, 2 and 3 represent the total, soluble and insoluble protein fractions respectively. Lane 4 represents the empty vector control

The *kdcA* ORF was placed under the regulation of a constitutive *GALI* promoter and introduced into *S. cerevisiae* W303. In medium containing 20g/L of valine as sole nitrogen source, cells overexpressing *kdcA* produced ~0.09g/L of isobutyraldehyde. This is two-fold higher than the amount produced by cells harboring the empty vector (fig 3.3). The *kdcA* overexpressing cells also produced ~0.2g/L isobutanol.

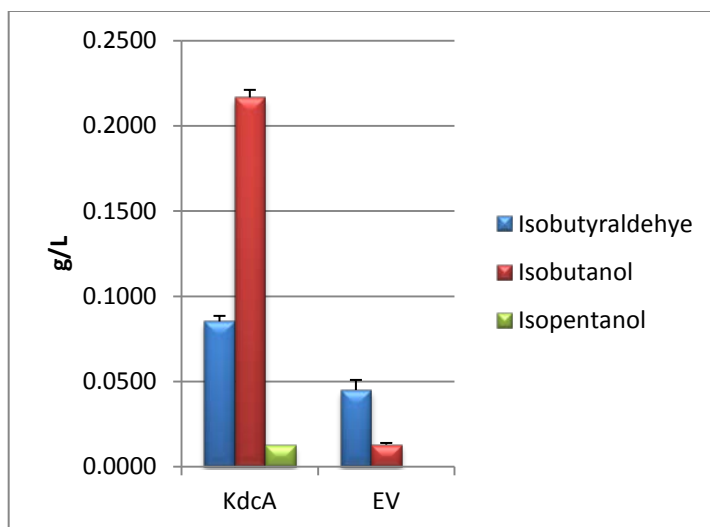


Figure 3.3: Alcohol production in yeast overexpressing *kdcA* versus Empty Vector (EV) control. Titer values are mean of three different samples from independent colonies. Error bars = standard deviation of biological triplicates

3.1.2 Determination of the optimal alcohol dehydrogenase activity for production of higher alcohol

Alcohol dehydrogenases (ADH) are oxidoreductases that catalyze the reversible oxidations of alcohols to aldehydes and ketones with the corresponding reduction of NAD^+ or NADP^+ [68]. ADHs constitute a large group of enzymes that can be subdivided into at least 3 distinct enzyme sub-families namely: short chain, medium chain and iron-activated alcohol dehydrogenases [68, 106]. The medium chain ADHs are the most well studied type. They use NAD(P) as a cofactor and a zinc ion at their active site.

The accumulation of isobutyraldehyde from yeast overexpressing *kdcA* (figure 3.3) suggests that alcohol dehydrogenase activity may be limiting for isobutanol production since some of the isobutyraldehyde produced was not converted to

isobutanol by the yeast's endogenous alcohol dehydrogenases. The optimal alcohol dehydrogenase activity for the conversion of branched-chain aldehyde to alcohols was evaluated by comparing the activities of three different ADH enzymes, namely; AdhA from *L. lactis*, YqhD from *E. coli* and the yeast Adh7. The AdhA from *L. lactis* has not been characterized biochemically; however, previous studies in *E. coli* [9] showed that the activity of AdhA towards isobutyraldehyde is quite high. Since we used the KdcA from *L. lactis* which showed broad-range substrate specificity, we reasoned that AdhA may have similar specificity. The crystal structure of the *E. coli* YqhD has been resolved. This indicates that it is an NADP(H)-dependent dehydrogenase and activity measurements with several alcohols demonstrate preference for >3-carbon alcohols [106]. Like the *E. coli* YqhD, Adh7 is an NADP(H)-dependent dehydrogenase. It is a homodimer of 40kDa. Adh7 is involved in fusel alcohol production in yeast and shows broad substrate specificity similar to Adh6 [68].

Cells overexpressing *kdcA* and one of *adhA*, *yqhD* or *ADH7* were grown in a medium enriched with valine as the sole nitrogen source for 96hrs and the supernatant was assayed for isobutanol. As shown in figure 3.4, cells expressing *E. coli yqhD* display a trend toward slightly higher isobutanol production than cells expressing *ADH7*. However, under these conditions, cells overexpressing *adhA* from *L. lactis* had the least activity. It is also worthy to note that due to the promiscuous nature of the KdcA and ADHs, isopentanol was also produced possibly from the degradation of leucine through the Ehrlich pathway.

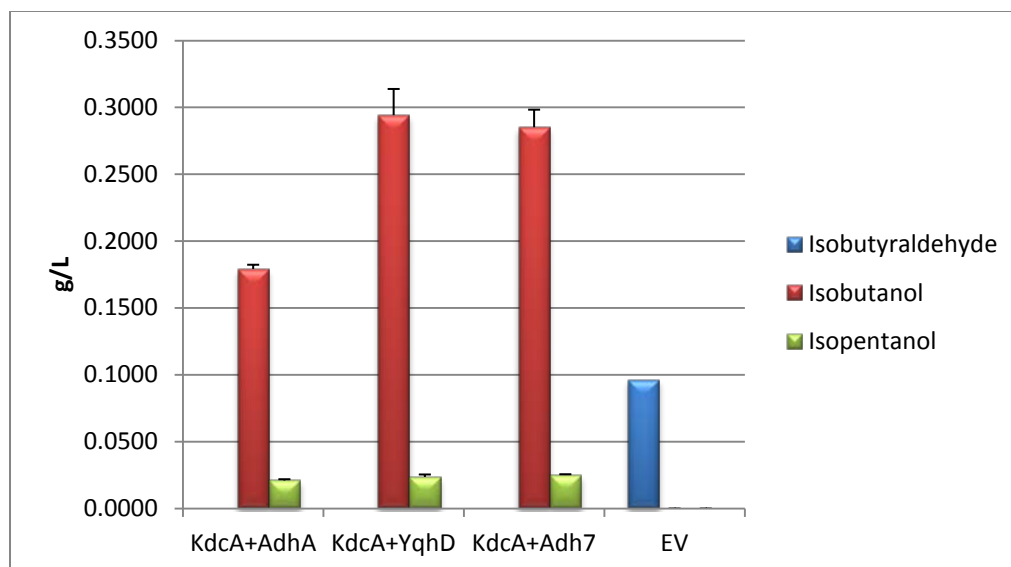


Figure 3.4: In vivo alcohol production for yeast overexpressing *kdcA* and different ADHs.

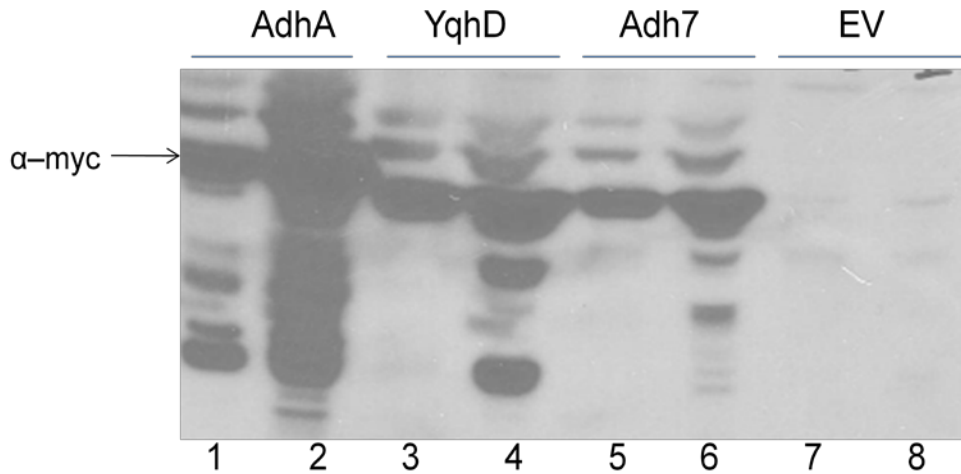
Values are mean of three different samples from independent colonies. Error bars = standard deviation of biological triplicates

Using western blotting we assessed the efficiency of expression and solubility of the MYC-tag ADHs overexpressed in yeast. Figure 3.5a shows that AdhA, YqhD and Adh7 enzymes are well expressed in yeast. The western blots also show that each of the enzyme is present in the soluble fraction.

The reductive ADH activity of the crude enzyme extract using isobutylaldehyde as the substrate was assessed by measuring the rate of oxidation of NADPH to NADP⁺ at 340nm. NADPH absorbs light maximally at 340nm while NADP⁺ does not. For a dehydrogenase that catalyzes the oxidation of NADPH, a decrease in absorbance at 340nm will be observed (figure 3.5b). The rate of change in absorbance at 340nm will be proportional to the quantity of alcohol dehydrogenase activity present.

As shown in Table 4, the specific activity for Adh7, YqhD and the empty vector were all in the same range. This indicates that the enzymes show no measurable activity.

a)



b)

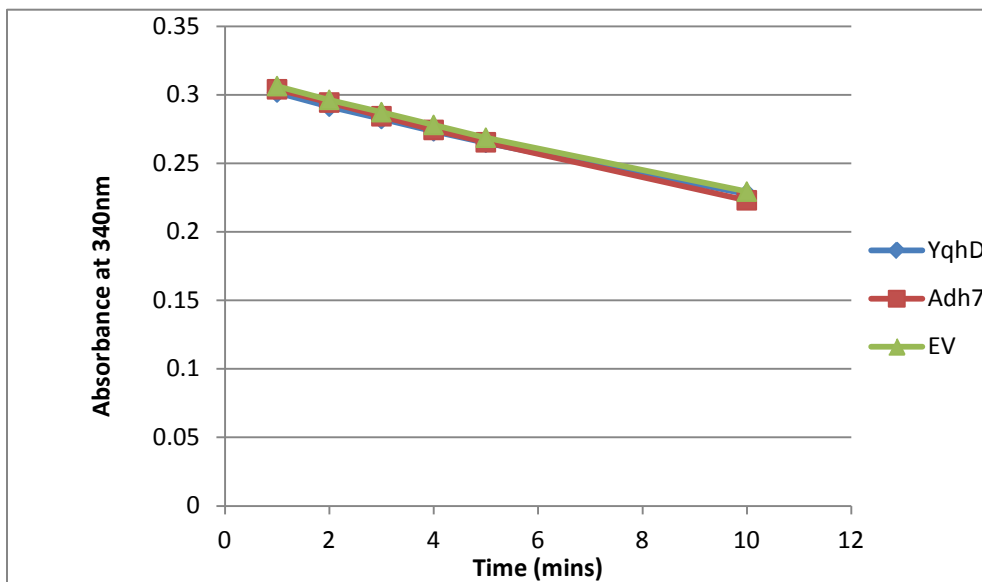


Figure 3.5: In vitro alcohol dehydrogenase activity

a) Western blot of myc-tagged ADH expressed in yeast. EV means empty vector control. Lane 1, 3, 5 and 7 represent the soluble protein fraction of AdhA, YqhD, Adh7 and EV respectively; Lane 2, 4, 6 and 8 represent the insoluble fractions of AdhA, YqhD, Adh7 and EV respectively. b) Characterization of ADH activity by measuring the rate of change in absorbance at 340nm corresponding to oxidation of NADPH. The OD_{340} are mean of three independent experiments.

Table 4: In vitro alcohol dehydrogenase activity.

| Enzyme | Initial rate (T ₁ and T ₅) | Total protein concentration (µg/mL) | Specific activity |
|--------|---|-------------------------------------|-------------------|
| YqhD | 0.0092 | 22.34 | 0.0004 |
| Adh7 | 0.0097 | 21.93 | 0.0004 |
| EV | 0.0094 | 24.31 | 0.0004 |

- Initial rate is equal the change in absorbance at 340nm between 1 and 5 minutes
- Total protein concentration in 5µl of crude enzyme was determined by Bradford's method and are mean of three independent samples
- Specific activity was determined by dividing the initial rate with the total protein concentration.

3.2 Alcohol production in a media with branched-chain amino acids as sole nitrogen source

Under conditions of nitrogen limitation, yeast cells can use amino acids as a source of nitrogen [35]. Fusel alcohols can be derived from the carbon skeleton of deaminated amino acids by the Ehrlich pathway. To investigate the potential for yeast to synthesize different varieties of fusel alcohol products, cells overexpressing *kdcA* and *ADH7* were grown in medium with 10% alanine, valine, leucine, isoleucine or casamino acids as sole nitrogen source. As shown in fig. 3.6, cells growing in alanine- or valine-enriched medium accumulated isobutanol. Whereas for the cells growing in leucine, isoleucine or casamino acid enriched media, the five-carbon alcohol - isopentanol was the predominant alcohol produced. In a casamino acid medium, the cells most likely extract nitrogen from glutamine and glutamic acid which are the preferred nitrogen source. The large error bars were probably due to variability in the copy number of the plasmids harboring the *kdcA* and *ADH7* genes.

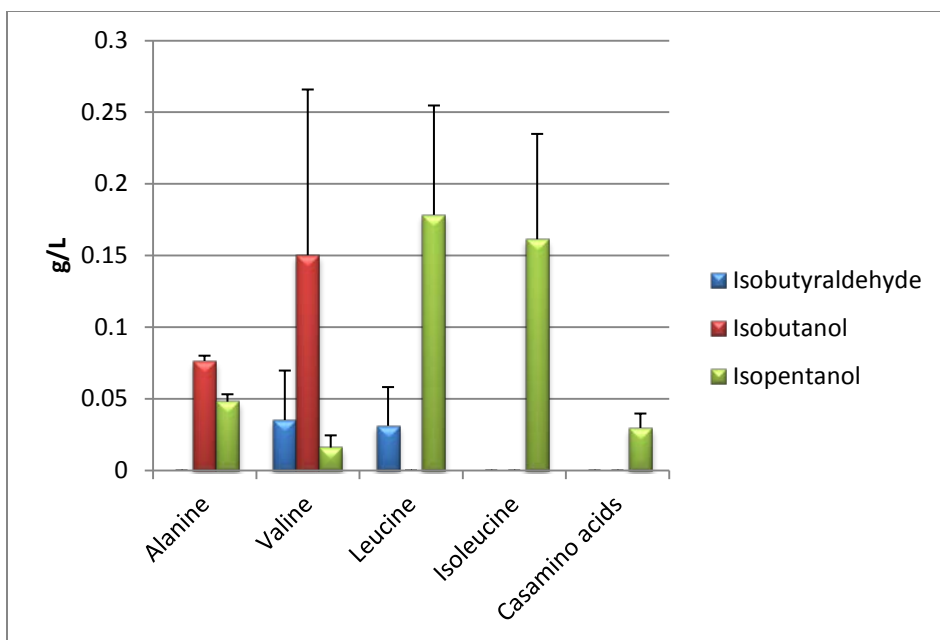


Figure 3.6: Fusel alcohol production under conditions of nitrogen limitation.

Cells overexpressing *kdcA* and *ADH7* were grown in a media enriched for each of the branched-chain amino-acid in the absence of ammonium sulphate. Values are mean of three different samples from independent colonies. Error bars = standard deviation of biological triplicates.

3.3 Fermentative production of isobutanol in *S. cerevisiae* by overexpressing genes in the valine biosynthetic pathway

The yeast *S. cerevisiae* synthesizes small amounts of isobutanol and other higher alcohols by the Ehrlich pathway through catabolism of valine and other branched-chain amino acids [92]. Recently, a strategy for aerobic production of isobutanol from glucose was reported in *E. coli* [3]. This approach involves the heterologous expression of the valine biosynthetic pathway which supplies 2-ketoisovalerate intermediate that can then be converted to isobutanol through the Ehrlich pathway.

In *S. cerevisiae*, 2-ketoisovalerate is produced from pyruvate in a three-step reaction that is catalyzed by Ilv2, Ilv6, Ilv5 and Ilv3 enzymes. The Ilv2 and Ilv6

are part of a multienzyme complex functioning as the catalytic and regulatory subunits respectively (fig 3.7).

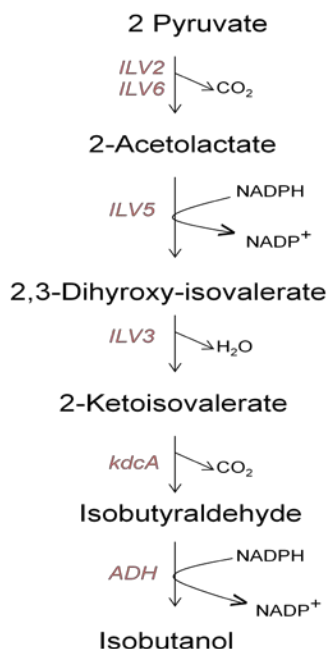


Figure 3.7: Pathway for isobutanol production from pyruvate in *S. cerevisiae*.

ILV2, *ILV6* encode acetolactate synthase (*ILV2* is the catalytic subunit of acetolactate synthase while *ILV6* is the regulatory subunit), *ILV5* encodes acetoxyacid reductoisomerase, *ILV3* encodes dihydroxyacid dehydratase, *kdcA* and *ADH* stands for 2-ketoacid decarboxylase and Alcohol dehydrogenase respectively.

3.3.1 Confirmation of *ILV* gene activity

In order to construct the isobutanol synthetic pathway in *S. cerevisiae*, each of *ILV2*, *ILV6*, *ILV5*, and *ILV3* ORF and 3' transcription termination sequences were ligated into a multi-copy plasmid under the regulation of the *FBA1*, *PDC1*, *P GKI1* and *HXT7* yeast promoters, respectively, as described in "Materials and Methods". The functionality of the cloned genes was confirmed by genetic complementation of valine auxotrophy as described in "Material and Methods". Figure 3.8 shows that the cloned *ILV2*, *ILV3* and *ILV5* genes are functional. The *ILV6* is the regulatory subunit for *ILV2* and has no detectable phenotype so there

is no genetic way of confirming its functionality. However, the *ILV6* gene was sequenced to ensure the correctness of the sequence.

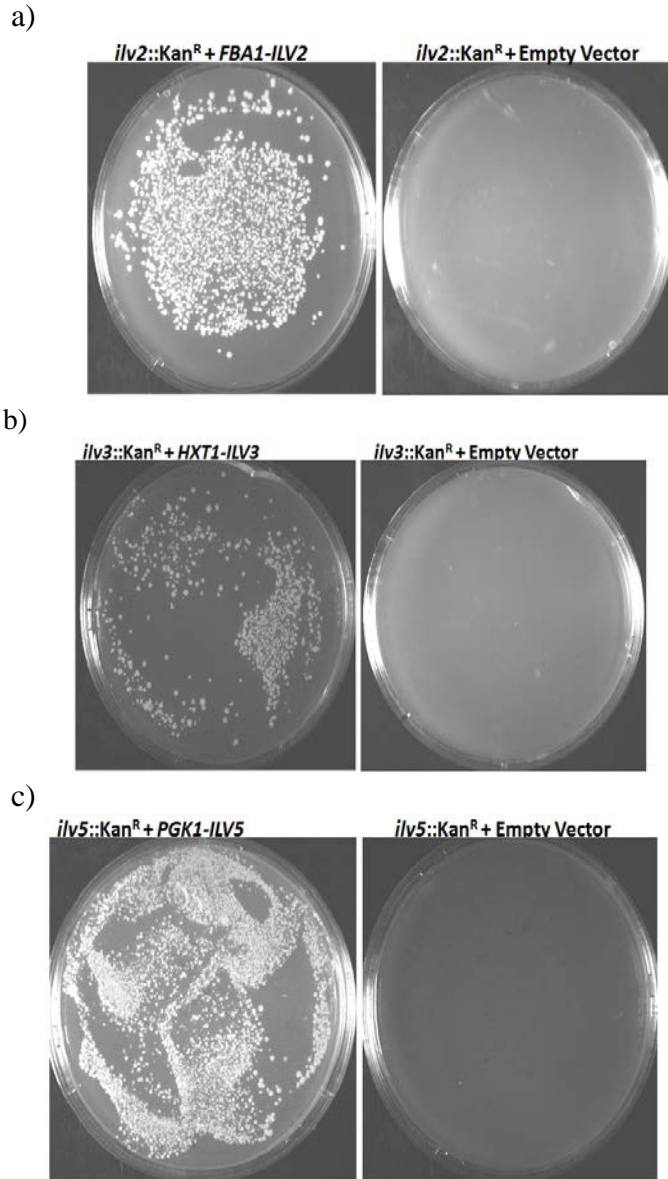


Figure 3.8: Confirmation of the activity of the cloned *ILV* genes.

a, b and c: FBA1-ILV2, HXT1-ILV3 and PGK1-ILV5 plasmids were used to transform mutant strains in which the *ILV2*, *ILV3* and *ILV5* genes respectively had been deleted using the *kan^R* cassette. These mutants are auxotrophic for valine. Genetic complementation was observed for the mutants harboring the plasmids when grown on valine-deficient media but not for the mutants containing the empty vector (controls).

3.3.2 Isobutanol production by cells overexpressing *ILV* pathway

The cloned *ILV2*, *ILV6*, *ILV5* and *ILV3* genes were sequentially assembled into a single plasmid (designated as *ILV* array) as described in “Materials and Methods” and was used to transform *S. cerevisiae* strain W303 (parental strain) together with a plasmid expressing *kdcA*. The strain was grown in 2% glucose medium under microaerobic conditions for 96 hours. The supernatant was assayed for isobutanol production by gas chromatography. As shown in Figure 3.9, this strain produced ~24mg/l of isobutanol. In contrast, a strain harboring the empty vectors produced no detectable isobutanol under these conditions.

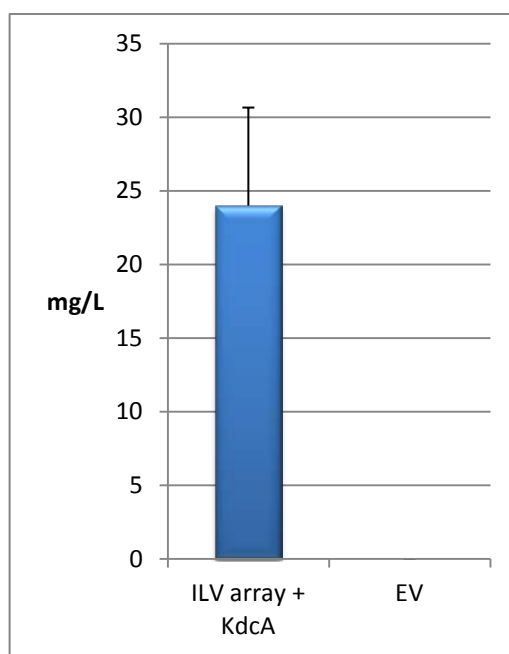
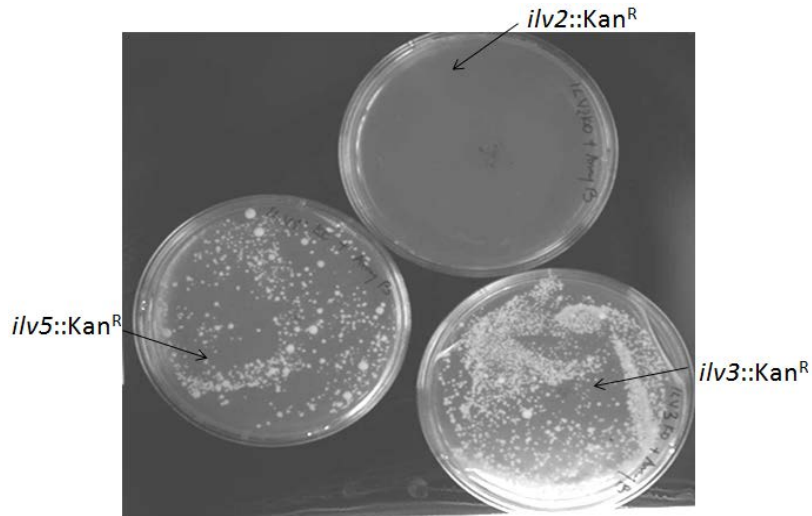


Figure 3.9: Isobutanol production in a strain overexpressing the *ILV* gene array and *kdcA* in 2% glucose. EV means empty vector control. Values are mean of three different samples from independent colonies. Error bar is the standard deviation of biological triplicates.

The isobutanol titer obtained was low compared to levels reported in *E. coli*. To further investigate if the low level of isobutanol observed was due to inactivity of some of the genes overexpressed in the pathway, genetic complementation was

performed to test whether the plasmid expressing all four *ILV* genes could rescue the auxotrophy of *ilv2*, *ilv3*, *ilv5* mutants. The plasmid containing the *ILV2*, *ILV6*, *ILV5* and *ILV3* genes was used to transform *ilv2::kan^R*, *ilv3::kan^R* and *ilv5::kan^R* mutants. While the plasmid effectively complemented the deficiency displayed by *ilv3* and *ilv5* strains, complementation of *ilv2::kan^R* took 2 weeks before colonies begin to appear (figure 3.10a), suggesting that the plasmid borne *ILV2* was poorly expressed or that the protein was defective. To confirm expression of Ilv2, a western blot was performed using anti-Ilv2 polyclonal antiserum (generously provided by Dr. Ralf Kölling from Universität Hohenheim, Germany). As shown in figure 3.10b, the Ilv2 protein is expressed, however the expression level within the *ILV* array plasmid seems to be weak (figure 3.10b, lane 2). To overcome this limitation, an extra copy of *P_{FBAI}-ILV2* was integrated at the *TRP1* gene (as described in section 2.2.3 of the “Material and Methods”) of all the strains investigated.

a)



b)

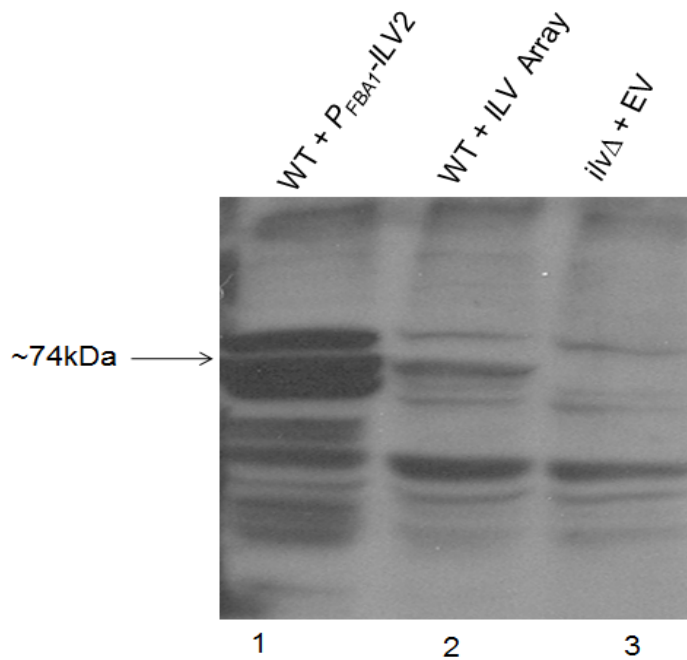


Figure 3.10: *ILV2* is weakly expressed within the *ILV* array plasmid.

a) No Genetic complementation of *ilv2::kan^R* when each of *ilv2::kan^R*, *ilv3::kan^R* and *ilv5::kan^R* mutant strains was transformed with *ILV* array plasmid. b) Western blotting using antibody against Ilv2. Lane 1 represents WT *S. cerevisiae* strain expressing a plasmid containing *P_{FBA1}-ILV2* gene only (positive control). Lane 2 represents WT *S. cerevisiae* strain expressing the plasmid containing all four *ILV* genes (*ILV* array) which previously did not complement *ilv2::kan^R* mutant. Lane 3 is the *ilv2::kan^R* mutant expressing an empty vector (EV) negative control.

3.4 Comparing the effects of competing pathways on isobutanol production

The valine biosynthetic pathway shares the intermediate; 2-ketoisovalerate with the leucine biosynthetic pathway (Figure 3.11). 2-ketoisovalerate can be converted to leucine in a four-step reaction that is catalyzed by Leu4, Leu9, Leu1, Leu2, Bat1 and Bat2 enzymes (Leu4 (major) and Leu9 (minor) are isozymes; Bat1 and Bat2 are isozymes found in the mitochondria and cytosol respectively [25]. 2-ketoisovalerate can be converted to valine by Bat2 in the cytosol, in reverse reaction from that used in the Ehrlich pathway whereas Bat1 converts 2-ketoisovalerate to valine in the mitochondria as part of predominant valine biosynthetic pathway. The other valine biosynthetic enzymes Ilv2, Ilv6, Ilv5 and Ilv3 all reside within the mitochondria.

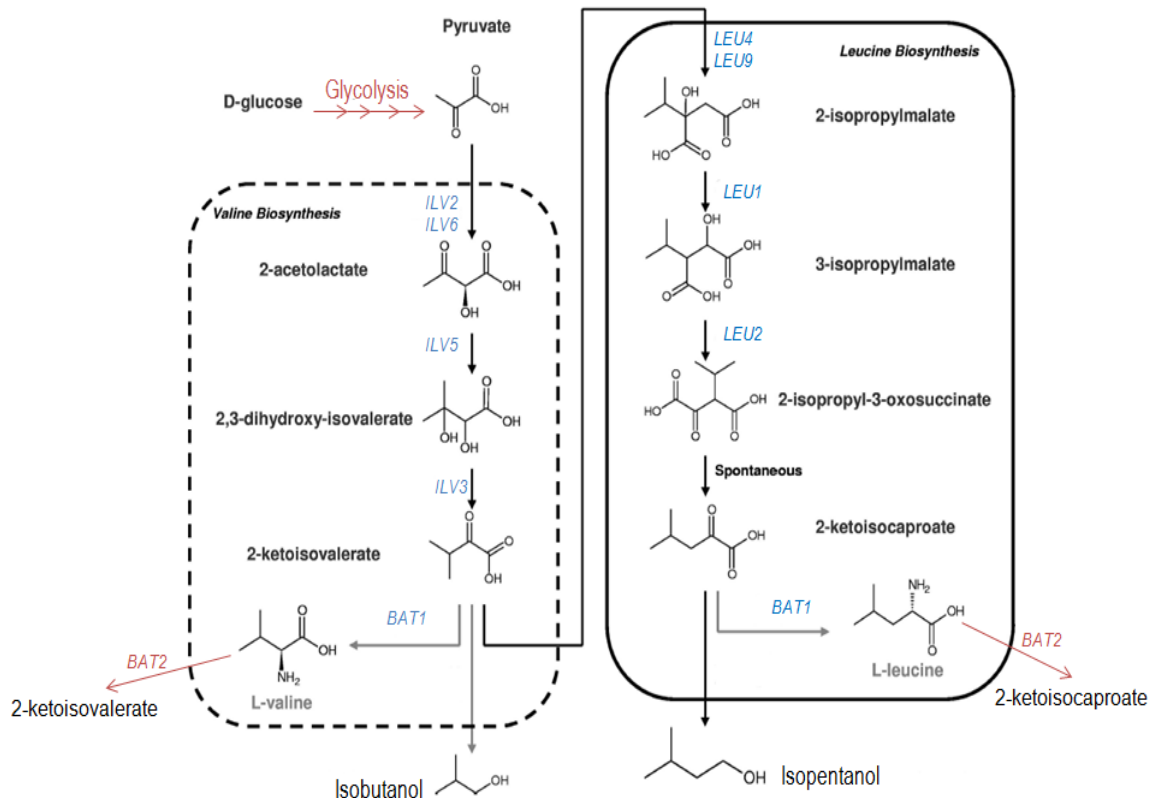


Figure 3.11: Pathways for valine and leucine biosynthesis in yeast.

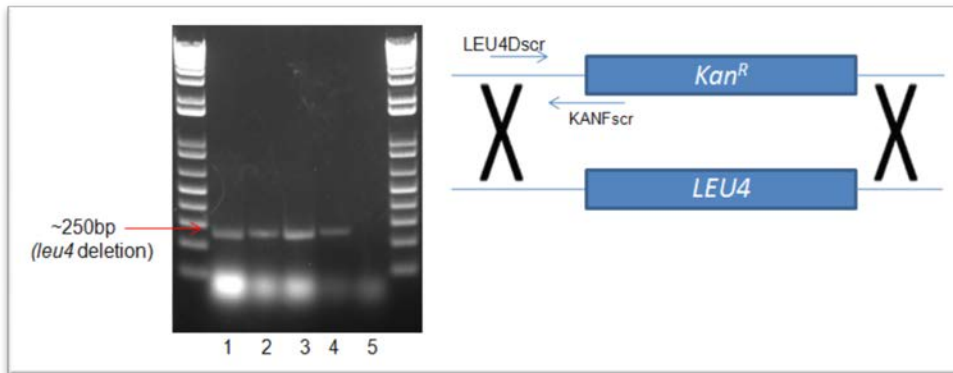
ILV2, *ILV6* encode acetolactate synthase (*ILV2* is the catalytic subunit of acetolactate synthase while *ILV6* is the regulatory subunit), *ILV5* encodes acetoxyacid reductoisomerase, *ILV3* encodes dihydroxyacid dehydratase, *LEU4* encodes alpha-isopropylmalate synthase, *LEU9* encodes alpha-isopropylmalate synthase minor isozyme, *LEU1* encodes isopropylmalate isomerase, *LEU2* encodes beta-isopropylmalate dehydrogenase, *BAT1* encodes branched-chain amino acid aminotransferase, *BAT2* encodes branched-chain amino acid transaminase. The broken and solid boxes represent pathways for valine and leucine biosynthesis in the mitochondria respectively. Red arrows indicate reactions occurring in the cytosol.

Adapted from Connor et al. [26]

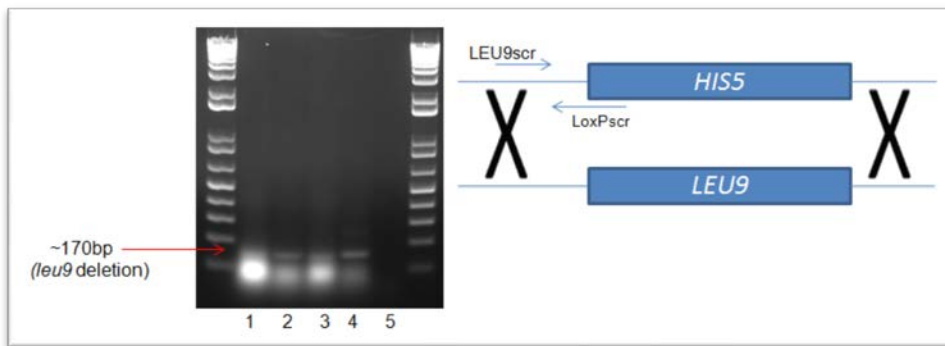
The effects of deleting *LEU4* and *LEU9* genes which catalyze the first step in the leucine biosynthesis or *BAT1* which catalyzes the conversion of 2-ketoisovalerate to valine in the mitochondria were investigated. The *LEU4*, *LEU9* and *BAT1* genes were deleted from the yeast chromosome by homologous integration as described in section 2.2.7 of “Materials and Methods”. Fig 3.12 shows the schematic diagram and diagnostic PCR for these deletions. *leu4::kan^R* deletion

was confirmed by PCR using LEU4Dscr and KANFscr external oligonucleotides to screen for integration at the correct site. These oligonucleotides hybridize 5' upstream of the *LEU4* gene and within the promoter of the *kan^R* gene, respectively. This primer set yielded a ~250bp fragment which corresponds to the product expected from the replacement of *LEU4* ORF with *kan^R* cassette (figure 3.12a). *leu9::HIS5* deletion was confirmed by PCR using LEU9scr and LoxPscr oligonucleotides. LEU9scr hybridizes 5' upstream of the *LEU9* gene while LoxPscr binds the LoxP site and allows synthesis upstream away from *HIS5* and towards the 5' end of the gene being replaced. This gave a ~170bp fragment (figure 3.12b). Finally, *bat1::HIS5* deletion was also confirmed by diagnostic PCR using Bat1e 5' and LoxPscr oligonucleotides which produced a fragment of ~350bp (figure 3.12c). Bat1e 5' hybridizes 5' upstream of the *BAT1* gene and the LoxPscr oligonucleotide hybridizes the LoxP site and allows synthesis upstream away from *HIS5* and toward the 5' end of the gene being replaced.

a) *leu4::kan^R*



b) *leu4::kan^R leu9::HIS5* double deletion



c) *leu4::kan^R leu9::loxP bat1::HIS5* triple deletion

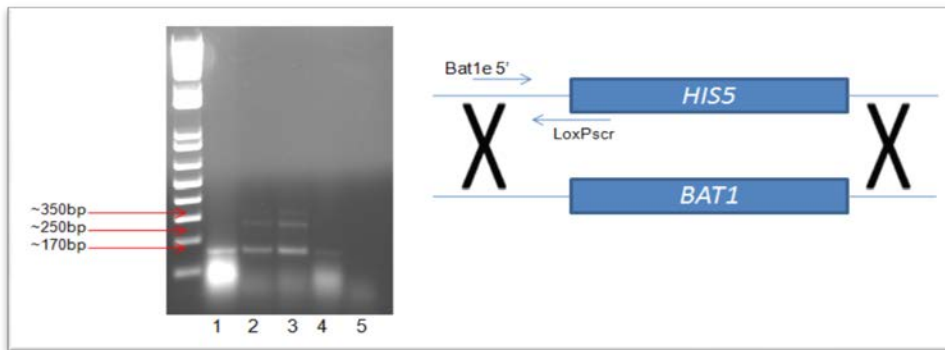


Figure 3.12: Gene deletions by homologous recombination.

a) Diagnostic PCR and schematic diagram for *leu4::kan^R* deletion. LEU4Dscr and KANFscr oligonucleotides bind at the regions shown by the blue arrows; the X sign shows regions of homology. Lanes 1, 2, 3 and 4 represent strains with correct deletions. Lane 5 is the negative control. b) Diagnostic PCR and schematic diagram for *leu4::kan^R leu9::HIS5* deletions using LEU9scr and LoxPscr oligonucleotides. This oligonucleotide pair binds at the regions shown by the blue arrows; the X sign shows regions of homology. Lanes 2, 3 and 4 represent strains with correct deletions. Lane 5 is the negative control. c) Diagnostic PCR and schematic diagram *leu4::kan^R leu9::loxP bat1::HIS5* deletions. Bat1e 5' and LoxPscr oligonucleotides bind at the regions shown by the blue arrows; the X sign shows regions of homology. Lanes 3 and 4 represent strains with all three deletions when diagnostic PCR was performed with LEU4Dscr and KANFscr; LEU9scr and LoxPscr; Bat1e 5' and LoxPscr oligonucleotides pairs. Lane 5 is the negative control. The red arrows in a, b and c points to the size of PCR fragment.

To further increase the isobutanol production, alcohol dehydrogenase (*yqhD* or *ADH7*) was added to the *ILV* gene array and an extra copy of the *ILV2* gene was integrated at the *TRP1* gene (*TRP1::P_{FBAI}-ILV2*) in all the strains investigated.

Table 5 shows the relevant genotype of all the strains tested.

Table 5: List and composition of strains used for isobutanol production

| | Strain name | <i>leu4::kan^R</i> | <i>leu9::loxP</i> | <i>bat1::loxP</i> | <i>TRP1::P_{FBAI}-ILV2</i> <i>P_{FBAI}-ILV2</i> <i>P_{HXT7}-ILV3</i> <i>P_{PGKI}-ILV5</i> <i>P_{PDCI}-ILV6</i> | <i>kdcA</i> | <i>yqhD</i> | <i>ADH7</i> |
|---|----------------|------------------------------|-------------------|-------------------|--|-------------|-------------|-------------|
| 1 | WT ADH7 | - | - | - | + | + | - | + |
| 2 | WT YQHD | - | - | - | + | + | + | - |
| 3 | LEUKO ADH7 | + | + | - | + | + | - | + |
| 4 | LEUKO YQHD | + | + | - | + | + | + | - |
| 5 | BATI KO ADH7 | - | - | + | + | + | - | + |
| 6 | BATI KO YQHD | - | - | + | + | + | + | - |
| 7 | TRIPLE KO ADH7 | + | + | + | + | + | - | + |
| 8 | TRIPLE KO YQHD | + | + | + | + | + | + | - |

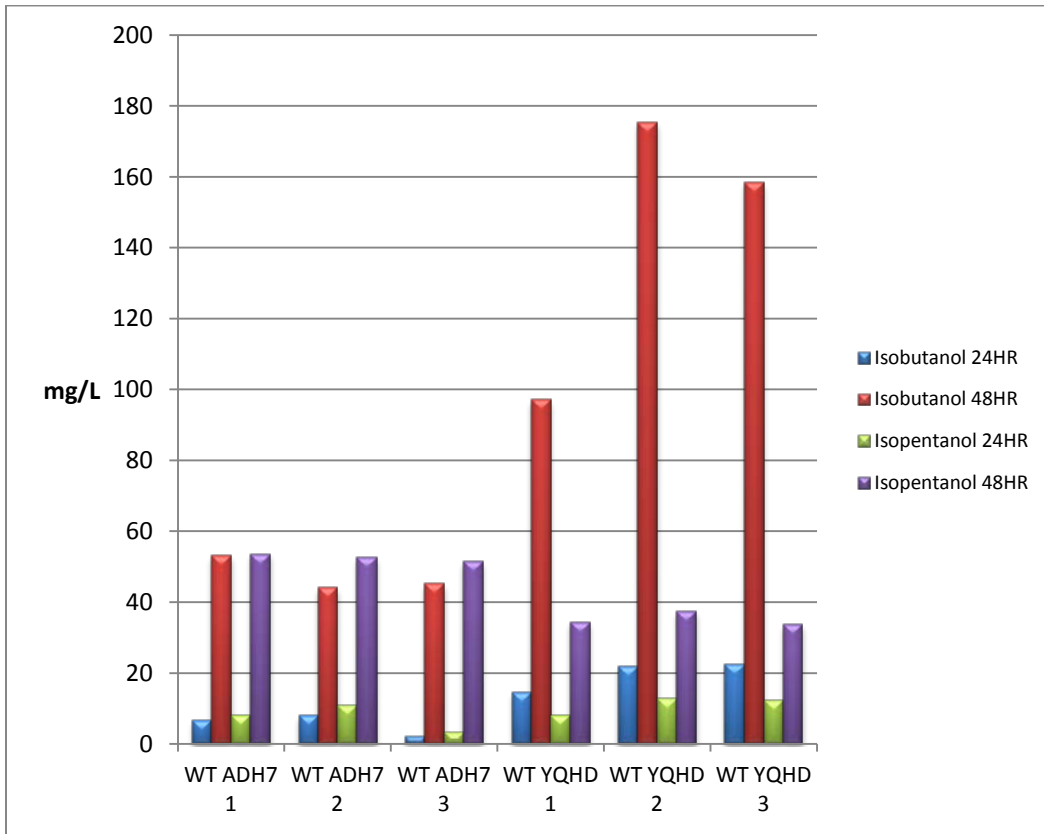
3.4.1 Isobutanol production in parental strain (WT) and *leu4::kan^R leu9::loxP* strains

To determine the effect of deletion of *LEU4* and *LEU9* genes, isobutanol production for parental the strain and *leu4::kan^R leu9::loxP* strains were compared. These strains were grown in a media containing 8% glucose. Figure 3.13 a and b reveals that cells overexpressing the *E. coli yqhD* alcohol dehydrogenase produced more isobutanol than those overexpressing the yeast's *ADH7*. After 48hours of culture, (figure 3.13a), the WT cells overexpressing the

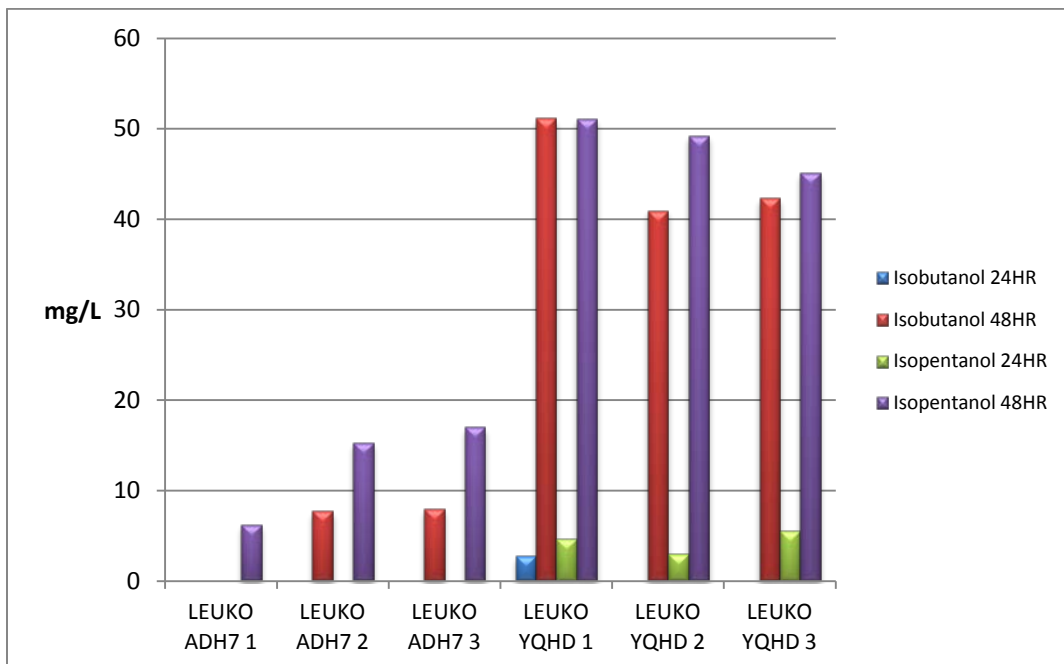
ILV genes with the *E. coli yqhD* produced ~3 times more isobutanol than the *leu4::kan^R leu9::loxP* strains (figure 3.13b) probably because the deletions cause decreased growth as shown in Figure 3.13c. After 48 hours of culture, the OD₆₀₀ of WT YQHD and LEUKO YQHD were ~10 and 6 respectively. A similar trend was observed for WT ADH7 and LEUKO ADH7 strains (figure 3.13c). This data suggests that the *LEU4 LEU9* gene deletions may not be beneficial for isobutanol production. There is variation in alcohol production between independent colonies of the same strain. For example the isobutanol production for 48HR cultures of 3 different colonies of the WT YQHD strain (WT YQHD 1, 2, and 3) are 97, 175, 158 mg/L, respectively (Figure 13.3a). This variation is likely due to the copy number of the plasmid in each strain.

It is also worthy to note the WT strain produced some isopentanol. This is not surprising as isopentanol can be produced in yeast by catabolism of leucine and since leucine shares the 2-ketoisovalerate intermediate with valine, it is possible for some of the 2-ketoisovalerate produced to be channeled to the leucine biosynthesis pathway and in the presence of KdcA and Adh be catabolized to isopentanol. In the *leu4::kan^R leu9::loxP* strains, the leucine biosynthetic pathway has been ablated and the cells must therefore use exogenous leucine, some of this may undergo deamination and be converted to isopentanol by KdcA and Adh.

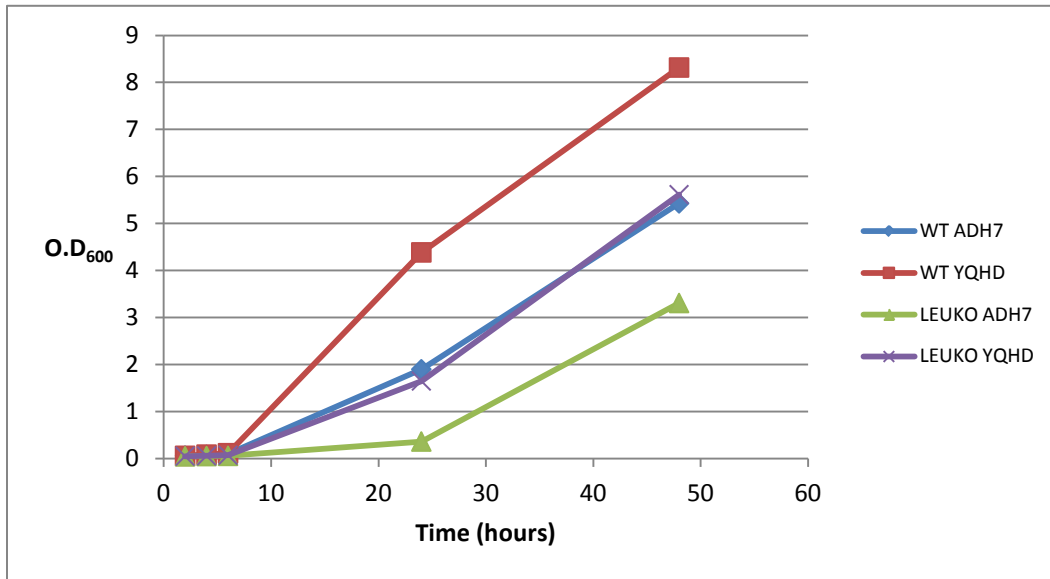
a)



b)



c)



d)

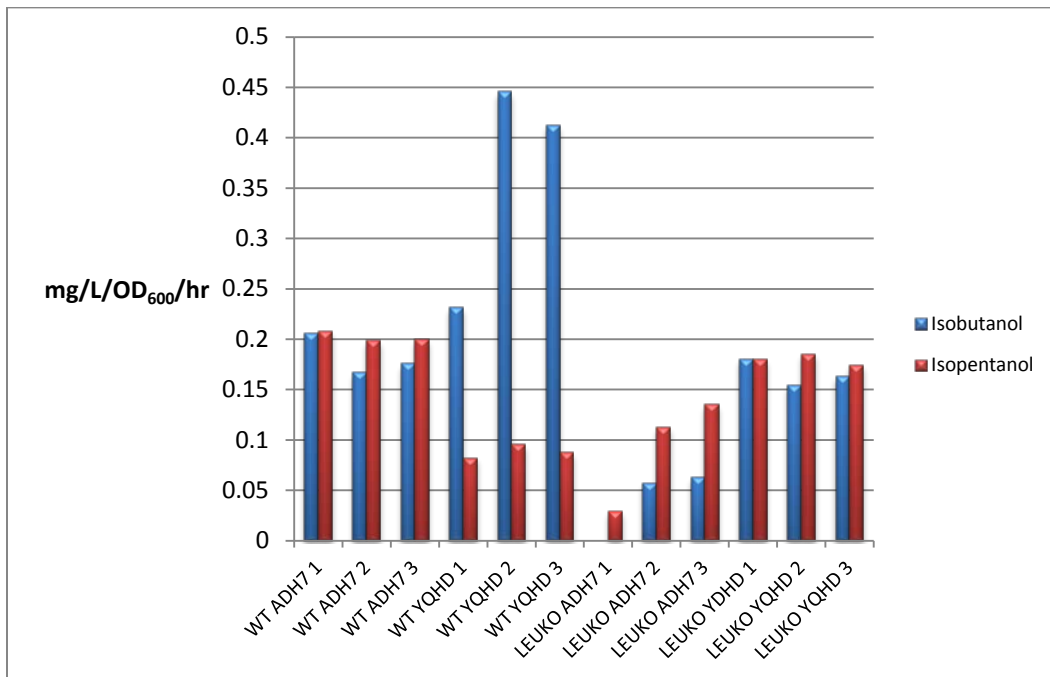


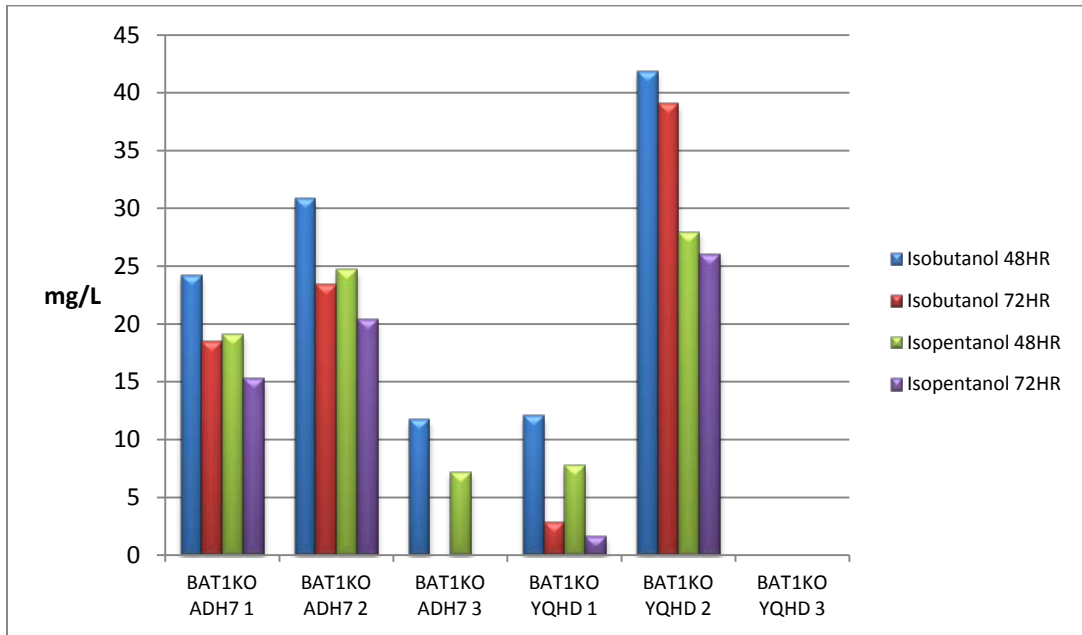
Figure 3.13: Alcohol production by WT and *leu4::kan^R leu9::loxP* strains in 8% glucose.

a) Alcohol titer for 24 and 48 hours cultures of WT strains overexpressing *kdcA*, *ILV* gene array and one of *ADH7* or *yqhD*. b) Alcohol titer of 24 and 48 hours cultures of *leu4::kan^R leu9::loxP* strains overexpressing *kdcA*, *ILV* array and one of *ADH7* or *yqhD*. c) Growth curve for strains in a) and b). Values are mean of 3 independent colonies in a) and b). d) Rate of alcohol production for WT and *leu4::Kan^R leu9::loxP* strains. The “1, 2, 3” behind each strain represent independent colonies from the same strain.

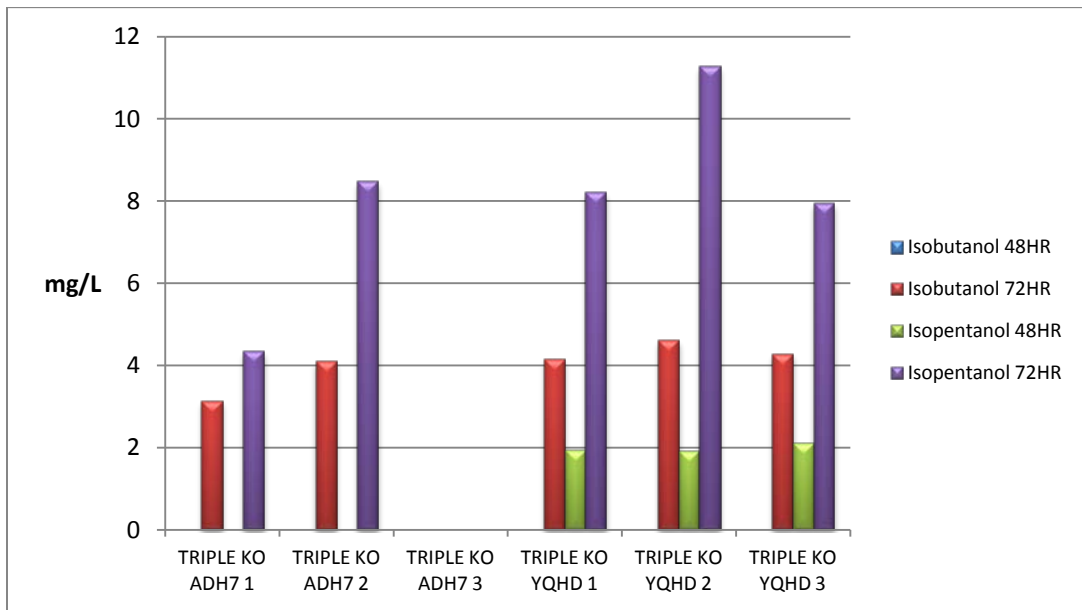
3.4.2 Isobutanol production in *bat1::loxP* and *leu4::kan^R leu9::loxP bat1::loxP* strains

The strains with the *BAT1* single or *LEU4 LEU9 BAT1* triple deletions were investigated for isobutanol production in 2% glucose media. Surprisingly, the increased availability of 2-ketoisovalerate that was predicted for these strains did not translate to increased isobutanol production. These strains performed poorly probably because the mutations caused great defects in growth to the cells. Cells lacking the *BAT1* gene cannot synthesize any of the branched-chain amino acids. As shown in figure 3.14c, after 72 hours of growth, triple mutants barely reached an OD₆₀₀ of 2.0. This defect in growth may explain the low levels of isobutanol observed in these strains when compared to the WT strains. There is also very large variation in alcohol production for independent colonies of the same strain. As shown in figure 3.14a, BAT1KO YQHD 2 produced almost 3 times more isobutanol than BAT1KO YQHD 1. This is probably due to difference in the copy number of the plasmids. Again, some of the strains e.g., BAT1KO YQHD 3 (figure 3.14a) did not produce any detectable alcohol. This may be due to loss of the plasmid by this strain, or inactivation of one or more of the plasmid borne genes. Since the product isobutanol is toxic, any cells that harbor a plasmid that has lost function might have a growth advantage.

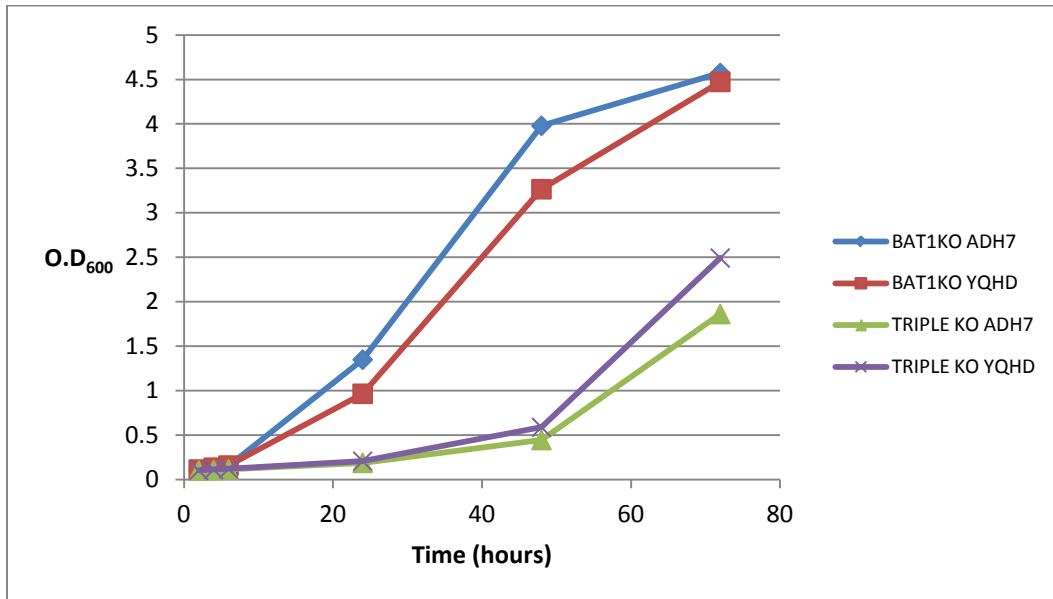
a)



b)



c)



d)

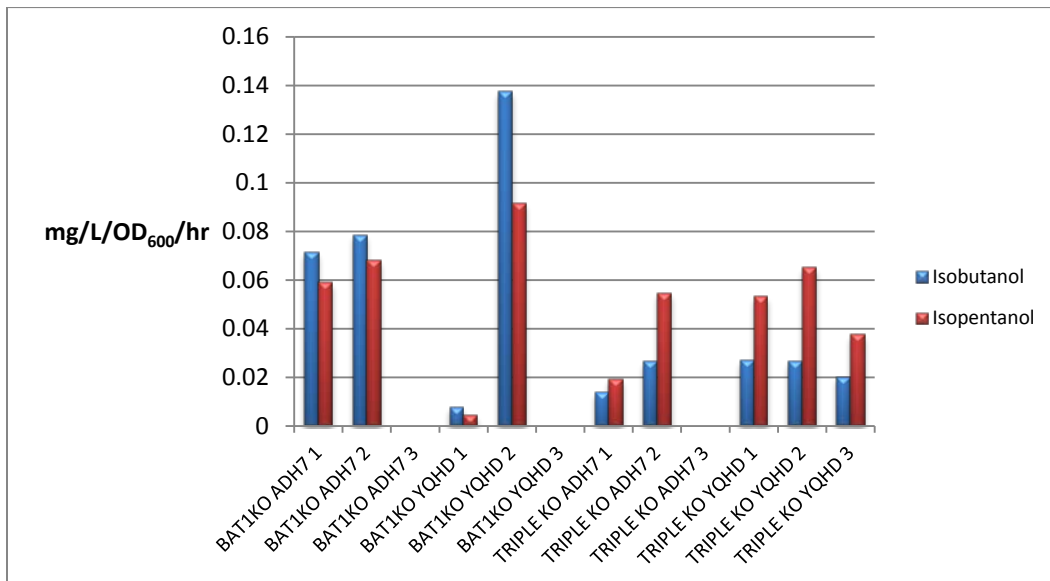


Figure 3.14: Alcohol production in *bat1::loxP* and *leu4::kan^R leu9::loxP bat1::loxP* strains in 2% glucose.

a) Alcohol titer for 24 and 48 hours cultures of *bat1::loxP* strains overexpressing *kdcA*, *ILV* gene array and one of *ADH7* or *yqhD*. b) Alcohol titer of 24 and 48 hours cultures of *leu4::kan^R leu9::loxP bat1::loxP* strains overexpressing *kdcA*, *ILV* array and one of *ADH7* or *yqhD*. c) Growth curve for strains in a) and b). Values are mean of 3 independent colonies from a) and b). d) Rate of alcohol production for *bat1::loxP* and of *leu4::kan^R leu9::loxP bat1::loxP* strains. The “1, 2, 3” behind each strain represent independent colonies from the same strain.

3.4.3 Comparing isobutanol production for WT, *leu4::kan^R leu9::loxP*, *bat1::loxP*, and *leu4::kan^R leu9::loxP bat1::loxP* strains

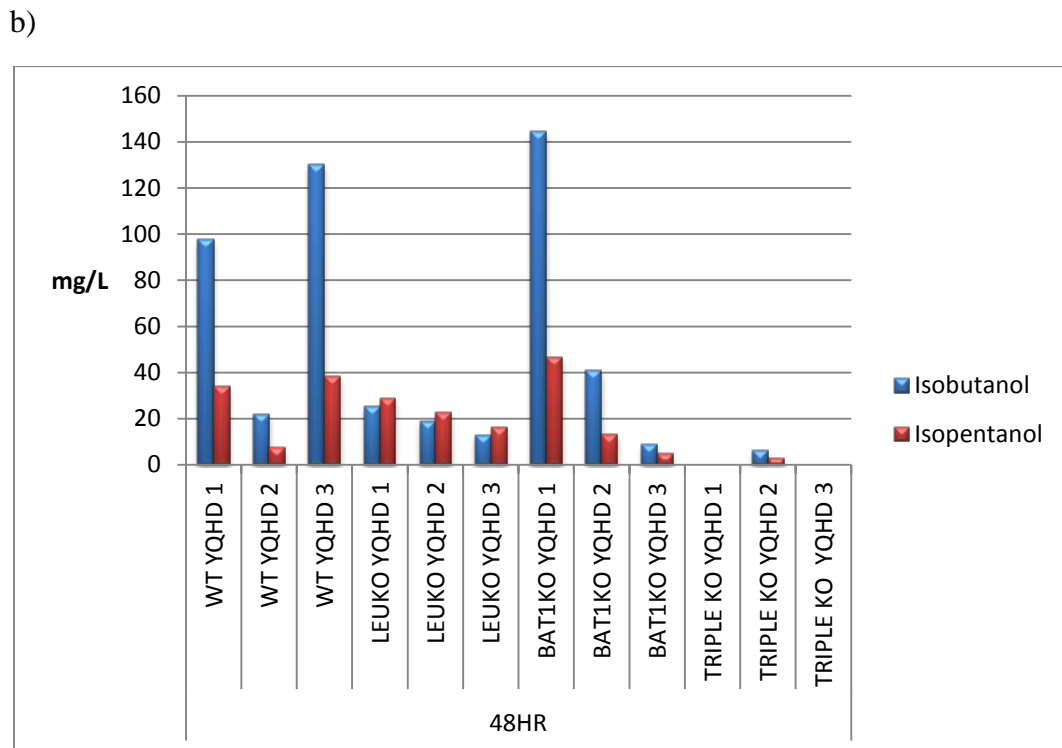
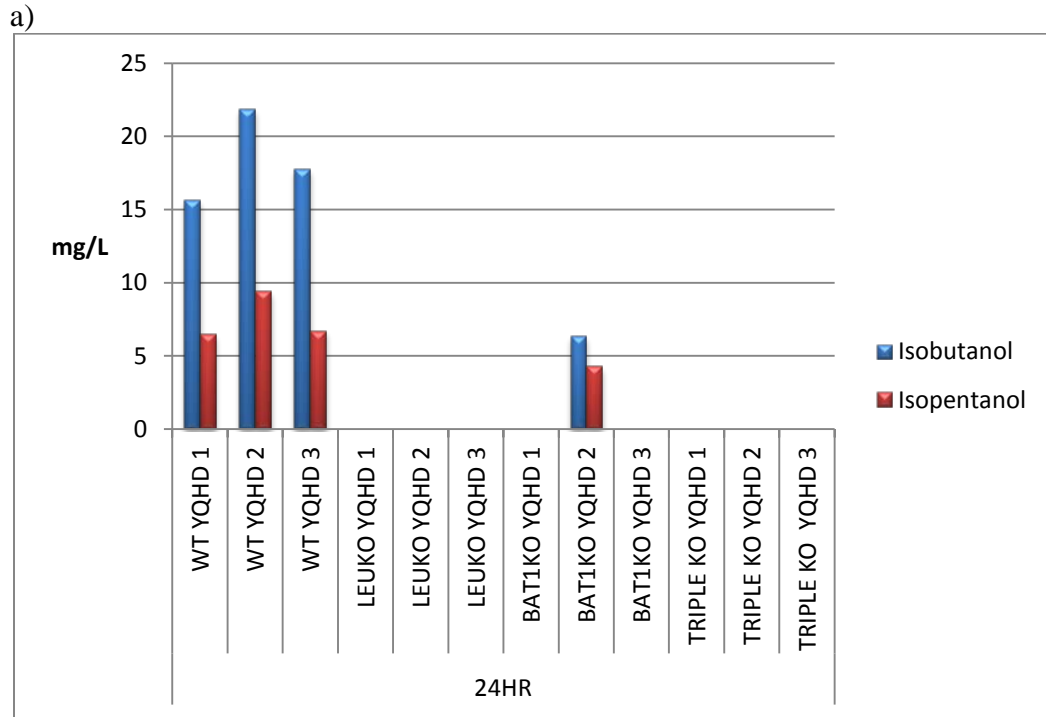
We compared the isobutanol production of all four strains namely; WT, *leu4::kan^R leu9::loxP*, *bat1::loxP*, and *leu4::kan^R leu9::loxP bat1::loxP* overexpressing the *ILV* array, *yqhD* and *kdcA* in 4% glucose. It should be noted that there is a wide discrepancy in the amount of isobutanol produced for independent colonies of the same strain because the copy number of the plasmid in each colony cannot be controlled. That notwithstanding, colonies 1 and 3 of the WT strains produced ~100 and 130mg/L of isobutanol after 48 hours (figure 3.15b). One colony from the *bat1::loxP* strains (BAT1KO YQHD 1 figure 3.15b) outperformed the WT strains. This strain may have acquired additional mutations that suppressed the loss of *BATI*. This will be worthy of further investigation.

The specific growth rate μ as described in Widdel F. [116] calculated as

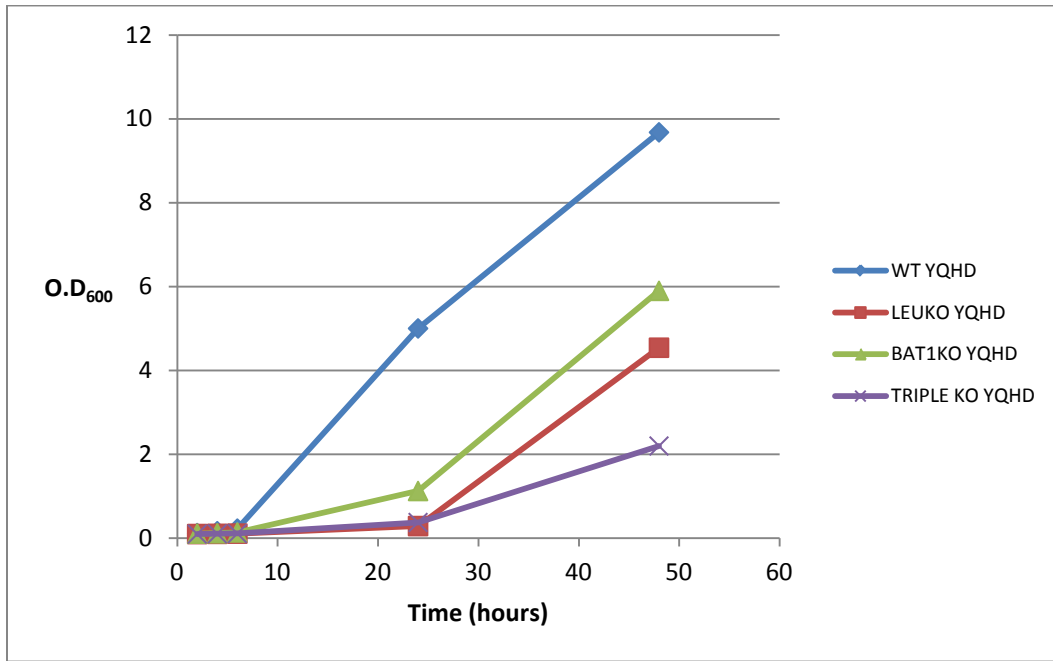
$$\mu = \frac{2.303 (\log OD_2 - \log OD_1)}{(t_2 - t_1)}$$

of all the four strains in figure 3.15c are as follows: WT = 0.095, *leu4::kan^R leu9::loxP* = 0.083, *bat1::loxP* = 0.087 and *leu4::kan^R leu9::loxP bat1::loxP* = 0.067. These figures indicate that the amount of isobutanol correlates with the specific growth rates of the strains. The wild type strains reached an OD₆₀₀ of ~10 after 48hours whereas, the OD₆₀₀ for the *leu4::kan^R leu9::loxP*, *bat1::loxP* and *leu4::kan^R leu9::loxP bat1::loxP* after 48hours are of 4.5, 6 and 2.2 respectively (figure 3.15c). The *bat1::loxP* that outperformed the WT strains reached an OD₆₀₀ of ~8. The strains containing the *leu4::kan^R leu9::loxP* and *leu4::kan^R*

leu9::loxP bat1::loxP deletions (LEUKO and TRIPLE KO) performed poorly indicating that the deletions are not beneficial for isobutanol production.



c)



d)

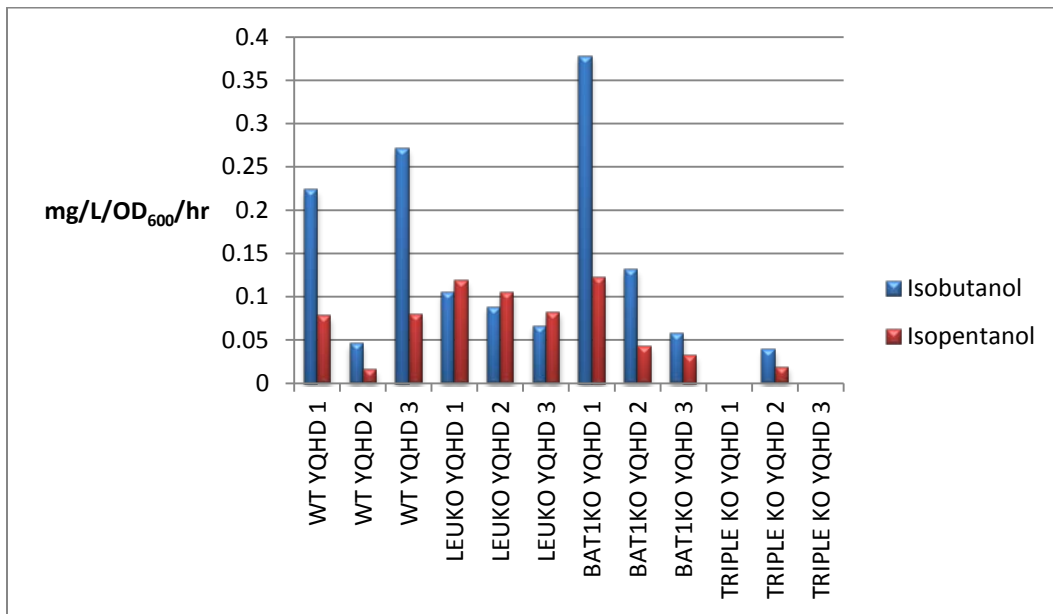


Figure 3.15: Comparing the isobutanol production of WT, *leu4::kan^R leu9::loxP, bat1::loxP,* and *leu4::kan^{R} leu9::loxP bat1::loxP}* strains in 4% glucose.

a) and b) 24 and 48 hours cultures of WT, *leu4::kan^{R} leu9::loxP, bat1::loxP,}* and *leu4::kan^{R} leu9::loxP bat1::loxP}* strains overexpressing *kdcA, ILV* array and *yqhD*. c) Growth curve for strains in a) and b). Values are mean of 3 independent colonies from a) and b). d) Rate of alcohol production for all strains tested. The “1, 2, 3” behind each strain represent independent colonies from the same strain.

3.4.4 Isobutanol production in valine and isoleucine deficient media

Amino acid biosynthetic pathways are regulated by their products. Valine and isoleucine are known to decrease flux through their pathways. To investigate whether isobutanol production can be increased by relieving this potential repressive effect, the best isobutanol producing strains (WT YQHD) were grown in a media deficient in valine and isoleucine. Growth of these strains in a media deficient in these branched-chain amino acids will likely increase expression of the genes involved in the isobutanol pathway due to the pressure on the cells to synthesize these amino acids endogenously. After 72 hours of growth in 4% glucose, isobutanol titer of ~74mg/L was accumulated (figure 3.16 WT YQHD 2). This result indicates that isobutanol was produced by the fermentation of glucose and not the degradation of exogenous valine in the media through the Ehrlich pathway. Additionally, the use of a single biological isolate in this experiment shows that the strain is relatively stable since there is little variation (60, 74 and 60mg/L) in the isobutanol production titer among the triplicate cultures.

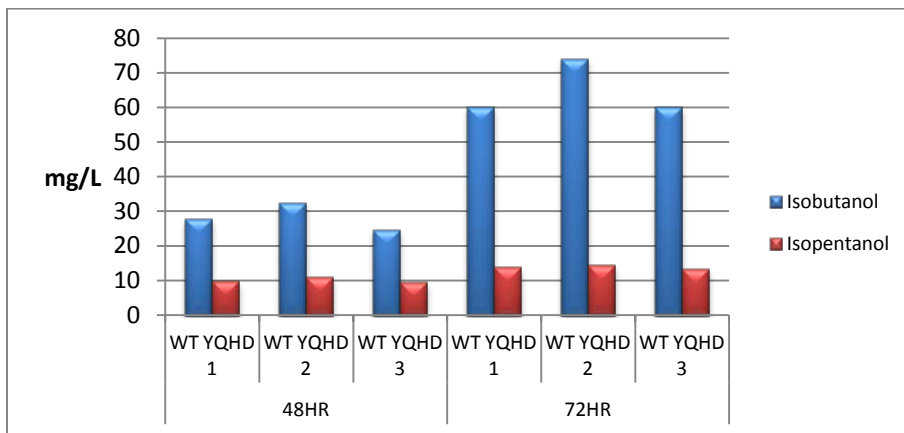


Figure 3.16: Isobutanol production in a media deficient in valine and isoleucine.

Chapter four: Conclusions

4.1 Discussion

Isobutanol is produced biologically as a by-product of yeast fermentation. Isobutanol is specifically produced from catabolism of L-valine in the cytoplasm after the amine group of L-valine is harvested as a nitrogen source; the resulting α -ketoacid is decarboxylated and reduced to isobutanol by enzymes of the Ehrlich pathway. Yields of fusel oil and/or its components achieved during beverage fermentation are typically low. For example, the concentration of isobutanol produced in beer fermentation is reported to be less than 16 parts per million [69]. Isobutanol can be produced in increased titer by adding valine exogenously to the media. Using this approach, a yeast strain overexpressing *kdcA* from *Lactococcus lactis* produced ~200mg/L of isobutanol when the growth media was enriched with valine. This represents an isobutanol yield of 10mg/g of valine. This strain also produced 90mg/L of isobutyraldehyde (a yield of 4.5mg/g of valine) due to incomplete conversion to isobutanol by endogenous yeast alcohol dehydrogenases. With the addition of the *E. coli yqhD*, the *kdcA* overexpressing strain produced 300mg/L of isobutanol; representing a yield of 15mg/g of valine. Clearly, much of the valine utilized is not being converted into isobutanol; some of the carbon skeleton of the valine may be shunted to gluconeogenesis. The yields of isobutanol and isobutyraldehyde reported here may be an underestimation of the actual yields as these compounds are volatile and some of it may be lost to the gas phase of the culture. Strategies such as gas stripping coupled with fermentation can be used to condense volatile solvents such

isobutanol and isobutyraldehyde produced during fermentation and enable easy recovery. This has successfully been applied to isobutanol production in *E. coli* [10].

The use of valine as a feed-stock would be cost prohibitive for industrial scale isobutanol production. There is a need for attaining higher amounts of isobutanol through yeast fermentation without addition of valine or other isobutanol production intermediates. Atsumi et al. [3, 4, 9] engineered *E. coli* for fermentative production of isobutanol from glucose by overexpressing the Ehrlich pathway enzymes (KdcA and Adh2 from *L. lactis* and *S. cerevisiae* respectively) in addition to an acetohydroxyacid synthase *alsS* from *Bacillus subtilis* and the native *E. coli ilvC and ilvD* to increase the carbon flux from pyruvate to isobutanol. Furthermore, the deletion of *adhE, ldhA, frdAB, fnr, pta* and *pflB* (encoding alcohol dehydrogenase, D-lactate dehydrogenase, fumarate reductase, transcriptional regulator FNR, phosphateacetyltransferase and formate lyase respectively) involved in competing reactions led to an isobutanol production of 22g/L (a yield of 0.35 g/ g glucose) which is 86% of the theoretical maximum [3].

Despite the successes achieved with isobutanol production in *E. coli*, the yeast *S. cerevisiae* has properties that make it a potentially better chassis for fermentative production of isobutanol. Yeast is a more robust organism; it is more tolerant to isobutanol and can withstand the harsh conditions used in industrial fermentations. Again, yeast genetics and physiology are well understood and there are many tools for sophisticated genetic manipulation. Several yeast strains have

been engineered to degrade cellulose, hemicellulose, and lignin; this makes it easy for isobutanol production to be coupled to lignocellulosic feedstock [21].

Fermentative production of isobutanol by *S. cerevisiae* has been reported by two different groups of researchers. Kondo et al. [64] engineered a yeast strain that produced 143mg/L of isobutanol (6.6mg/g glucose) by overexpressing *ILV2*, *kdcA* and the yeast *ADH6* and deletion of *PDC1* gene to reduce pyruvate drain off to ethanol. On the other hand, Chen et al. [21] engineered isobutanol in yeast by overexpressing the *ILV2*, *ILV3*, and *ILV5* and achieved an isobutanol yield of 4.12mg/g of glucose under aerobic conditions. The study also revealed that under anaerobic conditions, *ILV6*; the regulatory subunit decrease isobutanol production by threefold whereas overexpressing *BAT2* in addition to *ILV2*, *ILV3*, and *ILV5* genes improved the isobutanol production two-fold.

In this study, the fermentative pathway for isobutanol production was engineered in *S. cerevisiae*. Firstly, by overexpressing the genes encoding Ilv2, Ilv6, Ilv5, Ilv3 and KdcA enzymes involved in conversion of pyruvate to isobutyraldehyde, an isobutanol titer of 24mg/L (1.2mg/g glucose) was achieved. By addition of *yqhD* alcohol dehydrogenase from *E. coli* and the overexpression of an additional Ilv2 enzyme from the yeast chromosome, the isobutanol titer was increased to ~150mg/L representing an isobutanol yield of 1.88mg/g of glucose. The strains overexpressing the *E. coli yqhD* performed better than those overexpressing the endogenous yeast *ADH7* possibly because the *yqhD* had a *COX4* signal sequence fused to it so that it is capable of importing the protein to the mitochondria where the 2-ketoisovalerate is produced by the valine biosynthetic pathway.

The reaction for the conversion of 1mol of glucose to isobutanol is shown below:



1 mole of glucose produces 1 mole of isobutanol. The maximum theoretical yield for isobutanol is 0.41g/g of glucose. The best isobutanol strain in this study (WT YQHD) produced 1.88mg/g glucose, which is only 0.46% of the theoretical maximum. The strain we engineered was also found to produce ~37mg/L of isopentanol – a yield of 0.46mg/g of glucose. We speculate that most of the glucose is lost as a result of pyruvate drain-off to ethanol, acetate, lactate, and all the other possible metabolic fates of pyruvate. Additionally, the medium used for isobutanol production contained 80g/L of glucose; perhaps, some of glucose were not metabolized and remained in the medium as residual glucose.

To conserve the intracellular 2-ketoisovalerate intermediate for isobutanol production, the genes encoding Leu4 Leu9 and Bat1 enzymes involved in competing reactions were deleted. This did not prove to be beneficial for isobutanol production as these deletions caused great defects in growth for these strains. As Chen et al. [21] have observed, other factors besides the enzyme activities for the supply of 2-ketoisovalerate may be responsible for the low isobutanol production yield in *S. cerevisiae* when compared to *E. coli*. These could include the valine inhibition of the Ilv2 enzyme, which limits the flux to isobutanol, the transportation of 2-ketoisovalerate to the cytosol and the lower affinity of *ILV2* for pyruvate when compared to other enzymes involved in pyruvate metabolism [21].

Maintaining a balanced redox state is important for an efficient production process. The isobutanol pathway we constructed requires 2 mols of NADPH/H⁺ per mol of isobutanol produced since the yeast Ilv5 and the *E. coli* YqhD enzymes are NADPH dependent. Given that glycolysis generates 2mols of NADH/H⁺ per mol of glucose, efficient isobutanol production will require a means of recycling NADH/H⁺ or some other ways of supplying NADPH/H⁺.

4.2 Future directions

In order to further increase the isobutanol production in *S. cerevisiae* beyond the current titer reported in this thesis the following measures are proposed:

1. Reconstruct the isobutanol pathway using a feedback-resistant acetolactate synthase (*ILV6*) mutant gene.

The acetolactate synthase catalyzes the first step that is common to the biosynthesis of the branched-chain amino acids [82]. The reaction involves the irreversible decarboxylation of pyruvate to a bound hydroxyethyl group that then condenses with either a second pyruvate molecule to form 2-acetolactate (valine and isoleucine biosynthetic precursor) or with 2-ketobutyrate to form 2-aceto-2-hydroxybutyrate (for leucine biosynthesis). Like in bacteria, the *S. cerevisiae* acetolactate synthase is made up of the large (Ilv2) and small (Ilv6) subunits [82]. The Ilv6 regulatory subunit has been shown to confer valine feedback-inhibition to the enzyme. Feedback resistant acetatolactate synthase (*ilvN*) has been created in *C. glutamicum* using site directed mutagenesis to the

small subunit of the enzyme [42]. 3 amino acids residues in position 20, 21 and 22 of the protein were changed from Gly-Ile-Ile to Asp-Asp-Phe thereby creating a mutant enzyme that was feedback resistant to valine, leucine and isoleucine [42]. It will be worthwhile to test if similar mutation to the *Ilv6* protein will make it feedback-resistant to valine in *S. cerevisiae* and then to reconstruct the isobutanol pathway using the feed-back resistant *ILV6* mutant. This may lead to deregulation of valine biosynthesis and increased isobutanol production.

2. Balancing redox carriers

The engineered isobutanol pathway from glucose produces 2 mols of NADH and consumes 2 mols of NADPH. This creates redox imbalance to the cells and limits isobutanol production to only aerobic conditions. Anaerobic conditions are preferred for large scale fermentations as they eliminate the need to supply and control oxygen and generally produced higher yields [109]. The strain we engineered produced high concentrations of ethanol, possibly as a way of recycling NADH. This cofactor imbalance problem can be resolved through a number of ways.

The first approach will be to replace NADPH-dependent enzymes of the isobutanol pathway with NADH-utilizing homologues [13]. Bastin et al. [13] used directed evolution to engineer the *E. coli* *IlvC* so that it utilizes NADH rather than NADPH. Furthermore, the group also engineered the NADH dependent *L. lactis* *AdhA* alcohol dehydrogenase to increase its activity towards isobutyraldehyde. The use of the engineered NADH-dependent *IlvC* and *AdhA*

for isobutanol production in *E. coli* led to anaerobic production of isobutanol at 100% theoretical yield [13].

An alternative approach for the production of NADPH is the use of biosynthetic pathway enzymes such as an NADH kinase that can phosphorylate NADH to NADPH [18]. Different NADH kinase uses NADH or NAD⁺ as the phosphoryl acceptor [61]. There are three structural genes that encode NAD(H) kinase in *S. cerevisiae* *UTR1*, *YEF1*, and *POS5* [61]. The mitochondrial *POS5* gene has been shown to have higher activity towards NADH rather than NAD⁺ and is the major source of NADPH in the mitochondria [79, 81]. An NADP(H) phosphatase which preferentially dephosphorylates NADP⁺ and not NADPH will also be needed to maintain NAD⁺ pool [18].

3. Increase intracellular pyruvate availability

Factors other than 2-ketoisovalerate availability may be limiting for isobutanol production. Of particular importance is pyruvate availability. The 2-acetolactate synthase enzyme has lower affinity toward pyruvate compared with other competing enzymes such as pyruvate decarboxylase (PDC), pyruvate dehydrogenase complex, or lactate dehydrogenase [14].

Pyruvate decarboxylase catalyses the oxidation of pyruvate to acetaldehyde thereby enabling the reduction of NADH produced during glycolytic fermentation [85]. There are three structural genes that can encode an active pyruvate decarboxylase in yeast, namely *PDC1*, *PDC5* and *PDC6*.

PDC1 is the major isozyme while the nearly identical *PDC5* is expressed only in the absence of *PDC1* [95]. Disruption of the activity of the *PDC1* and or *PDC5* genes may decrease pyruvate drain-off to ethanol production and possibly increase isobutanol production. Kondo et al [64] has shown that deletion of *PDC1* increased isobutanol production by 13-fold from 11mg/L to 143mg/L in *S. cerevisiae* overexpressing *ILV2*, *kdcA* and the yeast *ADH6* when compared to strains not expressing any of the above genes and without *PDC1* deletion.

In yeast, the conversion of pyruvate to acetyl-CoA in the mitochondria is catalyzed by the multienzyme pyruvate dehydrogenase complex [85]. Pyruvate dehydrogenase complex consist of 3 major catalytic components. The E1 component consists of the E1 α and E1 β subunits encoded *PDA1* and *PDB1* respectively. The E2 and E3 components are encoded by *LAT1* and *LPD1* respectively. An additional complex protein is encoded by *PDX1*, which links Lat1p to Lpd1p [69, 85]. The activity of any of these proteins may be reduced to affect the function of the pyruvate dehydrogenase complex. Larry et al. [69] found that disrupting *PDA1* component of pyruvate dehydrogenase complex in the mitochondria increased isobutanol production, suggesting that flow of pyruvate to 2-ketoisovalerate was increased.

Lactate formation is another possible metabolic fate of pyruvate during fermentation. The interconversion of pyruvate to D-lactate is catalyzed by lactate dehydrogenase. In yeast, there are 3 isozymes of this enzyme; *DLD1*, *DLD2* and *DLD3*. Disruption of activity of any or all of these proteins may improve isobutanol production.

4. Creation of fusion proteins of some of the isobutanol pathway enzymes

Sub-cellular compartmentalization may also be responsible for the low levels of isobutanol observed in *S. cerevisiae* when compared to *E. coli*. Unlike in *E. coli*, the valine biosynthesis enzymes Ilv2, Ilv6, Ilv5, and Ilv3 in yeast are located in the mitochondria while Ehrlich pathway enzymes are in the cytosol. It is likely that the 2-ketoisovalerate produced in the mitochondria gets converted to valine or leucine faster than it gets transported to the cytosol. Creation of an Ilv3-KdcA and or Ilv3-KdcA-Adh fusion protein may help import the KdcA and Adh proteins to mitochondria where the 2-ketoisovalerate is made and then commit it to isobutanol production rather than valine synthesis.

5. Disrupt glutamate and glutamine assimilation to increase other amino acids uptake and degradation through the Ehrlich pathway

Glutamine and glutamate are the preferred amino acids to supply the nitrogen requirement of cells in nitrogen-limited medium [77]. To increase the uptake of valine or other branched-chain amino acids in a nitrogen-limited medium used for higher production through the Ehrlich pathway, the glutamine and glutamate assimilation can be disrupted by knocking out their transporters. Additionally, overexpressing the general amino acid permease *GAP1* or branched-chain amino acid permease *BAP2* may increase the import and uptake of valine and other branched chain amino acids [38].

6. Construction of the isobutanol pathway using integrating plasmids

The isobutanol producing pathway we engineered was done using high-copy plasmid and had to be maintained in selective media. The growth of the strains in selective media may have affected the stability of the strains. Additionally, the isobutanol pathway was constructed using a two-plasmid system; one or both of the plasmids can be easily lost by the strains. This may explain why some of colonies from the same strain do not produce any detectable amount of isobutanol (examples are the BAT1KO YQHD 3 strain in Figure 3.14a and TRIPLEKO ADH7 3 in Figure 3.14b).

Engineering these strains so that they no longer use selective media can be done using integrating plasmids. Moreover, the use of integrating plasmid will eliminate the variability in copy number associated with the use of high-copy plasmids.

4.3 Summary

2-ketoacids are intermediates in amino acid biosynthetic pathways and can be converted to aldehydes by 2-ketoacid decarboxylases (KDCs) and then to alcohols by alcohol dehydrogenase (ADHs). We have found that a ketoacid decarboxylase from *Lactococcus lactis* (KdcA) efficiently utilizes the branched chain precursor 2-ketoisovalerate to produce isobutyraldehyde, which can then be converted to isobutanol by alcohol dehydrogenase. In the presence of high concentration of valine, overexpression of *kdcA* and the *E. coli* alcohol dehydrogenase *yqhD*, leads

to increased isobutanol production *in vivo* (0.3g/liter in 96hrs), a yield of 15mg/g of valine.

The valine biosynthetic pathway was also engineered for efficient production of alcohols from pyruvate. It is hypothesized that isobutanol can be produced by increasing the flux through the valine biosynthetic pathway to produce 2-ketoisovalerate, which can be decarboxylated to isobutanol. To increase the availability of 2-ketoisovalerate, we assembled an array of genes, which are involved in producing valine from pyruvate; *ILV2*, *ILV3*, *ILV5*, and *ILV6* under the regulation of different strong yeast promoters in a multi-copy plasmid. The overexpression of these enzymes in addition to the Ehrlich pathway enzyme gave rise to a strain which produced ~150mg/liter (1.88mg/g glucose) of isobutanol after 48 hours. Elimination of *LEU4*, *LEU9* and *BAT1* genes involved in competing reactions that drains off 2-ketoisovalerate did not prove to be beneficial for isobutanol production because the mutants cannot synthesize any of the branched chain amino acids and had great defects in growth.

To further increase isobutanol production, several measures including reconstructing the isobutanol pathway using a feedback-resistant acetolactate synthase (*ILV6*) mutant gene, switching the cofactor dependence of *ILV5* and *ADH7/yqhD* from NADPH to NADH, and increasing the intracellular pyruvate availability should be exploited.

References

1. Antoni, D., Zverlov, V.V., and Schewarz, W. H. (2007). Biofuels from microbes. *Appl. Microbiol. Biotechnol.* 77, 23-35.
2. Arnold, F. H. (2008). The race for new biofuels. *Eng. Sci.* 2, 12-19.
3. Atsumi, S., Hanai, T., and Liao, J. C. (2008). Non-fermentative pathways for synthesis of branched-chain higher alcohols as biofuels. *Nature.* 451, 86-90.
4. Atsumi, S., and Liao, J. C. (2008). Metabolic engineering for advanced biofuels production from *Escherichia Coli*. *Curr. Opinion biotechnol.* 19, 414-419.
5. Atsumi, S., Cann, A. F., Connor, M. R., Shen, C. R., Smith, K. M., Brynildsen, M. P., Chou, K. J. Y., Hanai, T., and Liao, J.C. (2008). Metabolic engineering of *Escherichia coli* for 1-butanol production. *Metab. Eng.* 10, 305-311
6. Atsumi, S., Li, S., and Liao, J. C. (2009). Acetolactate synthase from *Bacillus subtilis* serves as 2-ketoisovalerate decarboxylase for isobutanol biosynthesis in *Escherichia coli*. *Appl. Environ. Microbiol.* 75, 6306-6311
7. Atsumi, S., Higashide, W. and Liao, J. C. (2009). Direct photosynthetic recycling of carbon dioxide to isobutyraldehyde. *Nature Biotechnol.* 27, 1177-1182.
8. Atsumi, S., Wu, T-Y., Machado, L., Huang, W-C., Chen, P-Y., Pellegrini, M., and Liao, J. C. (2010). Evolution, genomic analysis, and reconstruction of isobutanol tolerance in *Escherichia coli*. *Molecular systems biology.* 6:449

9. Atsumi, S., Wu, T. Y., Eckl, E. M., Hawkin, S. D., Buelter T., Liao, J.C. (2010). Engineering the isobutanol biosynthetic pathway in *Escherichia coli* by comparison of three aldehyde reductase/alcohol dehydrogenase genes. *Appl. Microbiol. Biotechnol.* 85, 651-657.

10. Baez, a., Cho, K-M., Liao, J. C. (2011). High-flux isobutanol production using engineered *Escherichia coli*: a bioreactor study with in situ product removal. *Appl. Microbiol. Biotechnol.* 90, 1681–1690.

11. Bahler, J., Wu, J-Q., Longtine, M., Shah, N. G., Mckenzie, A., Steever, A. B., Wach, A., Philippsen, P., and Pringle, J. R. (1998). Heterologous modules for efficient and versatile PCR-base gene targeting in *Schizosaccharomyces pombe*. *Yeast.* 14, 943-951.

12. Basso, L. C., , de Amorim, H. V, de Oliveira, A. J., and Lopes, M. L. (2008). Yeast selection for fuel ethanol production in Brazil. *FEMS Yeast Res.* 8, 1155–1163

13. Bastin, S., Lui, X., Meyerowitz, J. T., Snow, C. D., and Chen, M. M. Y.(2011). Engineered ketol-acid reductoisomerase and alcohol dehydrogenase enable anaerobic 2-methylpropan-1-ol production at theoretical yield in *Escherichia coli*. *Met. Eng.* 13, 345-352.

14. Blombach, B., and Eikmanns, B. J. (2011). Current knowledge on isobutanol production with *Escherichia coli*, *Bacillus subtilis* and *Corynebacterium glutamicum*. *Bioengineering bugs.* 2, 346-350.

15. Bond-Watts, B., Bellerose, R. J., and Chang M. C. Y. (2011). Enzyme mechanism as a kinetic control element for designing synthetic biofuels pathways. *Nature Chem. Biol.* 7, 222-227

16. Brekke, K. (2007). Butanol: an energy alternative. *Ethanol Today.* 36-39.

17. Brynildsen, M. P., and Liao, J. C. (2009). An integrated network approach identifies the isobutanol response network in *Escherichia coli*. *Molecular Systems Biology.* 5:277.

18. Buelter, T., Meinhold, P., Feldman, R. M. R., Hawkins, A., Bastin, S., Arnold, F. and Urano, J. (2012). Engineered microorganism capable of producing target compounds under anaerobic conditions. United States patent application number: 20120058532. <http://www.faqs.org/patents/app/20120058532#ixzz1tg5UooyL>
19. Cann, A. F., and Liao, J. C. (2010). Pentanol isomer synthesis in engineered microorganism. *Appl. Microbiol. Biotechnol.* 85, 893-899.
20. Cann, A. E., and Liao, J.C. (2008). Production of 2- methyl-1-butanol in engineered *Escherichia Coli*. *Appl. Microbiol. Biotechnol.* 81, 89-98.
21. Chen, X., Nielsen, K. F., Borodina, I., Kielland-Brandt, M. C., and Karhumaa, K. (2011). Increased isobutanol production in *Saccharomyces cerevisiae* by overexpression of genes in valine metabolism. *Biotechnol. Biofuels.* 4:21.
22. Chisti, Y. (2007) Biodiesel from microalgae beats bioethanol. *Cell.* 26, 126-131.
23. Cho, A., Yun, H., Park, J. H., Lee, S. Y., and Park, S.(2010). Prediction of novel synthetic pathways for the production of desired chemicals. *BMC syst. Biol.* 4, 35.
24. Clomburg, J.M., and Gonzalez, R. (2010). Biofuel production in *Escherichia coli*: the role of metabolic engineering and synthetic biology. *Appl. Microbiol. Biotechnol.* 86, 419-434.
25. Colon, M., Hernandez, F., Lopez, K., Quezada, H., Gonzalez, J., Lopez, G., Aranda, C., and Gonzalez, A. (2011). *Saccharomyces cerevisiae* Bat1 and Bat2 aminotransferases have functionally diverged from the ancestral-like *Kluyveromyces lactis* orthologous enzyme. *PLoS One.* 6:e16099.

26. Connor, M. R., and Liao, J.C. (2008) Engineering of an *Escherichia coli* strain for the production of 3-methyl-1-butanol. *Appl. Environ. Microbiol.* 74, 5769-5775.
27. Connor, M. R., Cann A. F., and Liao J. C. (2009). 3-methyl-1-butanol production in *Escherichia coli*: random mutagenesis and two-phase fermentation. *Appl. Microbiol. Biotechnol.* 86, 1155-1164.
28. Connor, M. R., and Atsumi, S. (2010). Synthetic biology guides biofuel production. *J. Biomed. Biotechnol.* doi:10.1155/2010/541698.
29. Connor, M. R. (2010). Metabolic engineering of microbial systems for the production of advanced transportation fuels. Unpublished PhD thesis. University of California, Los Angeles.
30. Cullin, C., Baudin-Baillieu, A., Guillement, E., and Ozier-Kalogeropoulos, O. (1996). Functional analysis of YCL09C: Evidence for a role as the regulatory subunit of acetolactate synthase. *Yeast.* 12, 1511-1518.
31. Dasari, S. and Kölling R. (2011). Cytosolic localization of acetoxyacid synthase Ilv2 and its impact on diacetyl formation during beer fermentation. *Appl. Environ. Microbiol.* 77, 727-731.
32. De la Plaza, M., De Palencia, F., Pelaez, C., and Requena, T. (2004). Biochemical and molecular characterization of α -ketoisovalerate decarboxylase, an enzyme involved in the formation of aldehydes from amino acids by *Lactococcus lactis*. *FEMS Microbiol, Letters.* 238, 367-374.
33. Dellomonaco, C., Fava, F., and Gonzalez, R. (2010). The path to next generation biofuels: successes and challenges in the era of synthetic biology. *Microbial Cell Factories.* 9:3.

34. Deng, M. D., and Coleman, J. R. (1999). Ethanol synthesis by genetic engineering of cyanobacteria. *Appl. Environ. Microbiol.* 65, 523-528.
35. Derrick, S., and large, P. J. (1993). Activities of the enzymes of the Ehrlich pathway and formation of branched-chain alcohols in *Saccharomyces cerevisiae* and *Candida utilis* grown in continuous culture on valine or ammonium as sole nitrogen source. *Journal of General Microbiology.* 139, 2783-2792.
36. Dickinson, J. R., Harriot, S. J., and Hewline, M. J. E. (1998). An investigation of the metabolism of valine to isobutyl alcohol in *Saccharomyces cerevisiae*. *J. Biol. Chem.* 273, 25751-25756.
37. Dickinson, J. R., Salgado, L. E. J., and Hewlins, M. J. E. (2003). The catabolism of amino acids to long chain and complex alcohols in *Saccharomyces cerevisiae*. *J. Biol. Chem.* 278, 8028-8034.
38. Didion, T., Grauslund, M., Kielland-Brandt, M. C., and Andersen H. A. (1996). Import of branched-chain amino acids in *Saccharomyces cerevisiae*. *Folia Microbiol (Praha).* 41:87.
39. Dong, X., Quinn, P. J., and Wang, X. (2011). Metabolic engineering of *Escherichia coli* and *Corynebacterium glutamicum* for the production of L-threonine. *Biotechnol Adv.* 29, 11-23.
40. Dunlop, M. J. (2011) Engineering microbes for tolerance to next generation biofuels. *Biotechnol. Biofuels.* 4, 32-41.
41. Durre, P. (2007). Biobutanol: an attractive biofuel. *Biotechnol. J.* 2, 1525-1534.
42. Elisakova, V., Patek, M., Holatko, J., Nesvera, J., Leyval, D., Goergen, J. L., and Delaunay, S.(2005) Feedback-resistant acetohydroxy acid synthase increases valine production in *Corynebacterium glutamicum*. *Appl. Environ. Microbiol.* 71, 207-213.

43. Foiani, M., Liberi, G., Piatti, S. and Plevani, P. (1999). *Saccharomyces cerevisiae* as a model system to study DNA replication. In Eukaryotic DNA Replication: A Practical Approach (ed. S. Cotterill), pp. 185-200. Oxford: Oxford University Press.
44. Galazka, J. M., Tian, C., Beeson, W. T. Martinez, B., Glass, N. L., and Cate, H. D. (2010). Cellodextrin transport in yeast for improved biofuel production. *Science*. 330, 84-86.
45. Gibreel, A., Sandercock, J. R., Lan, J., Goonewardene, L. A., Zijlstra, R.T., Curtis, J. M., and Bressler D. C. (2009). Fermentation of barley as a feedstock for bioethanol production and value-added products. *Appl. Environ. Microbiol.* 75, 1363-1372.
46. Gibson, D. G. (2011). Enzymatic assembly of overlapping DNA fragments. *Methods. Enzymol.* 498, 349-361.
47. Gietz, R. D., and Sugino, A. (1988). New yeast-*Escherichia coli* shuttle vectors constructed with in vitro mutagenized yeast genes lacking six-base pair restriction sites. *Gene*. 30, 527-534.
48. Güldener, U., Heinisch, J., Köhler G.J., Voss, D., and Hegemann, J.H. (2002). A second set of loxP marker cassettes for Cre-mediated multiple gene knockouts in budding yeast. *Nucleic Acids Research* **30**, e23.
49. Hanai, T., Atsumi, S., and Liao, J. C. (2007). Engineered synthetic pathway for isopropanol production in *Escherichia coli*. *Appl. Environ. Microbiol.* 73, 7814-7818.
50. Hara, S., Takemori, Y., Yamaguchi, M., and Nakamura, M. (1985). Determination of α -keto acids in serum and urine by high-performance liquid chromatography with fluorescence detection. *J. Chromatography*. 344, 33-39.

51. Hazelwood, L. A., Daran, J.-M., Maris, A. J. A. V., Pronk, J. T., and Dickinson, J. R. (2008). The Ehrlich pathway for fusel alcohol production: a century of research on *Saccharomyces cerevisiae* metabolism. *Appl. Environ. Microbiol.* 74, 2259-2266.
52. Hentges, P., Driessche, B. V., Tafforeau, L., Vandenhoute, J., and Carr, A. M. (2005). Three novel antibiotic marker cassettes for gene disruption and marker switching in *Schizosaccharomyces pombe*. *Yeast.* 22, 1013-1019.
53. Huntley, M. E., and Redalje, D. G. (2007). CO₂ mitigation and renewable oil from photosynthetic microbes; a new appraisal. *Mitigation and Adaptation Strategies for Global Change.* 12, 573-603.
54. Iding, H. P., Siegert, K., and Pohl, M. M. (1998). Application of α -keto acid decarboxylases in biotransformation. *Biochimica et Biophysica Acta.* 1385, 307-322.
55. Ikeda, M. (2006). Towards bacterial strains overproducing L-tryptophan and other aromatics by metabolic engineering. *Appl. Microbiol. Biotechnol.* 69, 615-626.
56. Inoue, H., Nojima, H., and Okayama, H. (1990). High efficiency transformation of *Escherichia coli* with plasmids. *Gene.* 96, 23-28.
57. Jarboe, L. R., Zhang, X., Wang, X., Moore, J. C., Shanmugam, K. T., and Ingram, L. O. (2010). Metabolic engineering for production of biorenewable fuels and chemicals: contributions of synthetic biology. *J. Biomed. Biotechnol.* DOI:10.1155/2010/761042.
58. Jojima, T., Inui, M., and Yukawa, H. (2008). Production of isopropanol by metabolically engineered *Escherichia coli*. *Appl. Microbiol. Biotechnol.* 77, 1219-1224.

59. Karabektas, M., and Hosoz, M. (2009). Performance and emission characteristics of a diesel engine using isobutanol-diesel fuel blends. *Renewable Energy*. 34, 1554-1559.
60. Kaster, K. R., Burgett, S. G., and Ingolia, T. D. (1984). Hygromycin B resistance as dominant selectable marker in yeast. *Curr. Genetics*. 8, 353-358.
61. Kawai, S. and Murata, K. (2008). Structure and function of NAD kinase and NADP phosphatase: key enzymes that regulate the intracellular balance of NAD(H) and NADP(H). *Biosci. Biotechnol. Biochem.*, 72, 70738-1-12.
62. Kennedy, D. (2010). Beyond petroleum. *Science*. 329, 727.
63. Kiritani, K., Narise, S., and Wagner, R. P. (1966). The dihydroxy acid dehydratase of *Neurospora crassa*. *J. Biol. Chem.* 241, 2042-2046.
64. Kondo, T., Tezuka, H., Ishii, J., Matsuda, F., Ogino, C. and Kondo. A. (2012). Genetic engineering to enhance the Ehrlich pathway and alter carbon flux for increased isobutanol production from glucose by *Saccharomyces cerevisiae*. *J. Biotech.* 159, 32-37.
65. Krause, F. S., Blombach, B., and Eikmanns, B. J. (2010). Metabolic engineering of *Corynebacterium glutamicum* for 2-ketoisovalerate production. *Appl. Environ. Microbiol.* 76, 8053-8061.
66. Kwok, R. (2010). Five hard truths for synthetic biology. *Nature*. 463, 288-290.
67. Lange, B. M., Rujan T., Martin, W., and Croteau, R. (2000). Isoprenoid biosynthesis: the evolution of two ancient pathways across genomes. *Proc Natl Acad Sci USA*. 97, 13172-13177.

68. Larroy, C., pares, X., and Biosca, J. A. (2002). Characterization of a *Saccharomyces cerevisiae* NADP(H)-dependent alcohol dehydrogenase (ADHVII), a member of the cinnamyl alcohol dehydrogenase family. *Eur. J. Biochem.* 269, 5738-35745.
69. Larry, C.A., Lixuan, L. H., and Rick, W.Y. (2010). Isobutanol production in yeast mitochondria. United States patent application number: 2010012988
<http://www.faqs.org/patents/app/20100129886#ixzz1qWQYNlby>
70. Leonard, E., Nielsen, D., Solomon, K., and Prather, K. J. (2008). Engineering microbes with synthetic biology frameworks. *Trends Biotechnol.* 26, 674-681.
71. Li, S., Wen, J., and Jia, X. (2011). Engineering *Bacillus subtilis* for isobutanol production by heterologous Ehrlich pathway construction and the biosynthetic 2-ketoisovalerate precursor pathway overexpression. *Appl. Microbiol. Biotechnol.* 91, 577-589.
72. Liu, S., and Qureshi, N. (2009) How microbes tolerate ethanol and butanol. *New Biotechnol.* 26, 117-120.
73. Lynd, L R., Wyman, C. E., and Gerngross, T. U. (1999) Biocommodity engineering. *Biotechnol. Prog.* 15, 777-793.
74. Ma, F., Milford, A., and Hanna A. (1999). Biodiesel production: a review. *Bioresource Technol.* 70, 1-15.
75. Magee, P. T., and De Robichon-Szulmsjdter H. (1968). The regulation of isoleucine-valine biosynthesis in *Saccharomyces cerevisiae*. *European J. Biochem.* 3, 507-511.

76. Martin D. M., Faldt, J., and Bohlmann J. (2004). Functional characterization of nine Norway Spruce TPS genes and evolution of gymnosperm terpene synthases of the TPS-d subfamily. *Plant Physiol.* 135, 1908-1927.
77. Miller, S. M., and Magasanik, B. (1990). Role of NAD-linked glutamate dehydrogenase in nitrogen metabolism in *Saccharomyces cerevisiae*. *J. Bacteriology.* 172, 4927-4935.
78. Mitchell, D. (2008). A note on rising food prices. The World Bank development prospects group. Policy research working paper.
79. Miyagi, H., Kawai, S. and Murata, K. (2009). Two sources of mitochondrial NADPH in the yeast *Saccharomyces cerevisiae*. *J. Biol. Chem.* 284, 7553–7560.
80. Nevoigt, E. (2008). Progress in metabolic engineering of *Saccharomyces cerevisiae*. *Microbiol. Mol. Biol. Rev.* 72, 379-412.
81. Outten, C. E. and Culotta, V. C. (2003). A novel NADH kinase is the mitochondrial source of NADPH in *Saccharomyces cerevisiae*. *EMBO. J.* 22, 2015-2024.
82. Pang, S. S., and Duggleby, R. G. (1999). Expression, purification, characterization, and reconstitution of the large and small subunits of yeast acetohydroxyacid synthase. *Biochemistry.* 38, 5222-5231.
83. Peraita-Yahya, P. P., and Keasling, J. D. (2010). Advanced biofuel production in microbes. *Biotechnol. J.* 5, 147-162.
84. Phi Minh Do (2009). Metabolic engineering of microbial biocatalyst for fermentative production of next generation biofuels. Unpublished PhD thesis. University of Florida.

85. Pronk, J. T., Steensmays, H. Y and Van Dijken, J. P (1996). Pyruvate Metabolism in *Saccharomyces cerevisiae*. *Yeast*. 12, 1607-1633.
86. Radakovits, R., Jinkerson, R. E., Darzins, A., and Posewitz, M. C. (2010). Genetic engineering of algae for enhanced biofuel production. *Eukaryotic cell*. 9, 486-501.
87. Richard, T. L. (2010). Challenges in scaling up biofuels infrastructure. *Science*. 329, 793-796.
88. Roeb, M., and Muller-Steinhagen, H. (2010). Concentrating on solar electricity and fuels. *Science*. 329, 773-774.
89. Rossouw, D., Naes, T., and Bauer, F. F. (2008). Linking gene regulation and the exo-metabolome: a comparative transcriptome approach to identify genes that impact on the production of volatile aroma compounds in yeast. *BMC Genomics*. 9, 530.
90. Rude, M. A., and Schirmer, A. (2009). New microbial fuels: a biotech perspective. *Curr. Opinion Microbiol*. 12, 274-281.
91. Sakuragi, H., Kuroda, K., and Ueda, M. (2011). Molecular breeding of advanced microorganism for biofuel production. *J. Biomed. Biotechnol*. 2011, Article ID 416931, 11 pages, doi:10.1155/2011/416931.
92. Savrasova, E. A., Kivero, A. D., Shakulov, R. S., and Stoyanova, N. V. (2011) Use of the valine biosynthetic pathway to convert glucose into isobutanol. *J. Ind. Microbiol. Biotechnol*. 38, 1287-1294.
93. Schirmer, A., Rude, M., Li, X., Popova, E., Del Cardayre, S. B. (2010). Microbial biosynthesis of alkanes. *Science*. 329, 559-562.

94. Schoondermark-Stolk, S. A., Jansen, M., Veurink, J. H., Verkleij, A. J., Verrips, C. T., Euverink, G. W., Boonstra, J., and Dijkhuizen, L. (2006). Rapid identification of target genes for 3-methyl-1-butanol production in *Saccharomyces cerevisiae*. *Appl. Microbiol. Biotechnol.* 70, 237-246.
95. Seeboth, P. G., Bohnsack, K., and Hollenberg, C. P. (1990). *pdc1(0)* mutants of *Saccharomyces cerevisiae* give evidence for an additional structural PDC gene: cloning of PDC5, a gene homologous to PDC1. *J. Bacteriology.* 172, 678-685.
96. Sentheshanmuganathan, S. (1959). The mechanism of the formation of higher alcohols from amino acids by *Saccharomyces cerevisiae*. *Biochem J.* 74, 568-576.
97. Service, S. (2010). Is there a road ahead for cellulosic ethanol? *Science.* 329, 784-785.
98. Sikorski, R.S., and Hieter, P. (1989). A system of shuttle vectors and yeast host strains designed for efficient manipulation of DNA in *Saccharomyces cerevisiae*. *Genetics.* 122, 19-27.
99. Smit, B., Vlieg, J. E. T. V. H., Engels, W. J. M., Meijer, L., Wouters, J. T. M., and Smit, G. (2005) Identification, cloning, and characterization of a *Lactococcus lactis* branched-chain α -keto acid decarboxylase involved in flavor formation. *Appl. Environ. Microbiol.* 71, 303-311.
100. Smith, K. M., Cho, K. M., and Liao, J.C. (2010). Engineering *Corynebacterium glutamicum* for isobutanol production. *Appl. Microbiol. Biotechnol.* 87, 1045-1053.
101. Smith, K. M., and Liao, J. C. (2011). An evolutionary strategy for isobutanol production strain development in *Escherichia coli*. *Metab. Eng.* 13, 674-681.

102. Somerville, C., Youngs, H., Taylor, C., Davis, S. C., and Long, S. P. (2010). Feedstocks for lignocellulosic biofuels. *Science*. 329, 790-792.
103. Song L. (2006). A soluble form of phosphatase in *Saccharomyces cerevisiae* capable of converting farnesyl diphosphate into E,E-farnesol. *Appl Biochem Biotechnol*. 128, 149-158.
104. Steen, E. J., Kang, Y., Bokinsky G., Hu, Z., Schirmer, A., McClure, A., Del Cardayre, S. B., and Keasling, J. D. (2010). Microbial production of fatty-acid-derived fuels and chemicals from plant biomass. *Nature*. 463, 559-563.
105. Stephanopoulos, G. (2007). Challenges in engineering microbes for biofuels production. *Science*. 315, 801-804.
106. Sulzenbacher, G., Alvarez, K., Van den Heuvel, R. H. H., Versluis, C., Spinelli, S., Campanacci, V., Valencia, C., Cambillau, C., Eklund, H., Tegoni, M. (2004). Crystal structure of *E. coli* Alcohol dehydrogenase yqhD: Evidence of a covalently modified NADP coenzyme. *J. Mol. Biol*. 342, 489-502.
107. Survase, S. A., Jurgens, G., Heiningen, A. V., and Granstrom, T. (2011). Continuous production of isopropanol and butanol using *Clostridium beijerinckii* DSM 6423. *Appl. Microbiol. Biotechnol*. 91, 1305-1313.
108. Ter Schure, E.G., Flikweert, M. T., Van Duken, J. P., Pronk, J. T., and Verrips, C. T. (1998). Pyruvate decarboxylase catalyzes decarboxylation of branched-chain 2-oxo acids but is not essential for fusel alcohol production by *Saccharomyces cerevisiae*. *Appl. Environ. Microbiol*. 64, 1303-1307.
109. Trinh, C. T., Li, J., Blanch, H. W., and Clark, D. S. (2011). Redesigning *Escherichia coli* metabolism for anaerobic production of isobutanol. *Appl. Environ. Microbiol*. 77, 4894-4904.

110. US Energy Information Administration. (2011) International Energy outlook. DOE/EIA-0484
<http://www.eia.gov/forecasts/ieo/pdf/0484%282011%29.pdf>
111. US Energy Information Administration. Petroleum and other liquids
http://205.254.135.7/pub/oil_gas/petroleum/analysis_publications/oil_market_basics/demand_text.htm#Global%20Oil%20Consumption
112. Vaaje-Kolsstad, G., Westereng, B., Horn, S. J., Liu, Z., Zhai, H., Sorlie, M., and Eijsink, V. G. H. (2010). An oxidative enzyme boosting the enzymatic conversion of recalcitrant polysaccharides. *Science*. 330, 219-222.
113. Wach, A., Branchat, A., Pohlmann, R., and Philippsen, P. (1994). New heterologous modules for classical or PCR-based gene disruption in *Saccharomyces cerevisiae*. *Yeast*. 10, 1793-1808.
114. Walter, A., Dolzan, P., Quilodrán, O., Garcia, J., Da Silva, C., Piacente, F., and Segerstedt, A. (2008). A Sustainability analysis of the Brazilian ethanol. An independent report, supported by UK's Department for Environment, Food and Rural Affairs (Defra) and UK Embassy, in Brasília.
115. Wang, B. W., Shi, A Q., Tu, R., Zhang, X-L., Wang, Q-H., and Bai, F-W. (2011). Branched-chain higher alcohols. *Adv. Biochem. Eng. Biotechnol.* DOI: 10.1007/10_2011_121.
116. Widdel F. (2010). Theory and measurement of bacterial growth. *Grundpraktikum Mikrobiologie, 4. Sem. (B.Sc.) Universität Breme.*
117. Wijffels, B. H., and Barbosa, M. J. (2010). An outlook on microalgal biofuels. *Science*. 329, 796-799.
118. Woods, D. R. (1995). The genetic engineering of microbial solvent production. *TIBTECH*. 13, 259-264.

119. Yan, Y., and Liao, J.C. (2009). Engineering metabolic systems for production of advanced fuels. *J. Ind. Microbiol. Biotechnol.* 36, 471-479.
120. Zhang, K., Sawaya, M. R., Eisenberg, D. S., and Liao J.C. (2008). Expanding metabolism for biosynthesis of nonnatural alcohols. *Proc Natl Acad Sci USA* 105, 20653–20658.
121. Zhang Y. (2009). Metabolic Engineering of *Clostridium tyrobutyricum* for production of biofuels and bio-based chemicals. Unpublished MSc thesis. The Ohio state University.
122. Zhao, Y., Yang, J., Qin, B., Li, Y., Sun, Y., Su, S., and Xian, M. (2011). Biosynthesis of isoprene in *Escherichia coli* via methylerythritol phosphate (MEP) pathway. *Appl. Microbiol. Biotechnol.* 90, 1915-1922.
123. Renewable fuel association (2012). Ethanol industry outlook. www.ethanolrfa.org